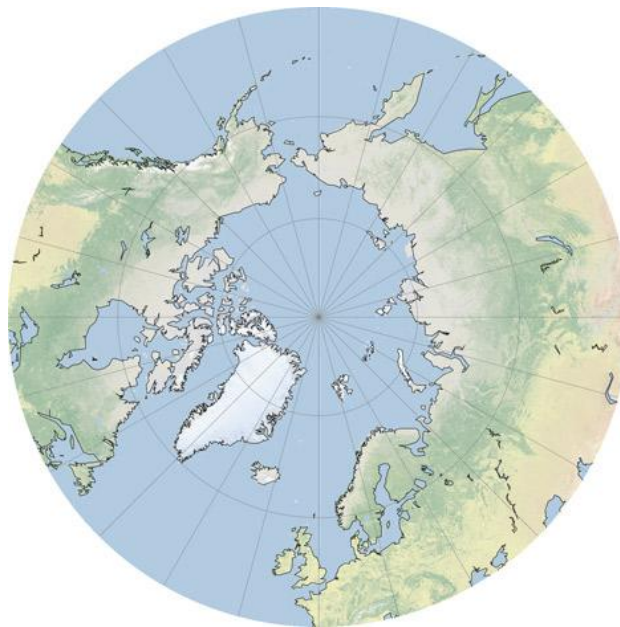


Submarine Geomorphology of the Continental Shelves of Southeast and Southwest Greenland from Olex Data

By Jonathan Ryan

Clare Hall



13th June 2013

**Dissertation is submitted for the degree of
Master of Philosophy**



**UNIVERSITY OF
CAMBRIDGE**



Scott Polar Research Institute
University of Cambridge

Abstract

Mass loss from the Greenland Ice Sheet remains the largest uncertainty in projections of sea level rise for the 21st century. Reconstructing the former history of the Greenland Ice Sheet during the Late Quaternary provides important constraints on how the ice sheet will behave in response to future environmental change. In order to improve our understanding of the extent, dynamics and deglacial retreat of the Greenland Ice Sheet during and after the Last Glacial Maximum (LGM), this study used geophysical bathymetric data to investigate the geomorphology of the continental margins of Southern Greenland. In particular, Olex data, which consist of multiple single-beam echo-sounder lines, were utilised.

Turbidity current-channel systems and gullies on the continental slopes, and moraines on the continental shelf edge of Southern Greenland indicate that the Greenland Ice Sheet extended to the continental shelf edge during the LGM. Drumlins and crag-and-tails, located in troughs, suggest that twenty ice streams drained the ice sheet in Southern Greenland at this time. After the LGM, the deglacial response of the Greenland Ice Sheet was spatially variable. Grounding-zone wedges in some troughs suggest that ice sheet retreat was punctuated by still-stands. In other troughs, the absence of sedimentary depocentres indicates that ice sheet retreat was rapid. In Southeast Greenland, iceberg ploughmarks suggest that initial retreat from the shelf edge was characterised by the calving of deep-keeled icebergs. In contrast, gullying offshore of inter-ice stream areas and evidence of meltwater sedimentation in Southwest Greenland, indicate that initial deglaciation was characterised predominantly by surface melting.

Acknowledgements

I would like to thank my supervisor Dr. Julian Dowdeswell for his guidance, advice and useful discussion throughout the course. I would also like to thank Dr Kelly Hogan. I am very grateful for the technical support and advice she provided which enabled me to complete this thesis. Christian Wilson from oceanDTM provided useful information about Olex and always responded quickly to my e-mails. I also acknowledge my fellow 'MPhils' who have made this year very enjoyable.

Declaration

I declare that this dissertation is entirely my own work. Where other sources of information have been used, they have been acknowledged. The dissertation does not exceed 20,000 words, excluding the abstract, tables of contents, list of figures, figure captions and bibliography.

Jonathan Ryan

June 2013

Contents

| | |
|---|------|
| Abstract..... | i |
| Acknowledgements..... | ii |
| Declaration..... | ii |
| Contents..... | iii |
| List of figures..... | vi |
| List of tables..... | viii |
| 1. Introduction..... | 1 |
| 1.1. The Greenland Ice Sheet..... | 2 |
| 1.2. The Greenland Ice Sheet during the Late Quaternary..... | 4 |
| 1.2.1. Extent of the LGM Greenland Ice Sheet in Southern Greenland..... | 4 |
| 1.2.2. Dynamics of the LGM Greenland Ice Sheet in Southern Greenland..... | 5 |
| 1.2.3. Deglaciation of the LGM Greenland Ice Sheet in Southern Greenland..... | 6 |
| 1.3. Thesis structure..... | 11 |
| 2. Methodology..... | 12 |
| 2.1. Introduction..... | 12 |
| 2.1.1. Olex data..... | 12 |
| 2.1.2. Multi-beam and IBCAO data..... | 13 |
| 2.2. Single-beam bathymetry..... | 13 |
| 2.2.1. Signal transmission and reception..... | 15 |
| 2.2.2. Navigation..... | 17 |
| 2.3. Multi-beam bathymetry..... | 18 |
| 2.4. Olex..... | 20 |
| 2.4.1. Interpolation..... | 21 |
| 2.4.2. Precision..... | 23 |
| 2.4.3. Accuracy..... | 25 |
| 2.5. Other data..... | 29 |
| 2.5.1. Multi-beam data collected onboard the RSS <i>James Clark Ross</i> (JCR)..... | 29 |
| 2.5.2. Multi-beam data archived in the NGDC..... | 30 |
| 2.5.3. IBCAO data..... | 31 |
| 2.6. Processing of multi-beam data..... | 31 |
| 2.7. Comparison of datasets..... | 31 |
| 2.7.1. Effective resolution..... | 31 |
| 2.7.2. Coverage..... | 36 |
| 2.8. Data interpretation..... | 36 |

| | | |
|---------|---|----|
| 3. | Geomorphology of the continental shelves of Southeast and Southwest Greenland | 38 |
| 3.1. | Introduction..... | 38 |
| 3.2. | Cross-shelf troughs | 42 |
| 3.2.1. | Description..... | 42 |
| 3.2.2. | Interpretation..... | 44 |
| 3.3. | Outward bulging bathymetric contours beyond cross-shelf troughs..... | 46 |
| 3.3.1. | Description..... | 46 |
| 3.3.2. | Interpretation..... | 47 |
| 3.4. | Elongate streamlined lineations | 48 |
| 3.4.1. | Description..... | 48 |
| 3.4.2. | Interpretation..... | 50 |
| 3.5. | Channels..... | 51 |
| 3.5.1. | Description..... | 51 |
| 3.5.2. | Interpretation..... | 53 |
| 3.6. | Meandering submarine channel | 53 |
| 3.6.1. | Description..... | 53 |
| 3.6.2. | Interpretation..... | 53 |
| 3.7. | Long sinuous ridges transverse to inferred ice flow direction | 55 |
| 3.7.1. | Description..... | 55 |
| 3.7.2. | Interpretation..... | 55 |
| 3.8. | Long ridges parallel to inferred ice flow direction..... | 57 |
| 3.8.1. | Description..... | 57 |
| 3.8.2. | Interpretation..... | 58 |
| 3.9. | Wide subdued ridges..... | 58 |
| 3.9.1. | Description..... | 58 |
| 3.9.2. | Interpretation..... | 58 |
| 3.10. | Curvilinear depressions or ploughmarks..... | 60 |
| 3.10.1. | Description..... | 60 |
| 3.10.2. | Interpretation..... | 62 |
| 3.11. | Features on the continental slope and rise..... | 62 |
| 3.11.1. | Set 1 - Gullies..... | 62 |
| 3.11.2. | Set 2 – Dendritic channel system and elongate depression with sidewall escarpment . | 66 |
| 3.11.3. | Set 3 - Wide flat-floored valleys with blocky terrain..... | 68 |
| 3.12. | Flat and featureless sea floor..... | 70 |
| 3.12.1. | Description..... | 70 |
| 3.12.2. | Interpretation..... | 70 |

| | | |
|--------|--|-----|
| 3.13. | Summary | 72 |
| 4. | Synthesis and identification of submarine landform assemblages on the Southern Greenland continental margin | 73 |
| 4.1. | Bedrock-dominated inner shelf..... | 73 |
| 4.1.1. | Meltwater channels | 73 |
| 4.1.2. | Streamlined landforms assemblages | 79 |
| 4.2. | Sedimentary outer continental shelf..... | 81 |
| 4.2.1. | Distribution of moraines and GZWs..... | 81 |
| 4.2.2. | Iceberg keel ploughing..... | 83 |
| 4.3. | Continental slope | 86 |
| 4.3.1. | Distribution of the presence and absence of TMFs..... | 86 |
| 4.3.2. | Spatial distribution of gullies, dendritic channel systems, blocky mass-transport deposits and glacial debris flows..... | 89 |
| 4.4. | Summary | 93 |
| 5. | Palaeo-glaciological implications and chronology | 94 |
| 5.1. | Extent of the LGM Greenland Ice Sheet in Southern Greenland..... | 94 |
| 5.1.1. | Southwest Greenland | 94 |
| 5.1.2. | Southeast Greenland | 95 |
| 5.2. | Dynamics of the LGM Greenland Ice Sheet in Southern Greenland..... | 97 |
| 5.2.1. | Ice streams | 97 |
| 5.2.2. | Inter-ice stream areas | 98 |
| 5.3. | Deglaciation of the LGM Greenland Ice Sheet in Southern Greenland..... | 101 |
| 5.3.1. | Nature of retreat | 101 |
| 5.3.2. | Mechanisms of retreat..... | 102 |
| 6. | Conclusions..... | 106 |
| 6.1. | Review of the main findings | 106 |
| 6.2. | Assessment of the Olex database and its limitations | 108 |
| 7. | References..... | 110 |

List of figures

| | |
|--|----|
| Figure 1.1. An idealised high-latitude continental margin..... | 2 |
| Figure 1.2. Location map of Greenland continent | 3 |
| Figure 1.3. Southern Greenland continental margin | 7 |
| Figure 1.4. Temperature in Greenland since the LGM | 8 |
| Figure 2.1. Olex data coverage on the margins of Southern Greenland | 12 |
| Figure 2.2. Multi-beam data coverage | 14 |
| Figure 2.3. Single-beam echo-sounding | 16 |
| Figure 2.4. Example of a sound speed depth profile..... | 17 |
| Figure 2.5 Multi-beam echo-sounding..... | 18 |
| Figure 2.6. Principles of multi-beam echo-sounding..... | 19 |
| Figure 2.7. Olex grid cell size | 20 |
| Figure 2.8. Single ship track-line in Olex | 21 |
| Figure 2.9. Trend projection interpolation using a linear spline..... | 22 |
| Figure 2.10. Result of large interpolation radius in Olex..... | 24 |
| Figure 2.11. Precision of Olex depth values | 25 |
| Figure 2.12. Stripe in Olex data caused by poor approximation of sound speed..... | 27 |
| Figure 2.13. Comparison of Olex and multi-beam depth values | 29 |
| Figure 2.14. Density of ship track-lines in Southwest Greenland | 33 |
| Figure 2.15. The identification of ploughmarks in Olex..... | 35 |
| Figure 2.16. Changing the azimuth in Olex | 37 |
| Figure 3.1. Location map of figures discussed in Chapter 3..... | 40 |
| Figure 3.2. Typical morphology of the Southern Greenland continental shelf..... | 41 |
| Figure 3.3. Seismic profile of Godthåb Trough | 42 |
| Figure 3.4. Example of typical cross-shelf trough in the Olex data..... | 43 |
| Figure 3.5. Reverse sloping long profiles of three troughs | 45 |
| Figure 3.6. Outward bulging bathymetric contours in the IBCAO data..... | 47 |

| | |
|---|-----|
| Figure 3.7. Streamlined elongate lineations in the Olex data | 49 |
| Figure 3.8. Oval-shaped protuberances in the Olex data | 50 |
| Figure 3.9. Large, V-shaped channels in the Olex data | 52 |
| Figure 3.10. Sinuous submarine channel in the Olex data..... | 54 |
| Figure 3.11. Long sinuous ridges in the Olex data | 56 |
| Figure 3.12. Long ridge parallel to cross-shelf trough in the Olex data | 57 |
| Figure 3.13. Large subdued ridges in the Olex data | 59 |
| Figure 3.14. Scatter plot of grounding-zone wedge thickness and length | 60 |
| Figure 3.15. Irregular curvilinear ploughmarks in the Olex data..... | 61 |
| Figure 3.16. Location map for features on the continental slope..... | 63 |
| Figure 3.17. Gullies in the multi-beam data..... | 64 |
| Figure 3.18. Gullies in the Olex data | 65 |
| Figure 3.19. Dendritic channel system in the multi-beam data | 67 |
| Figure 3.20. Wide flat-floored valley in the multi-beam data | 69 |
| Figure 3.21. Flat featureless floor in the Olex data..... | 71 |
| Figure 4.1. Location map of the figures discussed in Chapter 4..... | 74 |
| Figure 4.2. Distribution of landforms identified on the inner shelf | 76 |
| Figure 4.3. Long profiles of three channels in the Olex data..... | 78 |
| Figure 4.4. Drumlins and crag-and-tails on the inner shelf | 80 |
| Figure 4.5. Distribution of moraines and grounding-zone wedges on the shelf | 82 |
| Figure 4.6. Distribution of iceberg ploughmarks | 85 |
| Figure 4.7. Distribution of features on the continental slope..... | 87 |
| Figure 4.8. Diagram showing importance of processes on the continental slope..... | 91 |
| Figure 5.1. Inferred extent of the Greenland Ice Sheet at the Last Glacial Maximum | 96 |
| Figure 5.2. Locations of ice streams in Southwest Greenland..... | 99 |
| Figure 5.3. Locations of ice streams in Southeast Greenland..... | 100 |

List of tables

| | |
|--|----|
| Table 2.1. List of multi-beam data utilised in thesis | 30 |
|--|----|

1. Introduction

The Earth's climate is changing (IPCC, 2007) and the response of the Greenland Ice Sheet to warmer air and oceanic temperatures is a major issue in the debate surrounding future sea level change (Lenton et al., 2008). A comprehensive understanding of the dynamics of the Greenland Ice Sheet in response to past environmental change is therefore crucial for predicting its response to present and future environmental change.

Ice sheets respond dynamically to climate change over glacial-interglacial cycles through changes in their extent and spatial configuration. When ice advances and retreats across high-latitude continental margins, landforms are produced (Fig. 1.1). The relatively low energy marine environments in which these landforms are formed, means that they are often preserved on the sea floor, and provide comprehensive records of past glacial activity (Dowdeswell et al., 1998).

This thesis aims to investigate the morphology and distribution of submarine landforms on the continental margins of Southern Greenland¹ (Fig.1.2) in order to improve our understanding of the extent, dynamics and deglacial retreat of the Greenland Ice Sheet during and after the Last Glacial Maximum² (LGM). To do this, geophysical bathymetric data will be used to provide imagery of the sea floor. In particular, the Olex database will be utilised. The Olex database consists mainly of voluntarily contributed single-beam echo-sounder data from commercial fishing vessels. The database has been used for a number of geomorphological studies (e.g. Bradwell et al., 2008; Shaw et al., 2009, 2012; Spagnolo and Clark, 2009) but has yet to be critically analysed. A further aim of this thesis, therefore, is to assess the usefulness of the Olex database for identifying submarine landforms.

After a brief introduction to the modern Greenland Ice Sheet, this chapter reviews the current literature regarding the extent, dynamics and deglacial retreat of the ice sheet in Southern Greenland during the Late Quaternary.

¹ In this thesis, Southern Greenland is defined as the area south of Holsteinsborg Trough in Southwest Greenland and south of Kangerlussuaq Fjord in Southeast Greenland. The definition of 'Southwest' and 'Southeast' Greenland is shown in Figure 1.2.

² In this thesis, the Last Glacial Maximum (LGM) is defined as the period when the Greenland Ice Sheet attained its maximum extent. This is thought to have happened towards the end of the last glacial period at around 21,000 years before present (Alley et al., 2010).

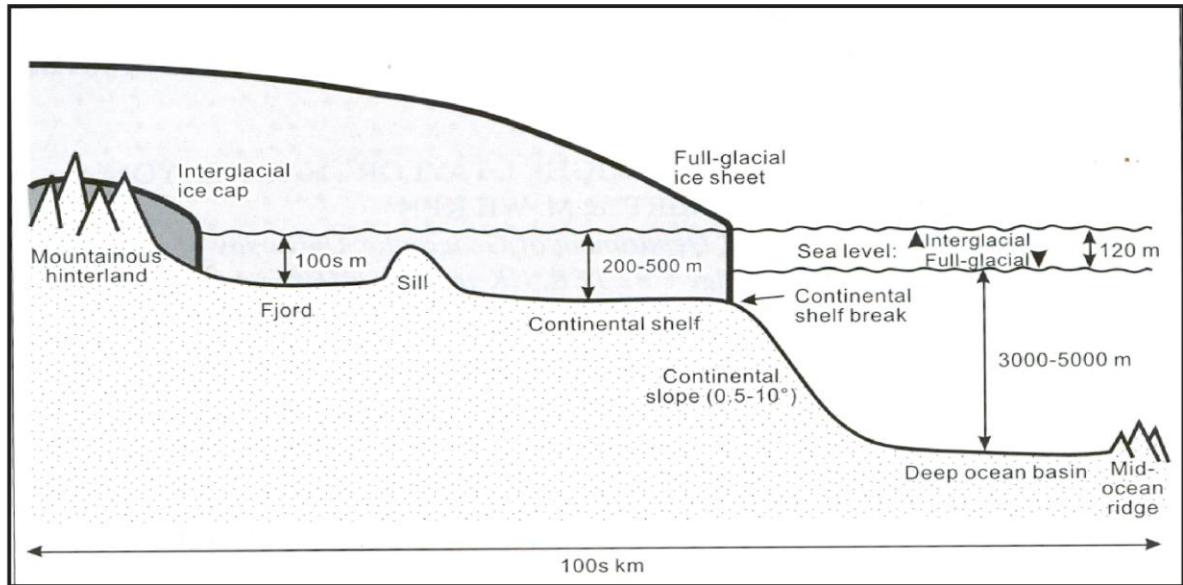


Figure 1.1. An idealised high-latitude continental margin with the locations of interglacial (dark shading) and full-glacial (lighter shading) ice sheets shown. As the ice sheet extends onto the shelf edge and retreats to the mountainous hinterland, a number of landforms are produced which are often preserved on the seafloor. Adapted from Dowdeswell et al., (2002).

1.1. The Greenland Ice Sheet

The island of Greenland has an area of 2,166,086 km². About 83% of its landmass is covered by the Greenland Ice Sheet which covers an area of 1,801,000 km² (Fig. 1.2) (Kargel et al., 2012). The Greenland Ice Sheet is the second largest ice mass on the planet, accounting for around 11% of the total global ice surface area. The ice sheet is composed of two separate domes. The southern dome contains about 15% of the ice volume and is a climatically sensitive, highland ice cap, resting on bedrock about 500 m a.s.l (Fig. 1.3) (Funder et al., 2011).

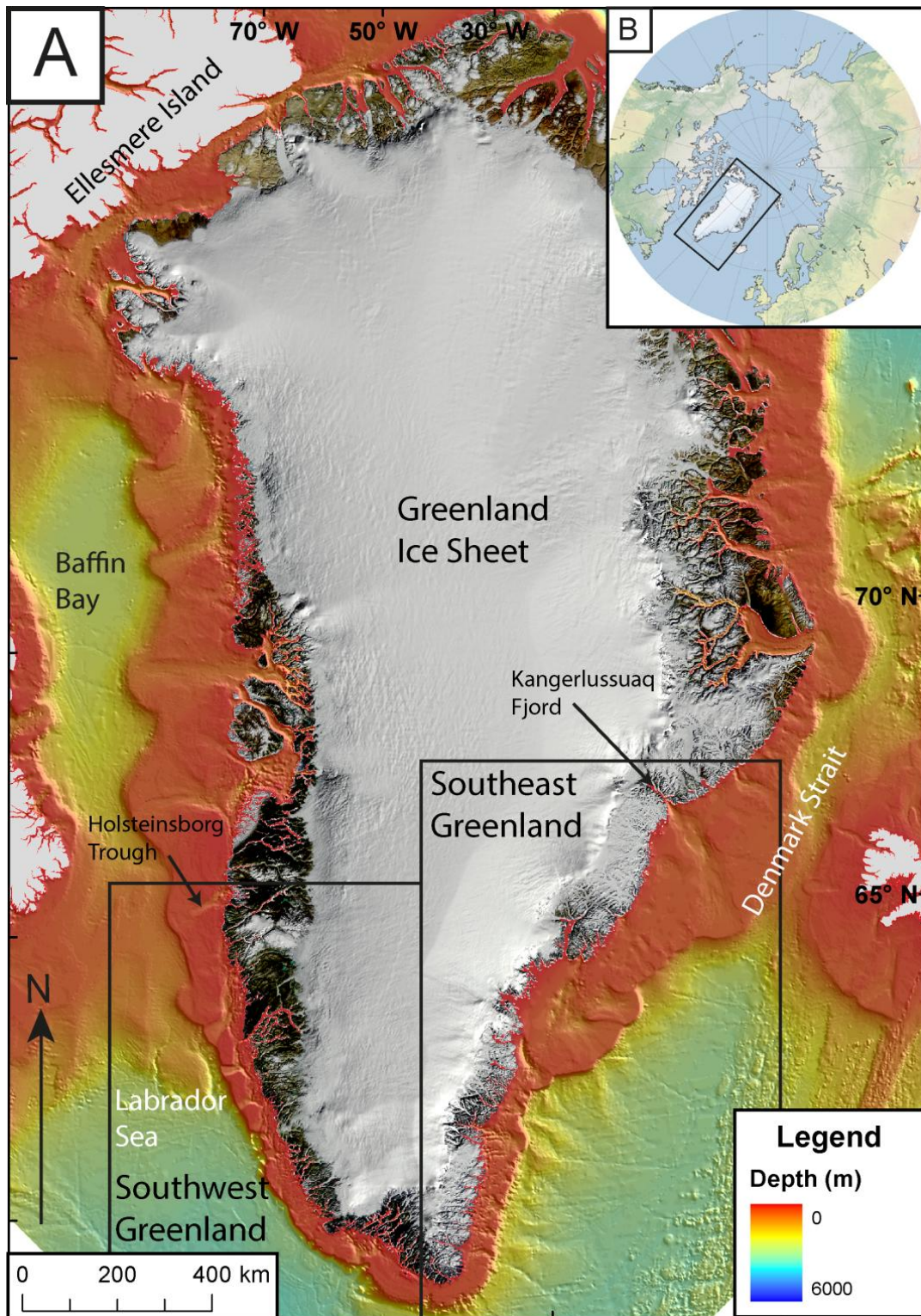


Figure 1.2. (A) Map of Greenland, the Greenland Ice Sheet and the bathymetry surrounding Greenland displayed with a Polar Stereographic projection. Black boxes show the study area and definition of ‘Southwest’ and ‘Southeast’ Greenland in this thesis. Bathymetric data is from IBCAO Version 3.0 (Jakobsson et al., 2012), and is discussed in Section 2.1.3. Greenland is displayed with a 250m resolution MODIS mosaic (Kargel et al., 2012). (B) Location map of Greenland in a Polar Stereographic projection.

1.2. The Greenland Ice Sheet during the Late Quaternary

1.2.1. Extent of the LGM Greenland Ice Sheet in Southern Greenland

Accurate reconstructions of the Greenland Ice Sheet during the Late Quaternary are necessary in order to constrain and improve models of ice sheet volume change and the associated global eustatic sea level rise. For example, a more extensive LGM Greenland Ice Sheet would make a higher contribution to deglacial global eustatic sea level rise than a smaller reconstructed extent. The reconstructed extent of the Greenland Ice Sheet in Southern Greenland during the LGM has, however, been the focus of much debate (e.g. Funder and Hansen, 1996; Funder et al., 2011).

Evidence from cosmogenic surface exposure dating and trimlines suggest that the Greenland Ice Sheet had a maximum ice thickness of around 500 to 810 metres above sea level (m a.s.l.) in the Sisimiut region, Southwest Greenland (Fig. 1.3) (Kelly, 1985; Rinterknecht et al., 2009; Roberts et al., 2009, 2010; Funder et al., 2011). This was used to argue that the Greenland Ice Sheet was relatively thin in Southwest Greenland during the LGM and that the ice sheet only extended to the inner continental shelf (Funder et al., 2011). This view was also taken by Nielsen and Kuijpers (2013), who interpreted five glacial debris flow units on the Davis Strait Drift Complex (Fig. 1.3) as evidence that the Greenland Ice Sheet extended to the shelf edge five times since the Early Pliocene and only to the mid-shelf during the LGM.

However, large isostatic uplift rates on the narrow continental shelf around Greenland's southern tip and fresh erosional features on coastal hills suggest that the Greenland Ice Sheet was up to 1500 m thick in the Nanortalik region (Fig. 1.3) (Bennike et al., 2002). This was used to argue that the ice sheet was thick enough to extend to the shelf edge during the LGM (Weidick et al., 2004). A new ice sheet model also predicts that the western sector of the Greenland Ice Sheet achieved at least a mid-shelf position in Southwest Greenland, with ice possibly extending as far as the Outer Hellefisk moraines at the shelf edge during the LGM (Fig. 1.3) (Simpson et al., 2009). Finally, a number of glacial debris flows on the continental slopes offshore of the Uummannaq and Egedesminde troughs have now been identified (Fig. 1.3) (Ó Cofaigh et al., 2013a, 2013b; Dowdeswell et al., In Press). These debris flows indicate that, during the LGM, large volumes of sediment were supplied to the continental slopes of West Greenland when ice streams extended to the continental shelf edge (Ó Cofaigh et al., 2013a; Dowdeswell et al., In Press). If the Greenland Ice Sheet extended

this far during the LGM, it suggests that the ice sheet could have also extended across the narrower shelf of Southwest Greenland.

In Southeast Greenland, traditional ice sheet reconstructions indicate that the Greenland Ice Sheet extended to the continental shelf edge during the LGM (Funder and Hansen, 1996; Funder et al., 2011). Turbidite sedimentation and glacial debris flows on the continental slope offshore of Kangerlussuaq Trough (Fig. 1.3) suggest that ice streams supplied sediment to the shelf edge (Jennings et al., 2002, 2006; Dowdeswell et al., 2010). Cosmogenic surface exposure dating from Sermilik Fjord indicates that the ice sheet reached thicknesses of at least 740 m a.s.l. (Roberts et al., 2008). This was used to argue that the ice sheet was thick enough to extend to the shelf edge during the LGM (Roberts et al., 2008).

In summary, the Greenland Ice Sheet probably extended to the shelf edge of Southeast Greenland. Whether it extended to the shelf edge of Southwest Greenland remains contested.

1.2.2. Dynamics of the LGM Greenland Ice Sheet in Southern Greenland

Ice streams drained ice sheets in the both Hemispheres during the LGM (Stokes and Clark, 2001; Ottesen et al., 2005; Livingstone et al., 2012a). Ice streams are important in controlling ice, fresh water and sediment flux to the oceans and significantly influence ice sheet mass balance and response to environmental forcing (Bennett, 2003; Ó Cofaigh et al., 2003). The identification of ice streams in the geological record is therefore important for assessing past and future dynamics of the Greenland Ice Sheet. In Southern Greenland, relatively little is known about the influence of ice streams on overall ice sheet dynamics during the Late Quaternary (Funder, 1989).

Onshore, a number of studies have attempted to reconstruct ice stream behaviour using glacial landforms and cosmogenic surface exposure dating (e.g. Long and Roberts, 2003; Roberts and Long, 2005; Weidick and Bennike, 2007; Rinterknecht et al., 2009; Roberts et al., 2009, 2010). In the marine environment, Kangerlussuaq Trough, in Southeast Greenland, and the Egedesminde and Uummannaq troughs, in West Greenland, are the only troughs south of 70° N which have been the subject of offshore geophysical and sedimentological investigations (Fig. 1.3) (Dowdeswell et al., 2010, In Press; Hogan et al., 2011, 2012; Ó Cofaigh et al., 2013a, 2013b). The International Bathymetric Chart of the Arctic Ocean Version (IBCAO) 3.0 suggests that twenty cross-shelf troughs exist on the continental shelf of Southern Greenland (Jakobsson et al., 2012; Batchelor and Dowdeswell, In Press) (Fig.

1.3). Several authors have suggested that the morphology of these troughs is likely to have been shaped by large ice streams during the LGM (Roberts and Long, 2005; Weidick and Bennike, 2007; Roberts et al., 2010). There is, however, no conclusive evidence to confirm this interpretation.

1.2.3. Deglaciation of the LGM Greenland Ice Sheet in Southern Greenland

1.2.3.1. Initial retreat from continental shelf

Since the LGM, the Greenland Ice Sheet has lost about 40% of its area and volume (Funder et al., 2011). This is much less than that of the warmer Laurentide and Fennoscandian ice sheets (100% loss) but is much more than the colder Antarctic Ice Sheet (Alley et al., 2010). Understanding the nature of Greenland Ice Sheet deglaciation since the LGM is important for understanding the response of the modern Greenland Ice Sheet to increasing oceanic and air temperatures (Joughin et al., 2004; Rignot and Kanagaratnam, 2006; Shepherd and Wingham, 2007; Holland et al., 2008; Christoffersen et al., 2011).

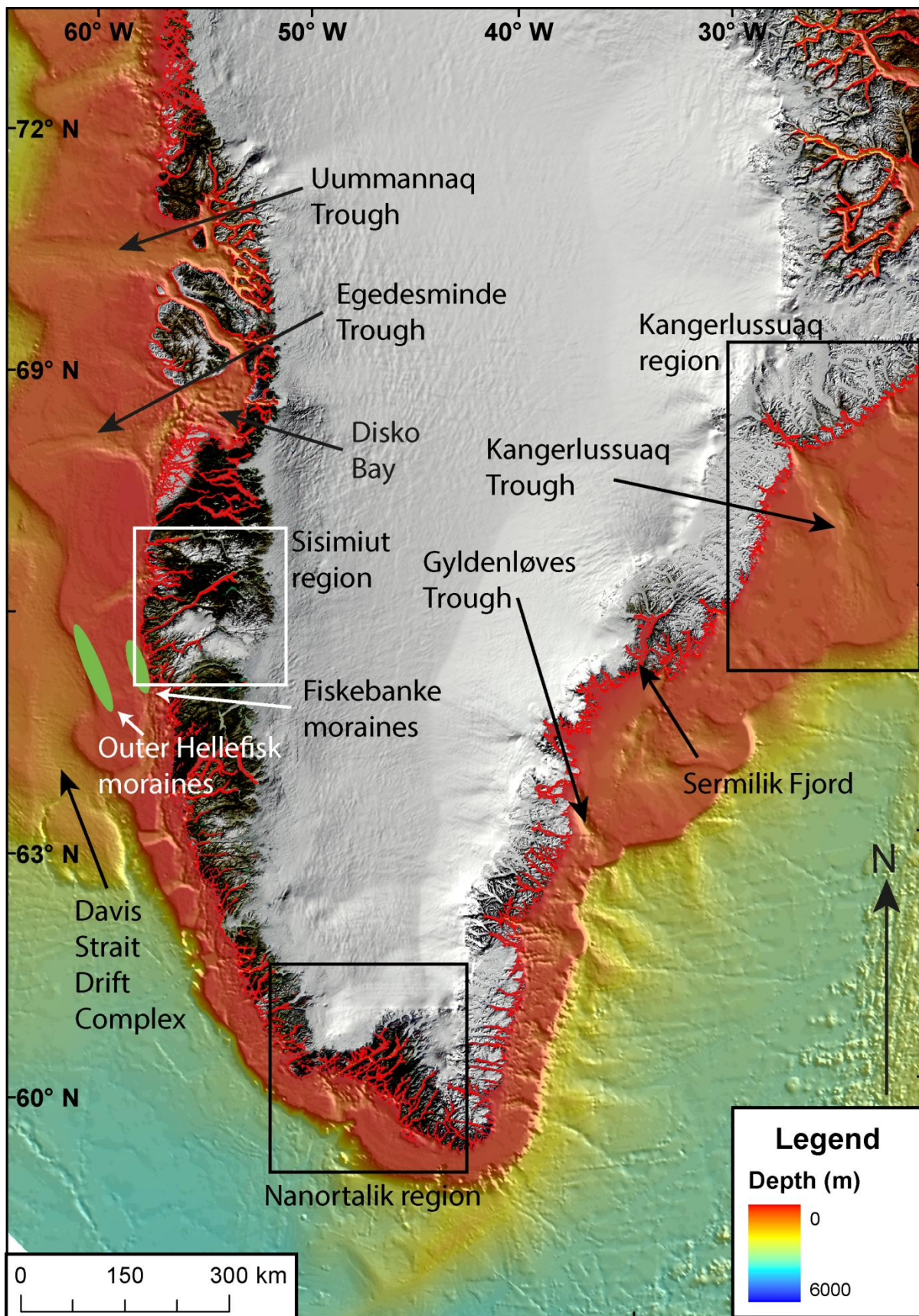


Figure 1.3. Map of Greenland showing the extent of the continental shelf around Southern Greenland and the regions and features mentioned in this chapter.

To date, there is only a limited chronological control on the deglaciation of the Greenland Ice Sheet since the LGM in Southwest Greenland (Alley et al., 2010). Cosmogenic exposure dating from coastal mountains in the Sisimiut region suggests that thinning began 21,000 years before present (BP) (Figs. 1.3, 1.4) (Roberts et al., 2009). Initial retreat from the continental shelf, however, may not have taken place until 15,000 years BP and could have occurred as recently as 10,000 years BP (Ingólfsson et al., 1990; Funder and Hansen, 1996; Roberts et al., 2009). North of Disko Bay, radiocarbon dating of benthic foraminifera from glacial marine mud above glacial till suggests that retreat from the outer continental shelf edge began at least 14,880 cal. years ago in this region (Fig. 1.3) (Ó Cofaigh et al., 2013b). South of Disko Bay, similar techniques suggest that retreat from the outer shelf edge began by 13,800 cal. years BP (Figs. 1.3, 1.4) (Ó Cofaigh et al., 2013b).

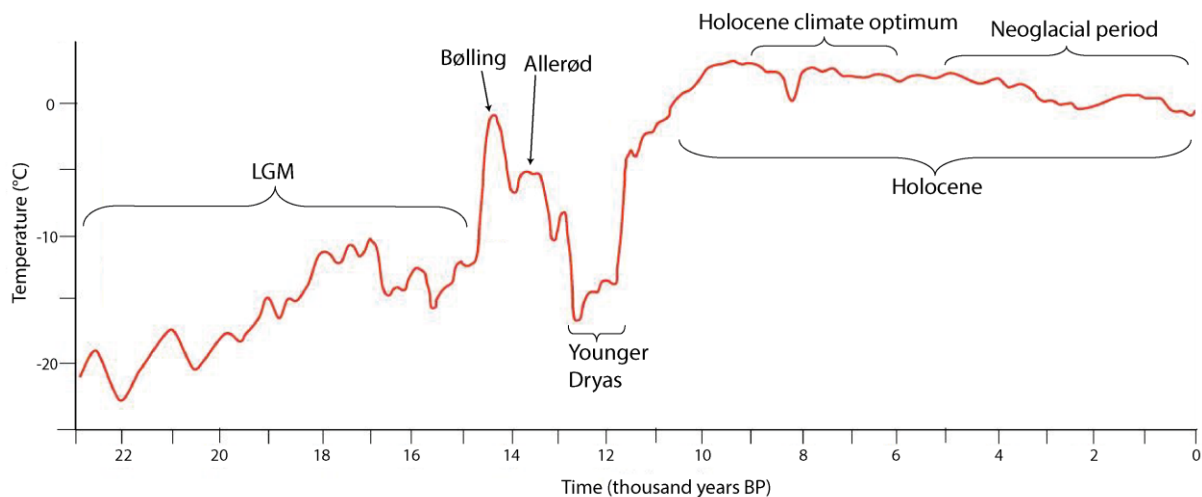


Figure 1.4. Trend of temperature development since the LGM, compiled from Greenland ice-core records (Dansgaard et al. 1984; Dahl-Jensen et al. 1998; Dansgaard 2004). The main events discussed in this thesis and their timings are labelled. Adapted from Weidick and Bennike (2007).

In Southeast Greenland, there is general agreement that initial retreat from the continental shelf edge began at around 17,000 years BP. This is much earlier than Southwest Greenland. Radiocarbon dating of foraminifera and molluscs in Kangerlussuaq Trough and cosmogenic exposure dating in Sermilik Fjord suggest that ice may have retreated from the shelf edge shortly after 17,000 cal. years BP (Figs. 1.3, 1.4) (Mienert et al., 1992; Roberts et al., 2008).

This is backed-up by pronounced decreases in planktonic foraminiferal $\delta^{18}\text{O}$ concentrations in sediment cores from the Labrador Sea, which indicate the transfer of isotopically light meltwater from the decaying Greenland Ice Sheet to the ocean at this time (Elliot et al., 1998; Knutz et al., 2011). A change in sedimentation rates in a deep sea core 600 km from the coast of Southeast Greenland suggests that initial retreat from the shelf edge of Kangerlussuaq Trough began at least 16,000 years BP (Kuijpers et al., 2003). Ice distal glacimarine sedimentation in sediment cores from the middle part of Kangerlussuaq Trough and the outer shelf of Gyldenløves Trough indicate that the ice sheet margin had retreated landward of the mid-shelf by 15,000 cal. years BP (Jennings et al., 2002; Kuijpers et al., 2003).

It is not clear which external factors were the most important for causing the initial break-up of the Greenland Ice Sheet after the LGM. For example, major sea level rises are thought to have occurred between 14,600 and 14,000 years BP (Hanebuth et al., 2000; Stanford et al., 2006). However, these sea level rises do not necessarily correspond with ice sheet mass loss, as indicated by the lack of change in the concentration of iceberg-rafted debris (IRD) in sediment cores from the Labrador Sea (Knutz et al., 2011). Likewise, oxygen isotope records from the Greenland ice-cores demonstrate very rapid increases in air temperatures in Greenland between 14,700 and 11,500 cal. years BP (Fig. 1.4) (Björck et al., 1998). However, the variation of ice sheet retreat from the continental shelf edge of Southeast and Southwest Greenland suggests that deglaciation was not driven solely by warming air temperatures.

These discrepancies indicate that the break-up of the Greenland Ice Sheet after the LGM was a complex and spatially variable process driven by a variety of different factors including sea level change, air temperature increase, oceanic warming, shelf bathymetry, ice stream drainage area and sea-ice conditions (Funder et al., 2011).

1.2.3.2. Re-advances and still-stands

The Younger Dryas is recorded by a prominent temperature signal in the Greenland ice-core record (Fig. 1.4) (Steffensen et al., 2008). The Fiskebanke moraines on the inner shelf of Southwest Greenland have been interpreted as evidence for a re-advance during the Younger Dryas, when air temperatures returned temporarily to glacial values (Fig. 1.3) (Bennike et al., 2002; Rinterknecht et al., 2009). Cores from the Disko Fan, offshore of Egedesminde Trough, indicate that Jakobshavn Isbræ underwent a major fluctuation during the Younger Dryas. An increase in IRD input to the Disko Fan at around 12,200 cal. years BP indicates that the ice

stream re-advanced onto the outer shelf during this period (Ó Cofaigh et al., 2013b). The ice stream then retreated rapidly to the mid-shelf. This suggests that the ice stream may have been out of phase with Younger Dryas temperatures (Ó Cofaigh et al., 2013b). In contrast, the Greenland Ice Sheet to the south of Disko Bay is thought to have been characterised by an increase in mass balance during the Younger Dryas (Knutz et al., 2011). Low IRD concentrations in sediment cores from the Labrador Sea suggest that the seaward mobility of icebergs was constrained by dense sea-ice formed in a cold ocean climate (Reeh et al., 1999; Knutz et al., 2011).

The presence of three grounding-zone wedges on the floor of Uummannaq Trough suggests that ice stream retreat in this region was episodic and punctuated by a number of still-stands (Dowdeswell et al., 2008; Ó Cofaigh et al., 2008). In the cross-shelf troughs of Southern Greenland, however, grounding-zone wedges have yet to be identified. This implies that retreat of the Greenland Ice Sheet from the continental shelf of Southern Greenland after the LGM was rapid and not characterised by still-stands (Dowdeswell et al., 2008; Ó Cofaigh et al., 2008). This is consistent with studies from Kangerlussuaq Trough and southernmost Greenland which have not documented a response of the Greenland Ice Sheet to a change in temperature during the Younger Dryas (Jennings et al., 2006; Sparrenbom et al., 2006).

1.2.3.3. Holocene

Radiocarbon dating of marine shells in the Sisimiut region indicates that the Greenland Ice Sheet retreated to the present coast by around 10,900 – 10,200 cal. years BP (Figs. 1.3, 1.4) (Bennike and Björck, 2002, Long and Roberts, 2003; Bennike et al., 2011). The ice margin in Southeast Greenland is inferred to have reached the present coast at a fairly similar time (Jennings et al., 2002, 2006; Roberts et al., 2008). During the Holocene climate optimum, the ice sheet is thought to have retreated behind its present margin (Fig. 1.4) (Weidick et al., 1990). The ice sheet then advanced close to its present position during the Neoglacial period as indicated by increasing concentrations of IRD at about 5,000 cal. years BP (Andrews et al., 1997; Jennings et al., 2002).

1.3. Thesis structure

A general introduction to this thesis, describing its aims, the Greenland Ice Sheet and the present understanding of the extent, dynamics and deglacial retreat of the ice sheet was provided in this chapter. The three bathymetric data sets (Olex, IBCAO and multi-beam) used to investigate the geomorphology of the continental margins of Southern Greenland are described in Chapter 2. The morphology of individual features identified in the bathymetric data will then be described and interpreted where possible in Chapter 3. The spatial distribution of the individual landforms will then be described in order to make further and more conclusive interpretations in Chapter 4. Finally, the palaeo-glaciological implications of the geomorphology of Southern Greenland and a comparison between the nature of the Greenland Ice Sheet in Southwest and Southeast Greenland will be investigated in Chapter 5. A summary of results and an assessment of the Olex data as a source of bathymetric data for geomorphological studies are presented in Chapter 6.

2. Methodology

2.1. Introduction

2.1.1. Olex data

The main source of geophysical bathymetric data used to investigate the geomorphology of the continental margins of Southern Greenland is the Olex database. The database consists of voluntarily contributed data from users of shipborne echo-sounders. Commercial fishing vessels using single-beam echo-sounders are the main contributors of data but measurements from specialist research vessels are also incorporated into the database. The Norwegian company Olex AS (http://www.olex.no/index_e.html) continuously adds the new information collected by the contributors to a central database. Olex AS provides a custom software package to view the Olex database which is presented as a digital elevation model (DEM) projected with a modified Mercator projection, with parallel and equidistant latitude and longitude lines (Fig. 2.1).

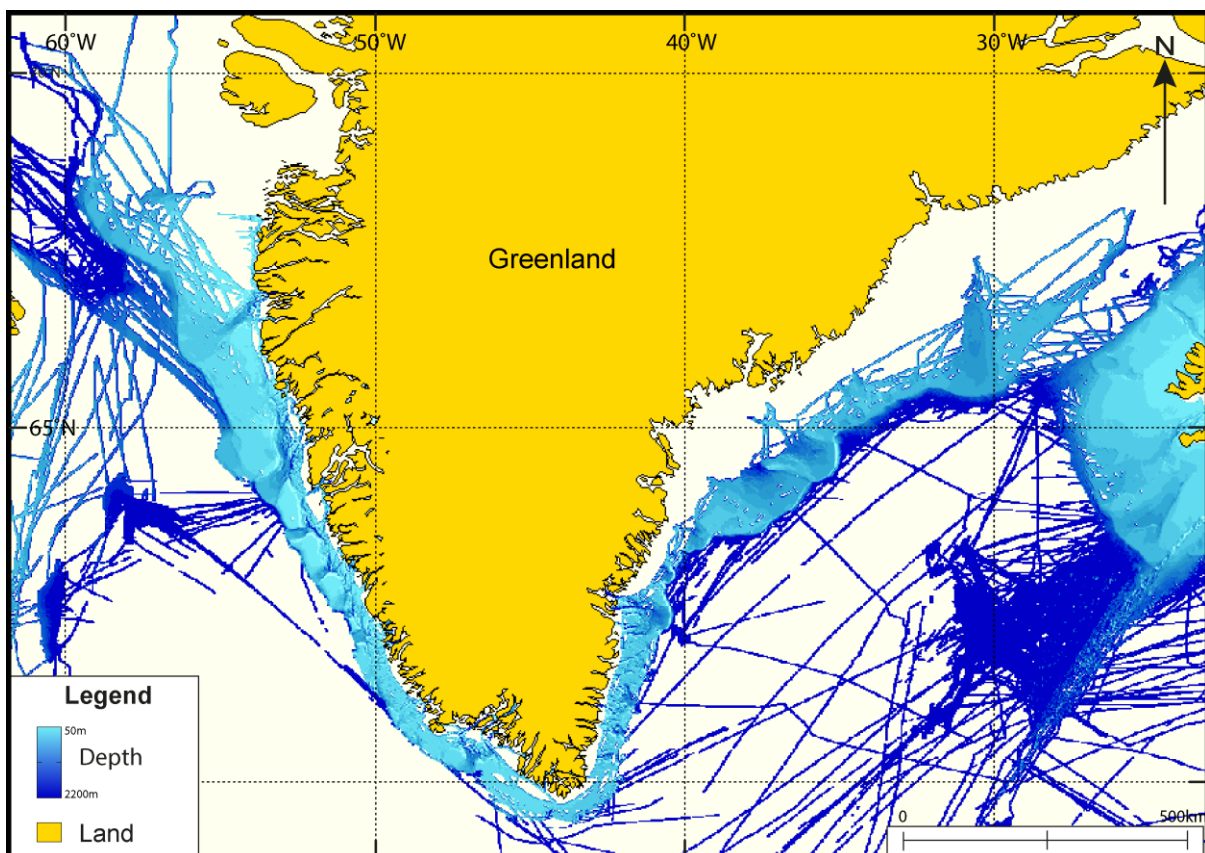


Figure 2.1. Example of the Olex DEM showing the bathymetric coverage of Olex data around Greenland. Lighter blues represent shallower water. Projected with a modified Mercator projection.

2.1.2. Multi-beam and IBCAO data

In addition to the Olex data, this thesis also utilises multi-beam bathymetric data collected onboard the British ice-strengthened research vessel, the RRS *James Clark Ross* (JCR) (Fig. 2.2), multi-beam data archived in the National Geophysical Data Centre (NGDC) (<http://www.ngdc.noaa.gov/mgg/bathymetry/multibeam.html>), and the International Bathymetric Chart of the Arctic Ocean (IBCAO) Version 3.0 (Fig. 2.2) (Jakobsson et al., 2012). The multi-beam data provide high resolution bathymetry for some areas of the sea floor and improve the data coverage over the continental shelf of Southern Greenland. The multi-beam data also allow a comparison with the Olex data. The IBCAO data provide comprehensive coverage of the Arctic Ocean at a resolution at a grid cell size of 500 x 500 m. These sources of data are discussed in Section 2.5.

2.2. Single-beam bathymetry

Acoustic methods are the principal means of mapping sea floor topography. Single-beam echo-sounders have been available since the 1920s and are used to measure the depth vertically below a ship. The echo-sounder records the time taken for a sound pulse ('ping'), usually at frequencies of tens of kHz, to travel from a transducer to an acoustic reflector, such as the sea floor, and back again (Lurton, 2002). For each transmitted ping, the user obtains a single point measurement of time delay, which is converted to water depth using the sound velocity of the water column (Section 2.2.1). Sequential depth profiles are compiled as the vessel advances and are combined to form a bathymetric map of the sea floor. Importantly, single-beam echo-sounder track-lines have to be close together in order to provide three-dimensional information (Section 2.7.1).

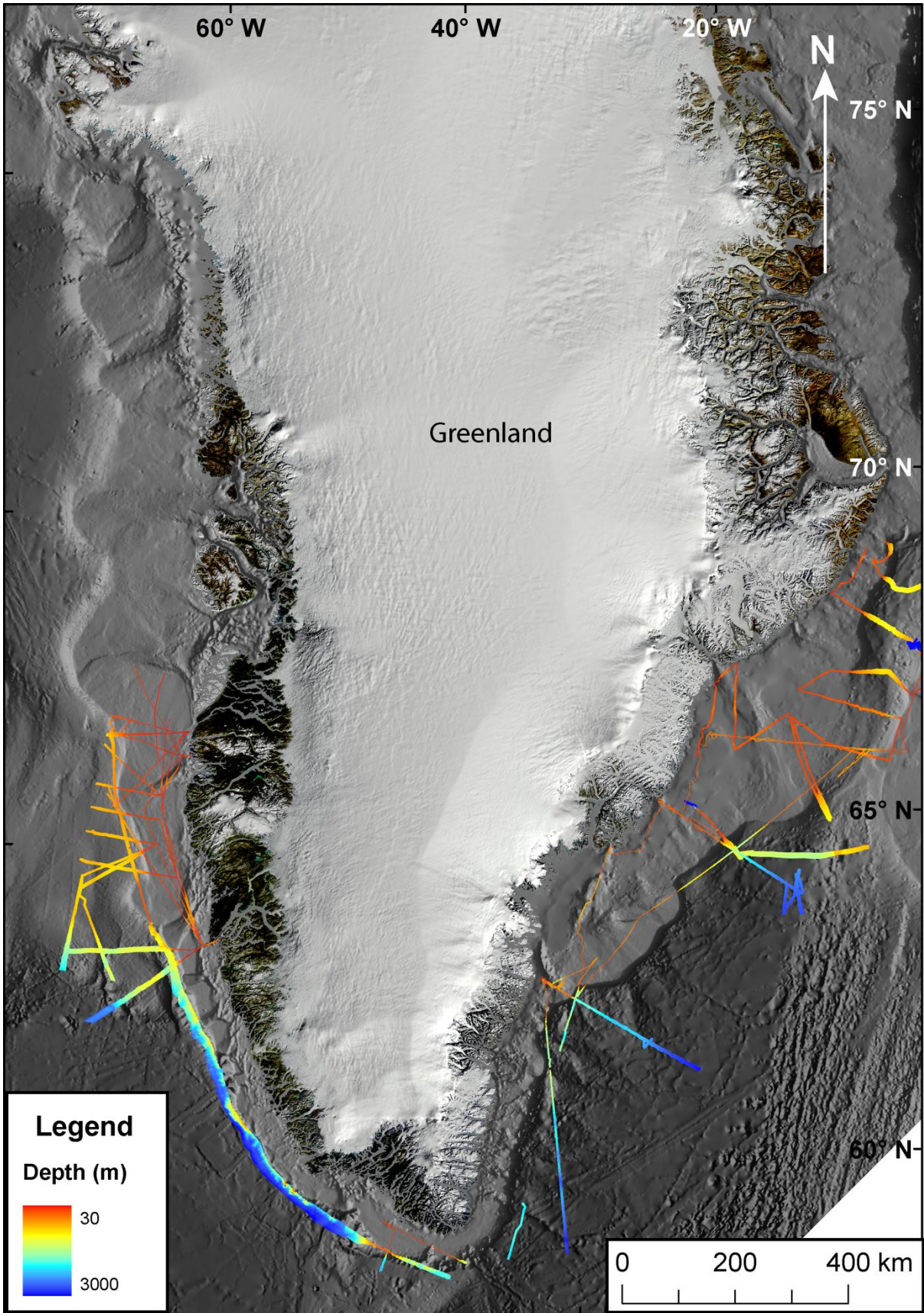


Figure 2.2. Map of bathymetric coverage of the multi-beam data used in this thesis. Multi-beam data are overlaid onto IBCAO data. Projected with a polar stereographic projection.

2.2.1. Signal transmission and reception

The sound pulse, or ping, of an echo-sounder is produced by energising a bank of piezoelectric transducers with a trigger signal from an inboard recorder (Fig. 2.3). The ping is transmitted below the ship and the echo from the sea floor is detected by the receiver. Therefore if the speed of sound through the water column is known, and the two-way travel time for the acoustic signal to reflect back from the sea floor to the transducer is measured accurately, then the water depth, 'z', can be calculated by:

$$z = \frac{1}{2} c \Delta t \quad (2.1)$$

where 'c' is the mean sound speed and 'Δt' is the difference in time between the transmission of the sound pulse and the reception of the reflected echo signal.

Water supports the propagation of acoustic pressure waves, or sound pulses, because it is an elastic medium. The speed of sound in water is about 1,484 m s⁻¹ but certain oceanic properties affect the spatial and temporal propagation of the sound pulse through the water column. The most important of these properties are temperature, *T* (Celsius (°C)), salinity, *S* (practical salinity unit (psu) which corresponds to parts per thousand (‰)), and hydrostatic pressure, *P*. Since *P* is nearly proportional to depth, *z* (metres (m)), depth usually replaces hydrostatic pressure. A failure to acknowledge these variables will result in errors when calculating water depth. Empirical equations have therefore been derived to calculate *c* more accurately using these oceanic variables. An example is Mackenzie's equation (Mackenzie, 1981) which has nine terms:

$$\begin{aligned} c = & 1448.96 + 4.591T - 5.304 \times 10^{-2}T^2 + 2.374 \times 10^{-4}T^3 \\ & + 1.34(S - 35) + 1.63 \times 10^{-2}z + 1.675 \times 10^{-7}z^2 \\ & - 1.025 \times 10^{-2}T(S - 35) - 7.139 \times 10^{-13}Tz^3 \end{aligned} \quad (2.2)$$

This equation has a domain of applicability of:

$$-2 < T < 30^\circ\text{C}$$

$$25 < S < 40 \text{ ‰}$$

$$0 < z < 8000 \text{ m}$$

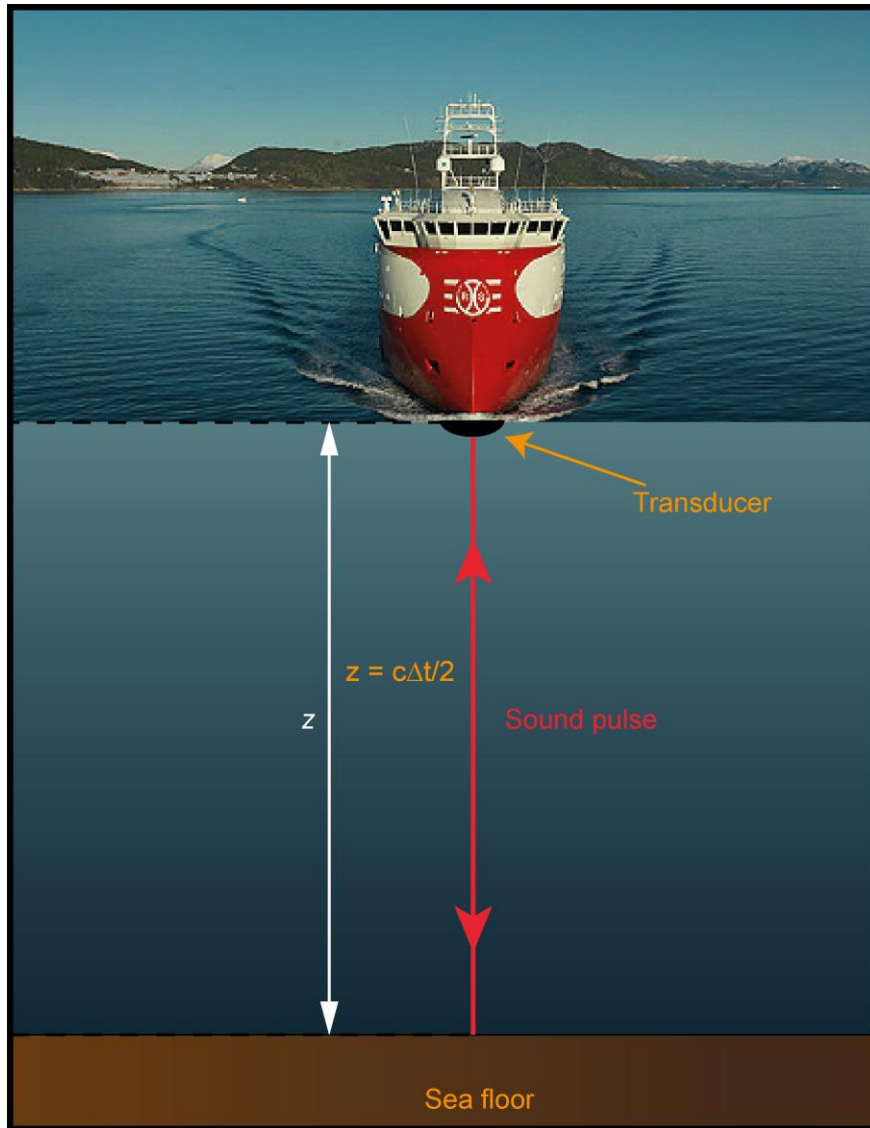


Figure 2.3. Diagram showing the basic principles of single-beam echo-sounding.

To measure the spatial and temporal sound speed variability, ships acquiring echo-sounding data often use expendable bathythermographs (XBT). XBTs measure T as a function of z using a known fall rate through the water column. c is then determined using an empirical relation (such as Equation 2.2) assuming constant S . Since temperature decreases with depth while pressure increases, the profile of sound speed with depth generally shows a characteristic curve which decreases to a minimum at a depth of several hundred metres and increases again with greater depth (Fig. 2.4)

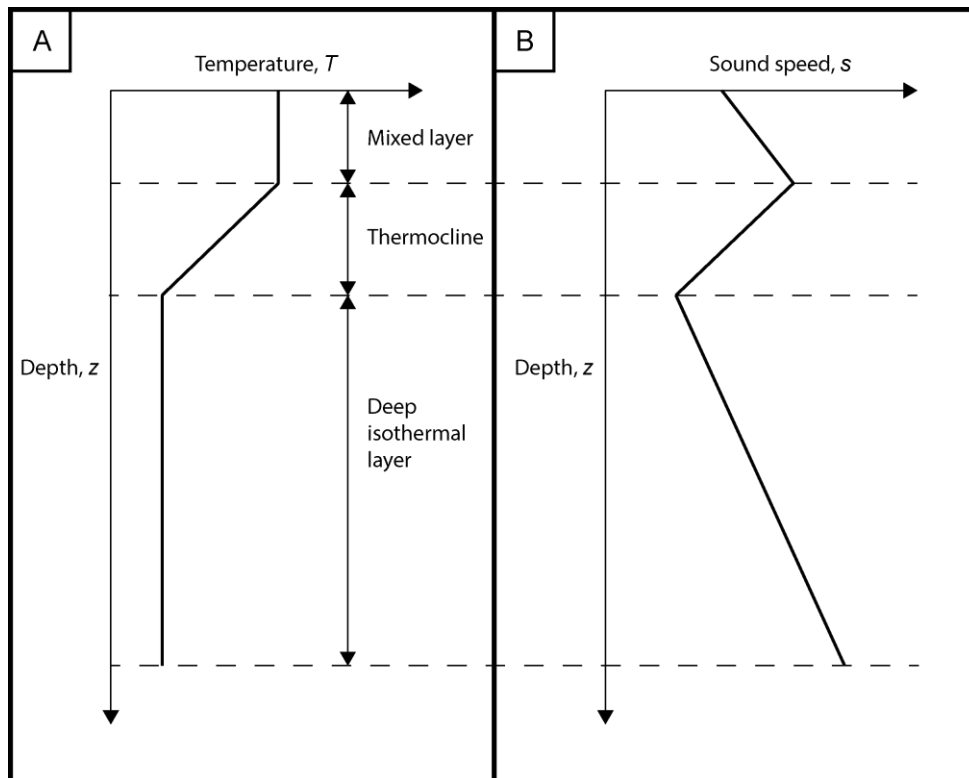


Figure 2.4. (A) Example of how temperature would be expected to vary with depth. (B) How the sound speed profile would respond to such changes (Adapted from <http://ocw.tudelft.nl/courses/geomatics/acoustic-remote-sensing-and-sea-floor-mapping/>).

For the receiver to locate an echo, measurements of depth using echo-sounders require a sharp leading edge to the transmitted and received sound pulse. The frequencies of single-beam echo-sounders depend on the application, and range between 10 kHz for deep water applications to 500 kHz for shallow water applications. The echo from a sediment interface is usually better observed at the lower frequencies. This is due to the decreasing sediment sound absorption with decreasing frequency. Therefore to produce the sharp pulses required in deep water, transducers will usually transmit in the 10 – 15 kHz range.

2.2.2. Navigation

Single-beam echo-sounders have to receive and process data from several ancillary systems in order to geographically locate the depth measurements accurately. This requires the echo-sounder to be connected to a ship-mounted Global Positioning System (GPS) which locates the soundings with respect to the surface of the Earth. Furthermore, the use of an attitude control unit allows for the correction of the ship's roll, pitch and yaw on the ocean surface.

Each single point measurement of time delay is then converted to water depth using the sound velocity of the water column and is time-stamped and referenced with the location at which it was collected. The georeferenced data are then stored digitally for later processing and analysis.

2.3. Multi-beam bathymetry

Multi-beam echo-sounder systems operate using the same theoretical principles as single-beam echo-sounders. While single-beam echo-sounders only return depth values along the track-line of a ship, multi-beam swath-bathymetric systems transmit and receive a fan of energy beams during each ping (Fig. 2.5). The fan of beams enables the possibility of a large number of simultaneous depth measurements (typically several hundred) along a swath of sea floor terrain.

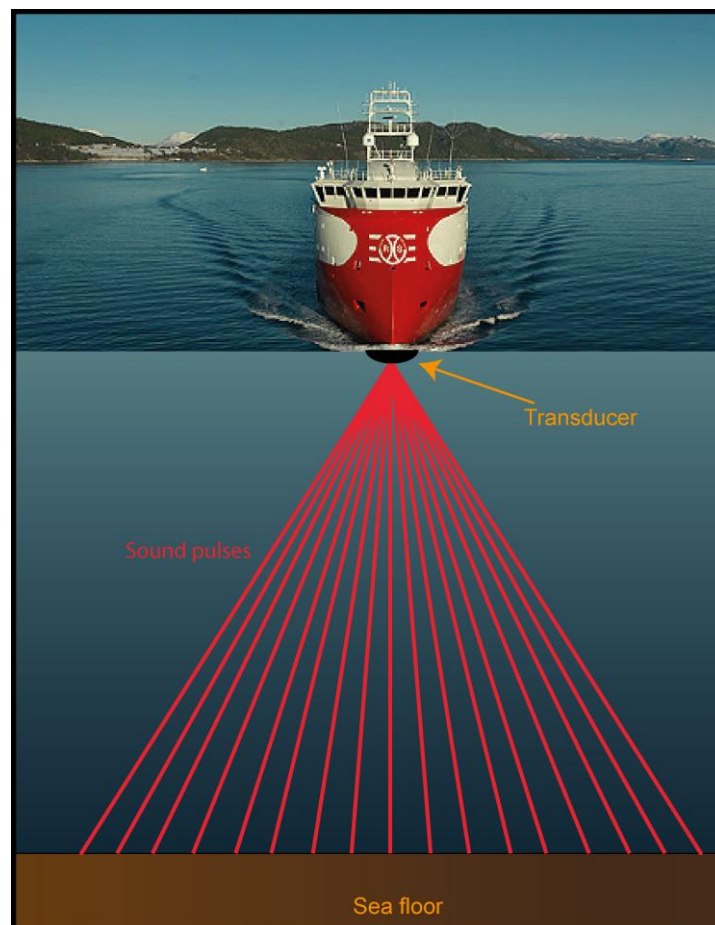


Figure 2.5. Example of a multi-beam swath-bathymetric system emitting a fan of beams that reflect off the seafloor. In shallower depths, the beams spread out less and width of surveyed sea floor is relatively narrow. At deeper depths the beams spread out more and the width of surveyed sea floor is wider.

Each ping of acoustic energy comprises of a number of beams orientated at known angles to the vertical in a plane perpendicular to the ship's motion (Fig. 2.5) (Lurton, 2002). The fundamental principle of bathymetric measurement is the joint estimation of time t and angle θ . Each pair (t, θ) is used to determine the position of one depth measurement. When the sound speed profile is constant over the entire water column, the acoustic paths from each beam are linear. The coordinates (y, z) of the measurement point, taking the sonar position as the origin (Fig. 2.6), are then:

$$y = \frac{ct}{2} \sin\theta \quad (2.3)$$

$$z = \frac{ct}{2} \cos\theta \quad (2.4)$$

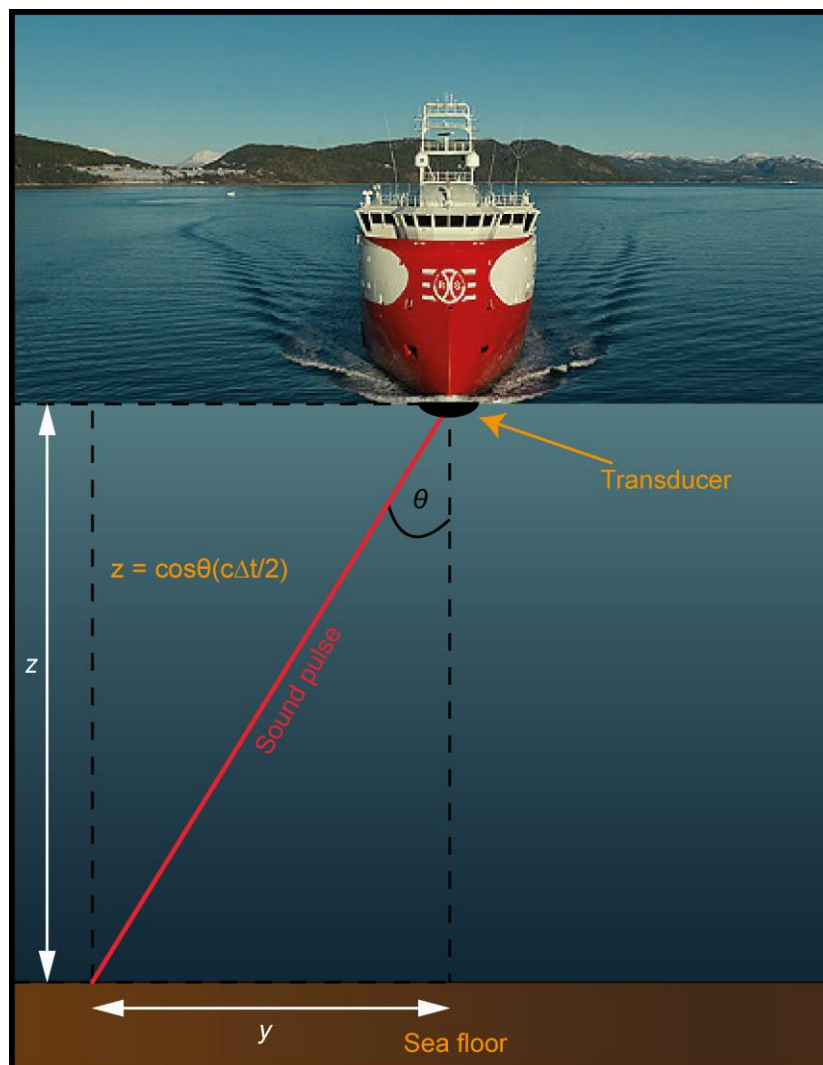


Figure 2.6. How a multi-beam echo-sounder calculates depth of the sea floor at a point on the sea floor using trigonometry.

2.4. Olex

The Olex database represents the Earth's surface as a grid consisting of an array of 5.6 x 5.6 m cells. Each cell contains a single depth value in metres (m) (Fig. 2.7).

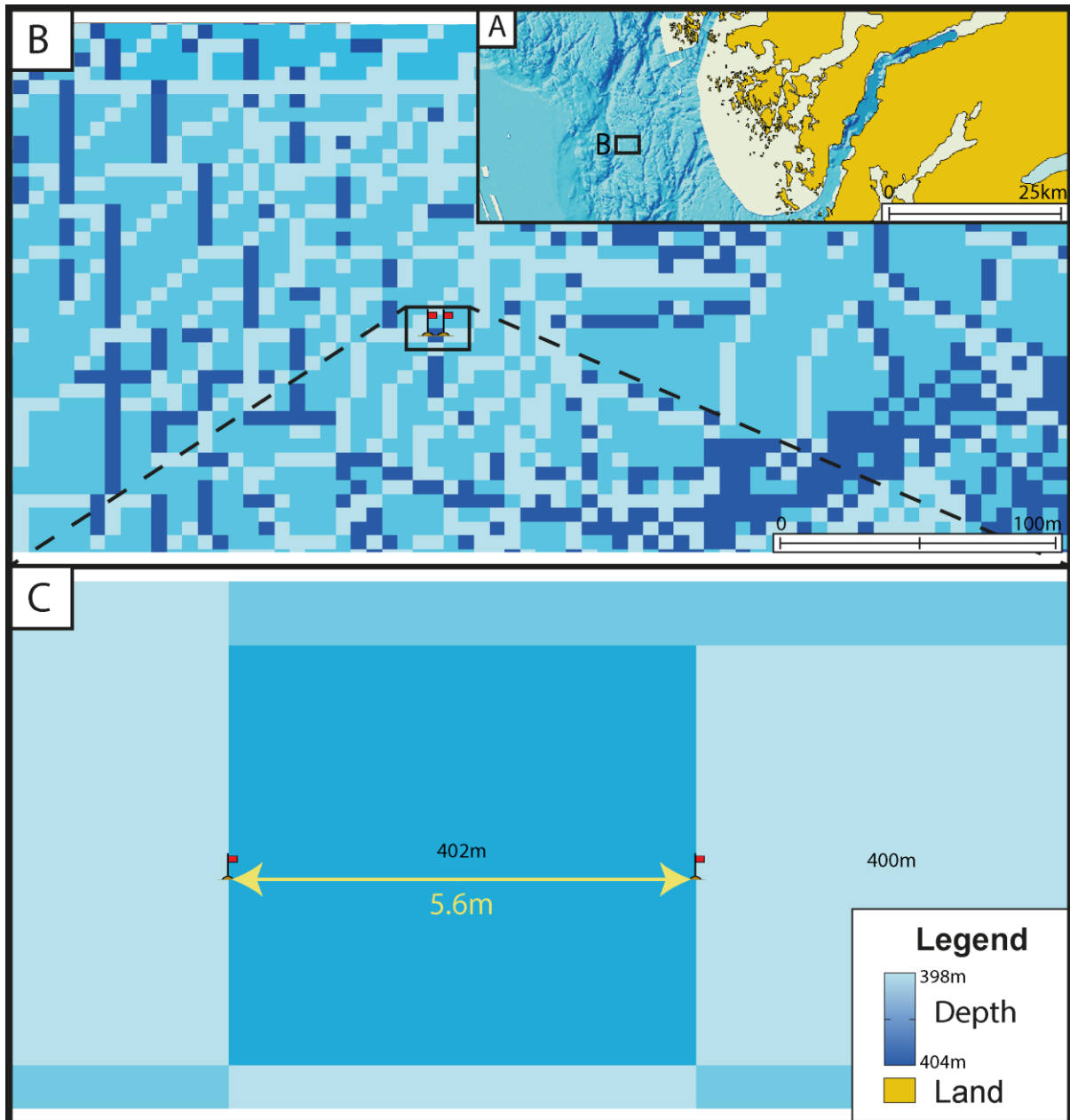


Figure 2.7. (A) Example of bathymetry displayed by the Olex database. (B) The Olex database represents the bathymetric data as a grid consisting of an array of cells. (C) These cells have a diameter of 5.6 m and contain a single depth value of 402 and 400 metres.

2.4.1. Interpolation

The Olex database consists of a grid of cells that have one of three states; measured, interpolated or unknown (Fig. 2.8A). A measured depth value is a cell which contains a point that has been measured directly by an echo-sounder (Fig. 2.8B). If more than one point has been measured in a 5.6 x 5.6 m cell, the mean of the measured depth values is calculated. The Olex software allows the user to visualise the location of the measured cells by changing their colour from blue to maroon.

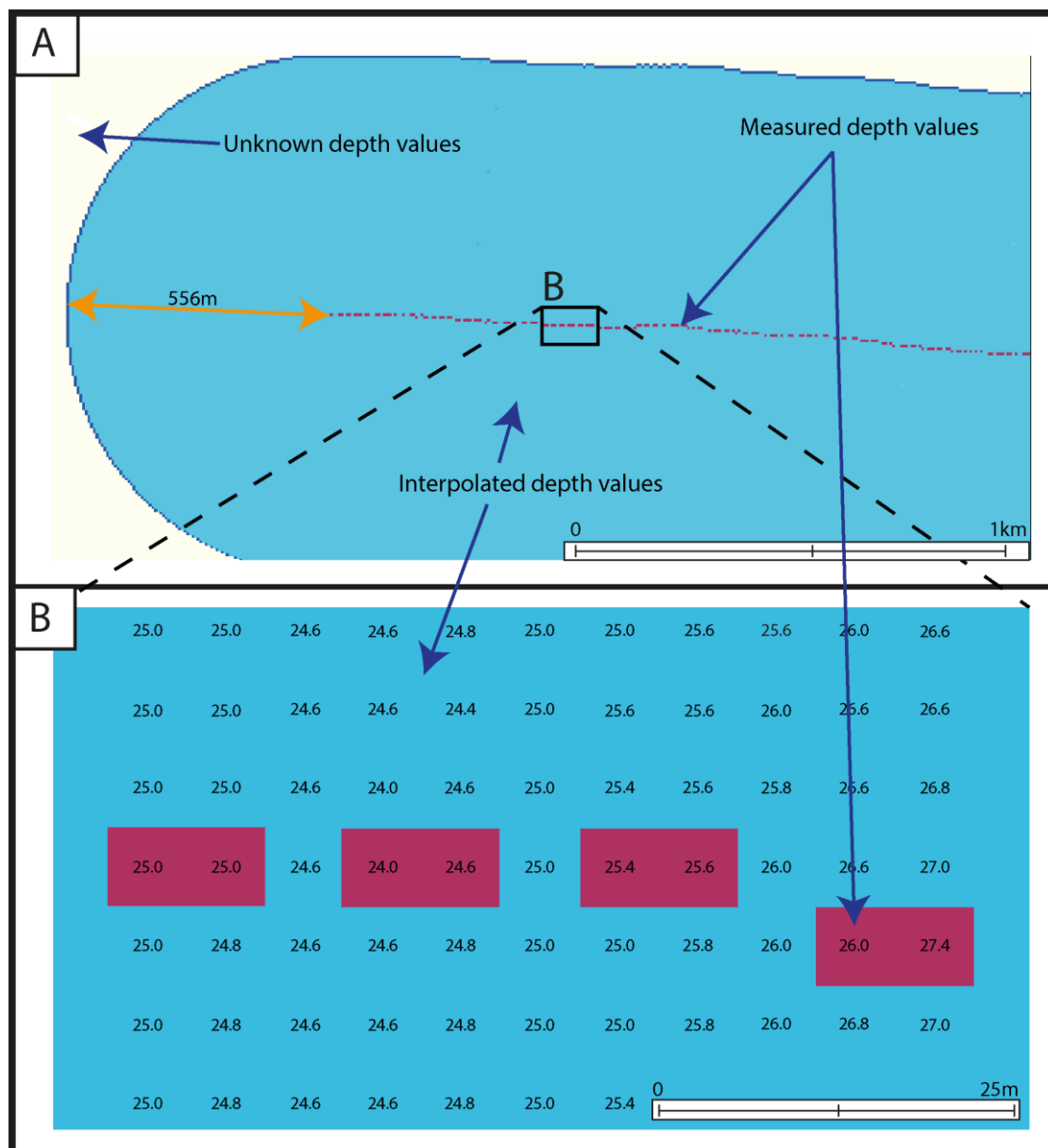


Figure 2.8. (A) Example of a single ship track-line in the Olex database and the location of the measured (maroon), interpolated (blue) and unknown cells (white). Depth values of cells within a 556 m radius from measured cells are interpolated. (B) Example measured (maroon) and interpolated (blue) cells. Each 5.6 x 5.6 m cell has a single depth value.

Interpolated depth values are cells at locations that lack measured depth values but are within a certain radius of a cell with a measured depth value. To derive these interpolated depth values, Olex uses a trend projection interpolation method. The specific details of this method are not disclosed by Olex but the basic approach is outlined in this thesis. Firstly, a region of cells around a cell containing a measured depth value is determined using a specified search radius. In Olex this radius is set to 556 m. A continuous mathematical function then fits a surface to this specified region of cells and the depth values of the unmeasured cells are calculated. In Olex, the mathematical function is a simple linear spline. Figure 2.9 shows how Olex calculates the depth value of an unmeasured cell using five cells with measured depth values.

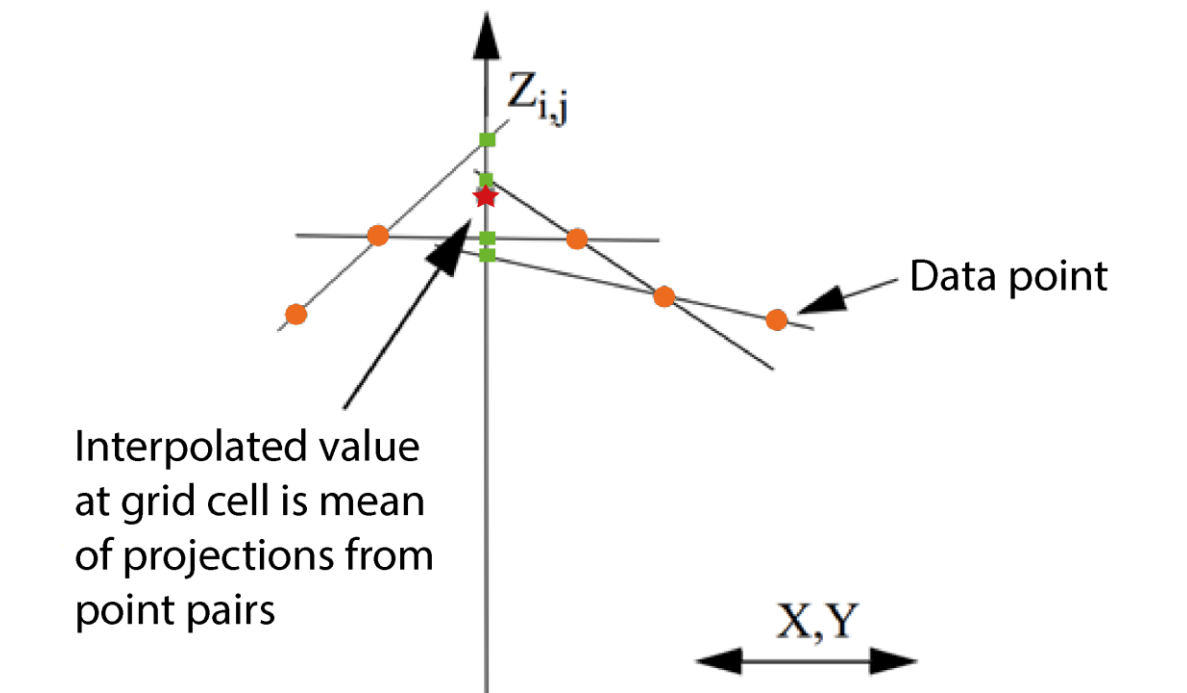


Figure 2.9. Trend projection interpolation using a linear spline estimate. $Z_{i,j}$ is the depth of the cell and x,y are the coordinates of the cell. Orange dots are measured depth values, green squares are the estimated depth values and the red star is the resulting interpolated depth value which is an average of these estimates. Adapted from Clarke (1995).

The search radius of the interpolation method (556 m) is quite large. This is perhaps so that the Olex database can present the bathymetric data as a continuous surface. This may be useful for navigational purposes but, for landform identification, the large area of interpolated depth values can mislead the user. For example, Figure 2.10 shows the bathymetry of two areas on the continental shelf of Southwest Greenland. The bathymetry of Figure 2.10A is characterised by some linear grooves and a meandering channel-like feature. Figure 2.10B is about 25 km inshore from Figure 2.10A and appears to have a relatively flat surface. When the ship track-lines are examined (Fig. 2.10C and Fig. 2.10D) it is clear that Figure 2.10A is much better surveyed than Figure 2.10B. The interpolation methods, however, have resulted in both areas appearing as continuous bathymetric surfaces. Whilst channels and grooves can be identified in Figure 2.10A, they cannot be identified in Figure 2.10B. It is therefore not clear whether channels and grooves do not exist in Figure 2.10B or whether they do exist, but the scarcity of measured depth values prevents the landforms from being identified.

Cells outside the defined radius of a measured cell are given unknown depth values. These cells represent the white areas in the Olex database (Fig. 2.8).

2.4.2. Precision

The precision of the depth values depends on the depth of the cell. At depths that are shallower than 100 m, the precision of the depth value is to the nearest decimetre or one decimal place (Fig. 2.11A). At depths deeper than 100 m, the precision of the depth value is to the nearest metre (Fig. 2.11B).

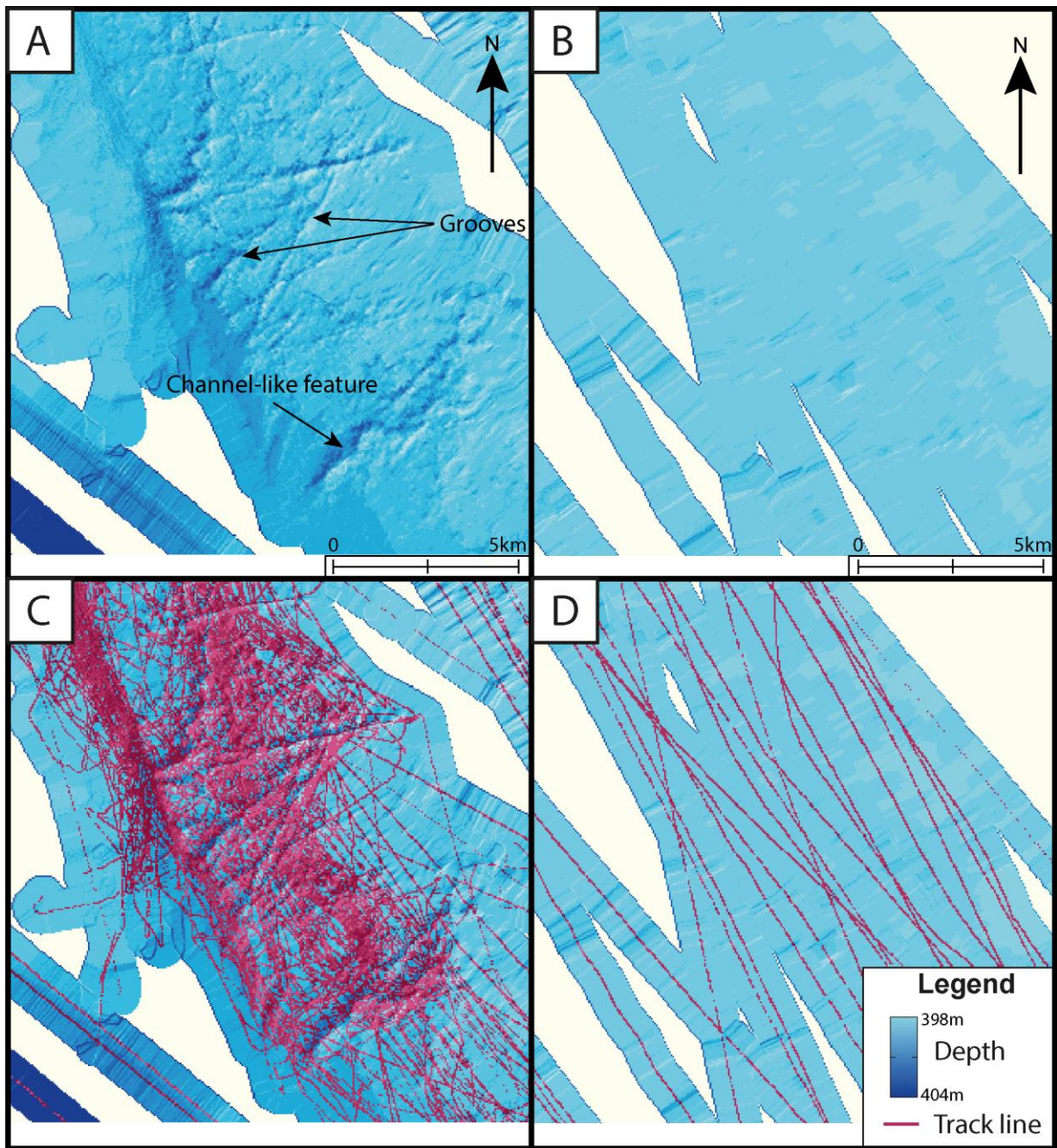


Figure 2.10. (A) Bathymetry of an area covered by Olex data showing grooves and channel-like features. (B) Bathymetry of a 25 km distant area covered by Olex data with no visible features. (C) The bathymetry of (A) is densely covered with ship track lines. (D) The bathymetry of (B) is sparsely covered with ship track lines.

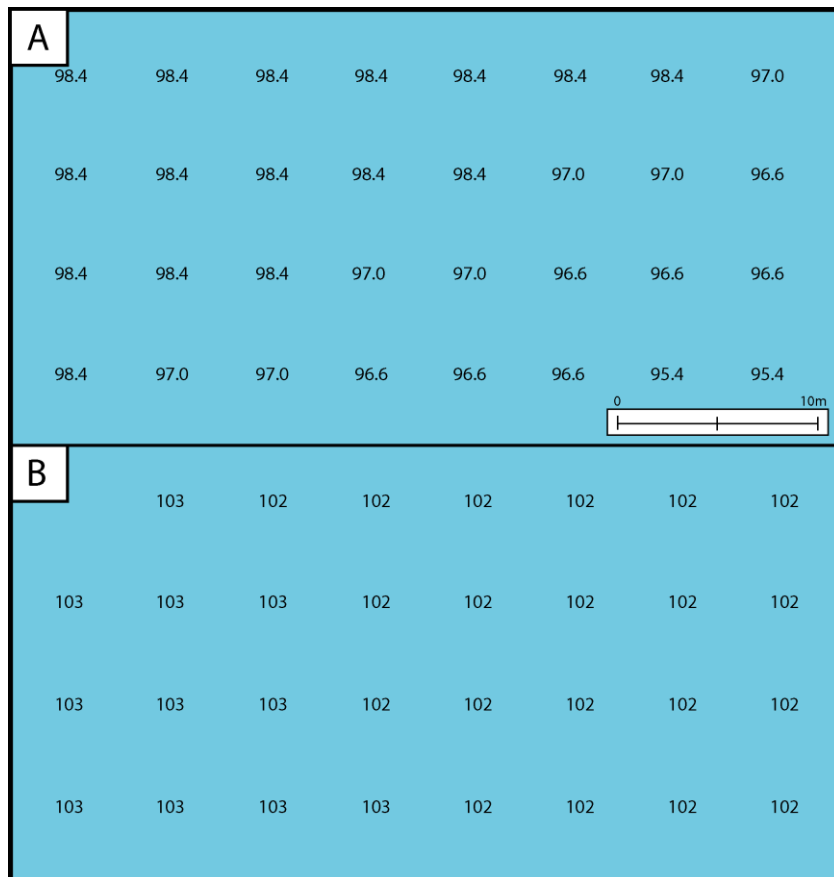


Figure 2.11. Examples of depth values that represent the bathymetry of the Olex database. (A) Depth values have a precision to the nearest decimetre when the depth value measured or interpolated is shallower than 100 m. (B) Depth values have a precision to the nearest metre when the depth value measured or interpolated is deeper than 100 m.

2.4.3. Accuracy

The data acquired by Olex are not associated with regular temperature and salinity profiles because they are collected mainly by commercial fishing vessels that do not need highly accurate depth measurements. Therefore, when the Olex database is compiled, a nominal average sound speed of a ping travelling vertically through the seawater is applied in the conversion between the two-way echo travel-time to depth. The sound speed chosen is usually between 1460 and 1480 m s⁻¹ (Jakobsson et al. (2012) pers. comm. O. B. Hestvik, Olex, 2011). This means that the absolute accuracy of the measured depth values is potentially variable. Error in measured depth values is exaggerated with greater depth.

The assumption that the sound speed is between 1460 and 1480 m s⁻¹ might be especially inaccurate in the North Atlantic offshore of Southern Greenland where seasonal variations in temperature of the water column can cause temporal changes in the sound speed profile (Bulgakov and Lomakin, 1994). The different properties of large water masses (e.g. the East Greenland Current and the Irminger Current) mean that the speed of sound could vary spatially as well (Bulgakov and Lomakin, 1994).

Olex AS claim that any errors in depth values are minimised during database compilation and processing by comparing an individual contributor (a ship) with the large number of other soundings covering the same area. However, there are still noticeable artefacts in the database. For example, Figure 2.12 shows an area of the continental slope of Southeast Greenland. The bathymetry has a number of 'stripes'. These 'stripes' are depth values that are shallower than other measured depth values in the vicinity. This could have been caused by assuming the speed of sound through the water column was between 1460 and 1480 m s⁻¹ when it might, in reality, have been lower. The linear spline interpolation between the measured depth values fits a surface through the erroneous depth values, causing the 'stripes' to appear on the bathymetry. This example demonstrates that errors in depth values are not always corrected for by Olex. Therefore, linear features in the bathymetry may not always be real and Olex data have to be interpreted with care.

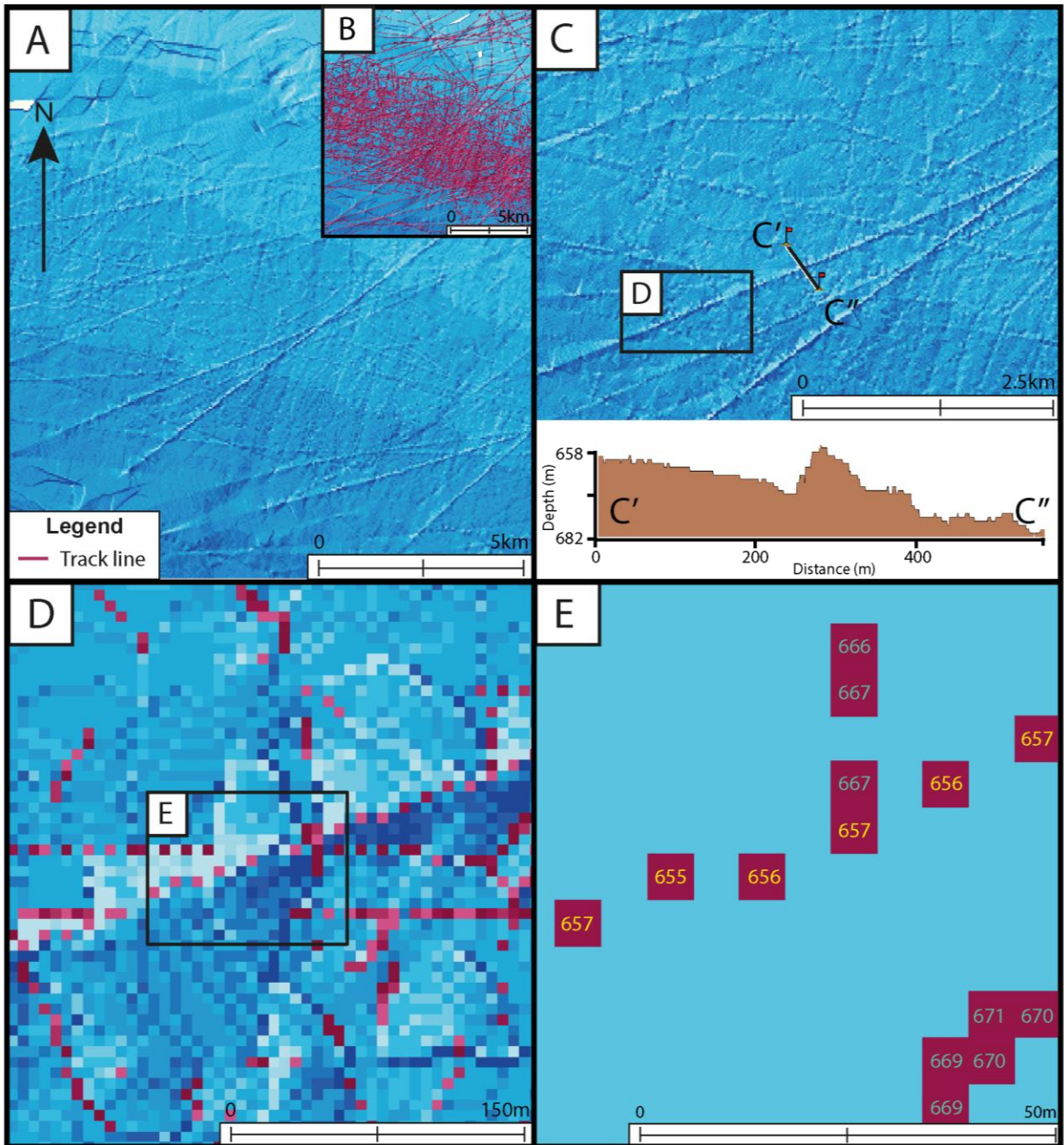


Figure 2.12. (A) The Olex database has a number of ‘stripes’ in the bathymetry. (B) This area is densely surveyed by ship track-lines. (C) The cross-sectional profile C’ – C’’ shows that these stripes are raised from the surrounding bathymetry. (D) This image reveals that the stripe is caused by one ship track-line. (E) The measured depth values of this track-line (yellow) are shallower than the depth values recorded by other ships’ track-lines (blue). This could be due to a poor approximation of sound speed through the water column.

To further investigate the absolute accuracy of the Olex data, some multi-beam data collected by the RRS *James Clark Ross* were imported into the Olex database. The multi-beam data were added as YXZ points so that they could be gridded in the same way as the voluntarily contributed data that the Olex database receives. Individual depths from the Olex data were then paired with depths from the multi-beam data for comparison (e.g. Fig. 2.13). The criterion used to form a pair of depth values was that the two must be located in adjacent 5.6 x 5.6 m cells.

There is general agreement between both sources of data but, in some places, there are slight differences. In depths of 300 to 500 m there was an average difference of 4.5 m between Olex depths and multi-beam depths. The Olex depths were both deeper and shallower than multi-beam depths. Jakobsson et al., (2012) applied a similar method to investigate the accuracy of the Olex data. They sampled 1999 depth values and found that the Olex depth values were on average 4.9 m deeper than the multi-beam data at a mean depth of 640 m.

This thesis also sampled much deeper depths of over a thousand metres. This further analysis revealed that the difference between Olex and multi-beam depths increased. In some places there was a difference of up to 27 m. The increase in error as depth increases indicates that the error could be due to a poor approximation of sound speed through the water column when collecting the echo-sounding data or due to systematic errors in the individual single-beam echo-sounder that was used to collect the data.

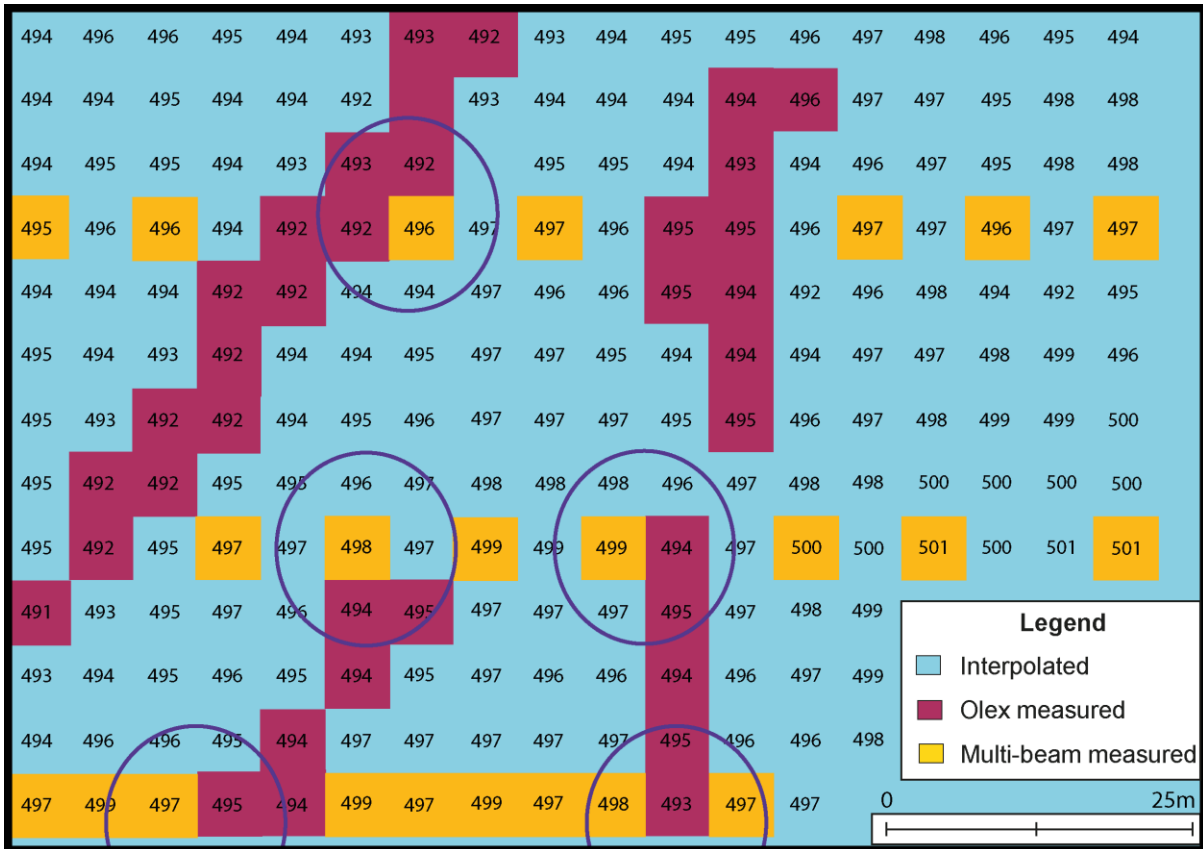


Figure 2.13. Depth values of cell colours explained by legend. Example of how the Olex depths and multi-beam depths were compared. The multi-beam data were imported into the Olex software and, where measured Olex and multi-beam grid cells were next to each other, the depths were compared. There is an average difference of about 4 m between the Olex and the multi-beam depth values in this image.

2.5. Other data

In addition to the Olex data, multi-beam data collected by research ships and IBCAO data were also incorporated into the investigation (Fig. 2.5).

2.5.1. Multi-beam data collected onboard the RSS *James Clark Ross* (JCR)

The first type of research cruise data was collected by JCR on cruises 106b in 2004 and 175 in 2009 (Table 2.1). A hull-mounted Kongsberg-Simrad EM120 multi-beam swath-bathymetric system was operated on both cruises. This system emits 191 acoustic beams during every swath ping and operates at a frequency of 12 kHz and a maximum port and starboard beam angle of 70°. The beam angle chosen during the cruises varied according to

sea conditions, water depth and seabed type but was generally between 60° - 68°. The speed of sound through the water column was measured regularly using XBT instruments. The sound velocity profiles (SVP) obtained from the XBT deployments were input to the EM120 system and used in the relevant surveys. The calculated SVPs generated by the XBT system software were transferred to the multi-beam data processing workstation and the data then imported into the multi-beam data acquisition system. An Ashtech ADU5 Differential Global Positioning System was used to record the attitude and geographical position of the ship every second. The raw data were digitally archived and transported to the Scott Polar Research Institute, University of Cambridge on DVD, where the files were transferred to a Linux machine for processing.

2.5.2. Multi-beam data archived in the NGDC

The NGDC is the US national archive for multi-beam bathymetric data and it presently holds over 15.7 million nautical miles of ship track-lines received from sources worldwide. Table 2.1 lists the datasets that were used in this thesis. These data were collected with a variety of multi-beam swath-bathymetric systems on different ships (Fig. 2.2, Table 2.1).

| Source | Ship | Cruise name | Instrument used | Date collected |
|--------|-------------------------|-------------|------------------------|----------------|
| SPRI | <i>James Clark Ross</i> | JR106b | Kongsberg-Simrad EM120 | 2004 |
| SPRI | <i>James Clark Ross</i> | JR175 | Kongsberg-Simrad EM120 | 2009 |
| NGDC | <i>Maurice Ewing</i> | EW9607 | Atlas Hydrosweep DS | 1996 |
| NGDC | <i>Healy</i> | HLY0004 | SeaBeam 2112 | 2000 |
| NGDC | <i>Knorr</i> | KN179L05 | SeaBeam 2100 | 2004 |
| NGDC | <i>Knorr</i> | KN194-02 | SeaBeam3012-P1 | 2008 |
| NGDC | <i>Knorr</i> | KN194-04 | SeaBeam3012-P1 | 2008 |
| NGDC | <i>Knorr</i> | KN199-02 | SeaBeam3012-P1 | 2010 |
| NGDC | <i>Knorr</i> | KN203-04 | SeaBeam3012-P1 | 2011 |

Table 2.1. List of the data used alongside the Olex data in this thesis. NGDC is the National Geophysical Data Centre.

2.5.3. IBCAO data

The IBCAO Version 3.0 is a digital bathymetric model which was released in 2012 and is the most up-to-date bathymetric portrayal of the Arctic Ocean sea floor (Figs. 1.2, 2.2, 3.1). The incorporation of recently acquired multi-beam data and the Olex database have allowed the sea floor to be gridded at a cell size of 500 x 500 m (Jakobsson et al., 2012).

2.6. Processing of multi-beam data

Processing of the raw multi-beam data was completed on a Linux platform and performed using the open-source, Unix-based software, MB-SystemTM (Caress et al., 1996). Data processing aimed to eliminate erroneous data points that were recorded by the acoustic beams. Erroneous data points were removed through a combination of automatic and manual editing. Automatic filters (the ‘mbclean’ tool in MB-System) flagged erroneous data points, very steep slopes, and outer pings using a variety of different algorithms. Manual editing (the ‘mbedit’ tool in MB-System) then followed to check the effectiveness of the automated filters and to edit erroneous data segments left unflagged by the automated filters.

The MB-System ‘mbgrid’ tool was then used to grid the processed bathymetry data at regular intervals. The multi-beam data from the Greenland margin were gridded with cell sizes between 30 and 100 m depending on the density of bathymetric data points, which is a function of depth. The grid files produced were then exported as ascii files and imported into ArcGIS where they were viewed and analysed.

2.7. Comparison of datasets

2.7.1. Effective resolution

The effective resolution of the Olex data is determined by the density of cells with measured depth values in a specified area. The density of cells with measured depth values is determined by echo-sounder output rates and the number of ship track-lines in a specified area.

In shallow areas, the time taken for the ping to be reflected by the sea floor and received is relatively rapid (0.134 seconds in 100 m of water with an average sound speed of 1500 m s⁻¹). Therefore the next ping can be produced quickly and the spacing between the measured depth values is small (Fig. 2.8). In deeper waters, pings take longer to travel twice through

the water column (1 second in 750 metres of water with an average sound speed of 1500 m s⁻¹) and, therefore, gaps between measured depth values in deeper water are larger.

More importantly for determining the effective resolution, is the density of ship track-lines, which is highly variable in the Olex database. This is because the majority of Olex users are fishermen and there is a strong bias in the data coverage towards good fishing areas on the continental shelf of Greenland. For example, in Southwest Greenland the troughs on the continental shelf are densely covered by track-lines (Fig. 2.14). This reflects the areas where commercial fishing vessels operate regularly. The effective resolution in the troughs is, therefore, relatively high and landforms such as grooves and channels can be identified easily (Fig. 2.10). In contrast, the banks on the continental shelf, the continental slope and the deep abyssal plain of Southwest Greenland are not densely covered with ship track-lines (Fig. 2.14). The effective resolution in these areas, therefore, is poor and landforms are more difficult to identify (Fig. 2.10).

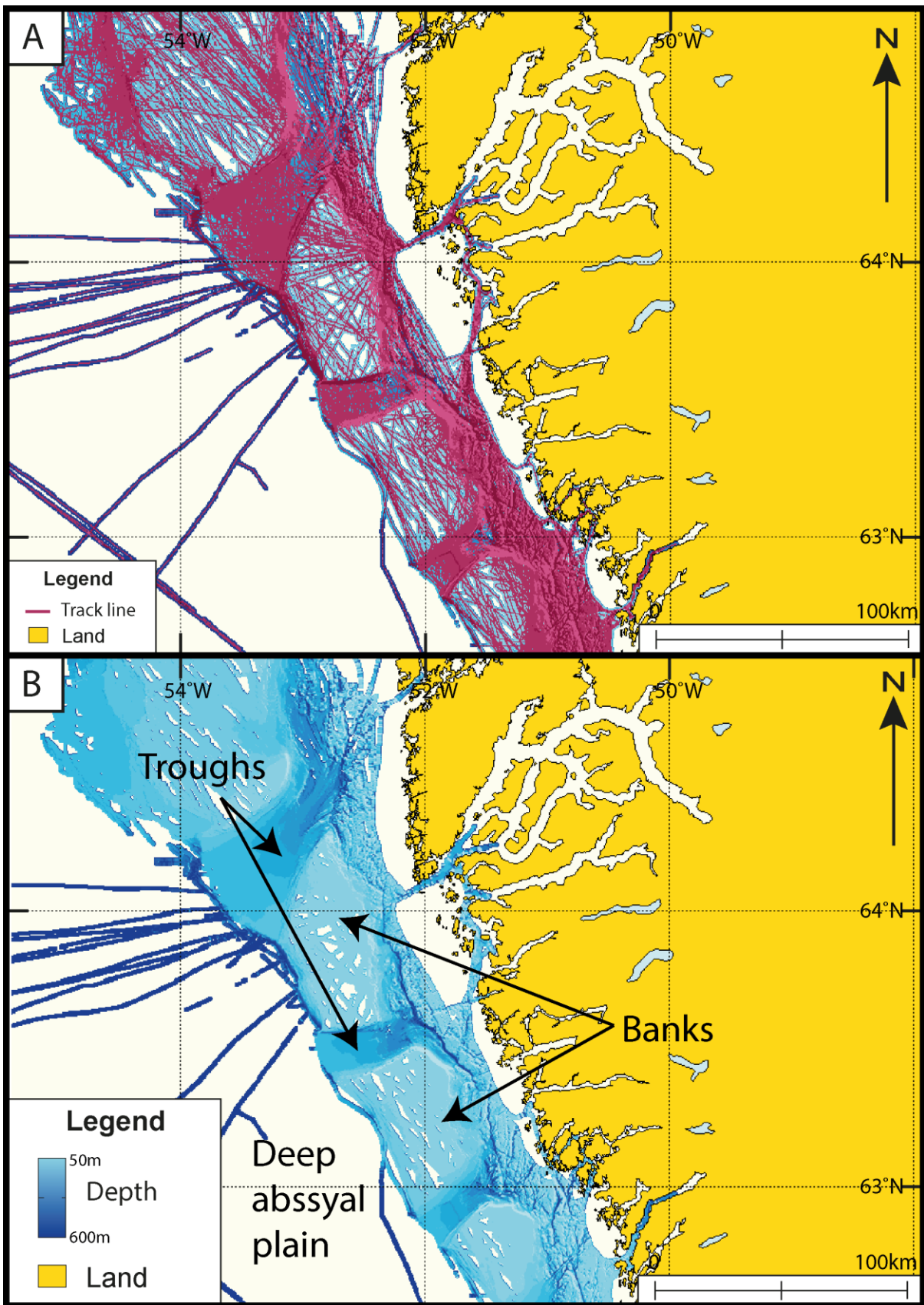


Figure 2.14. (A) Ship track-line coverage of Southwest Greenland. (B) Bathymetry produced by these track-lines. The shallow banks are not as densely covered as the troughs. Therefore the banks have poorer effective resolution than the troughs and fewer features are identified.

The number of track-lines also improves the reliability of the data since this increases the probability that a cell is measured more than once. When a cell is measured multiple times, an average depth value is taken and this value is more reliable through repeat measurement of cells.

To further investigate the effective resolution of Olex data in comparison with the multi-beam data collected by research vessels, the multi-beam data were imported into the Olex database (Fig. 2.15). For comparison with the original Olex data, a cell size of 5.6 x 5.6 m and an interpolation radius of 556 m around the measured cells were chosen when importing the data. The identification of iceberg ploughmarks on the continental shelf of Southern Greenland was then considered. The track-line density of the Olex data on the outer continental shelf of Southeast Greenland is very high. Therefore, it is in these places where the Olex data might be comparable to the multi-beam data that were collected onboard research vessels.

Figure 2.15A shows a multi-beam track-line in the Olex database. Ploughmarks are clearly identifiable in the bathymetry. In the same location, ploughmarks cannot be identified in the Olex data (Fig. 2.15C) even though the ship track-lines in Figure 2.15D are relatively closely spaced (2.3 track-lines per km²). In a nearby location, ploughmarks can be identified in the Olex data (Fig. 2.15E). Figure 2.15F is more magnified than Fig. 2.15D and has a much higher density of track-lines (12 track-lines per km²). These ploughmarks are around 50 m wide and so the effective resolution of the Olex data, where track-line density is 12 per km², is about 50 m. However, track-line densities of this magnitude are rare on the continental shelf of Southern Greenland and as the density of track-lines decrease, so will the effective resolution. Therefore, although the Olex data is gridded at 5.6 x 5.6 m, the effective resolution is about 50 m at best and is usually much worse in areas less densely covered with track-lines.

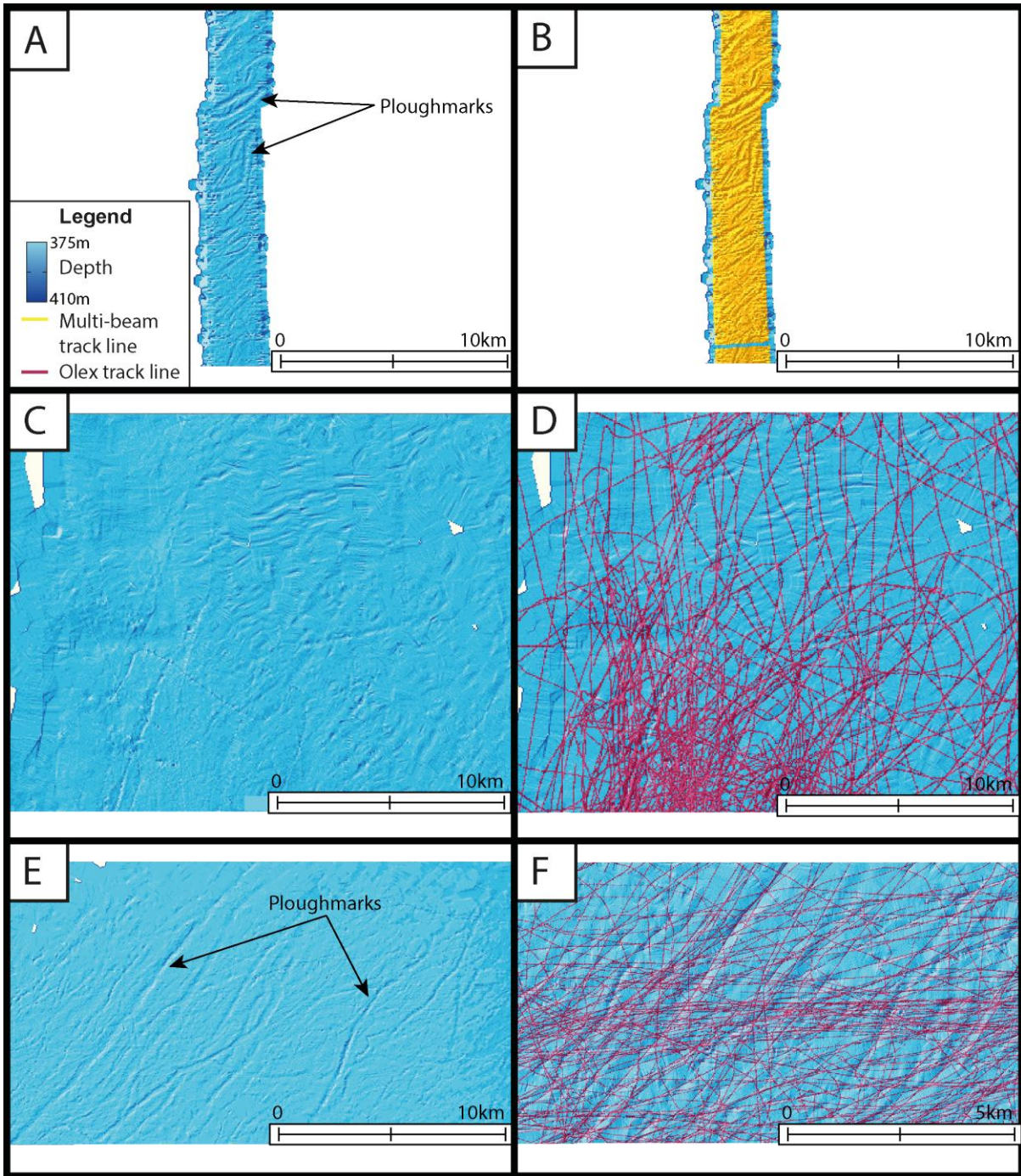


Figure 2.15. (A) Bathymetry measured using a multi-beam echo-sounder. Ploughmarks are easily identifiable in the bathymetry. (B) The multi-beam data points are so closely spaced that, at this scale, they cannot be distinguished. (C) The Olex bathymetry in the same location. No ploughmarks can be identified. (D) The track line density of Olex data. The track line density is 2.3 per km^2 . (E) The Olex bathymetry in a nearby location. Ploughmarks can be identified. (F) The track line density 12 per km^2 .

2.7.2. Coverage

The coverage of the Olex data is very high in comparison to the multi-beam data used in this thesis (Fig. 2.1). The Olex data cover most of the inner and outer continental shelves of Southwest Greenland and most of the outer continental shelf and continental slopes of Southeast Greenland (Fig. 2.1). In comparison, the coverage of the multi-beam data collected offshore of Southern Greenland is relatively limited (Fig. 2.2).

The strength of the Olex system lies in the integration of data contributed by a number of users over several years. Through time, the Olex data will improve as more depth values are recorded by commercial fishing vessels. The quality of data will also improve as cells are measured multiple times so that reliable depth values are obtained.

2.8. Data interpretation

Unfortunately, for commercial reasons, the Olex data cannot be exported into other geophysical data processing systems. Landform identification was therefore carried out using the Olex software package. A number of features provided by the Olex software, however, assisted in the identification of landforms. The Olex DEM can be viewed as a 2D shaded relief map and the software allows this bathymetric surface to be illuminated by an idealized light source either from the northeast (azimuth of 45°) or the northwest (azimuth of 315°). When identifying landforms this introduces azimuth-bias (the azimuth of the illumination is the angle formed between north and the direction of the light source). Changing the direction of the illumination can alter the apparent position of the break-in-slope so that features may change shape, appear or disappear (Fig. 2.16) (Smith and Clark, 2005).

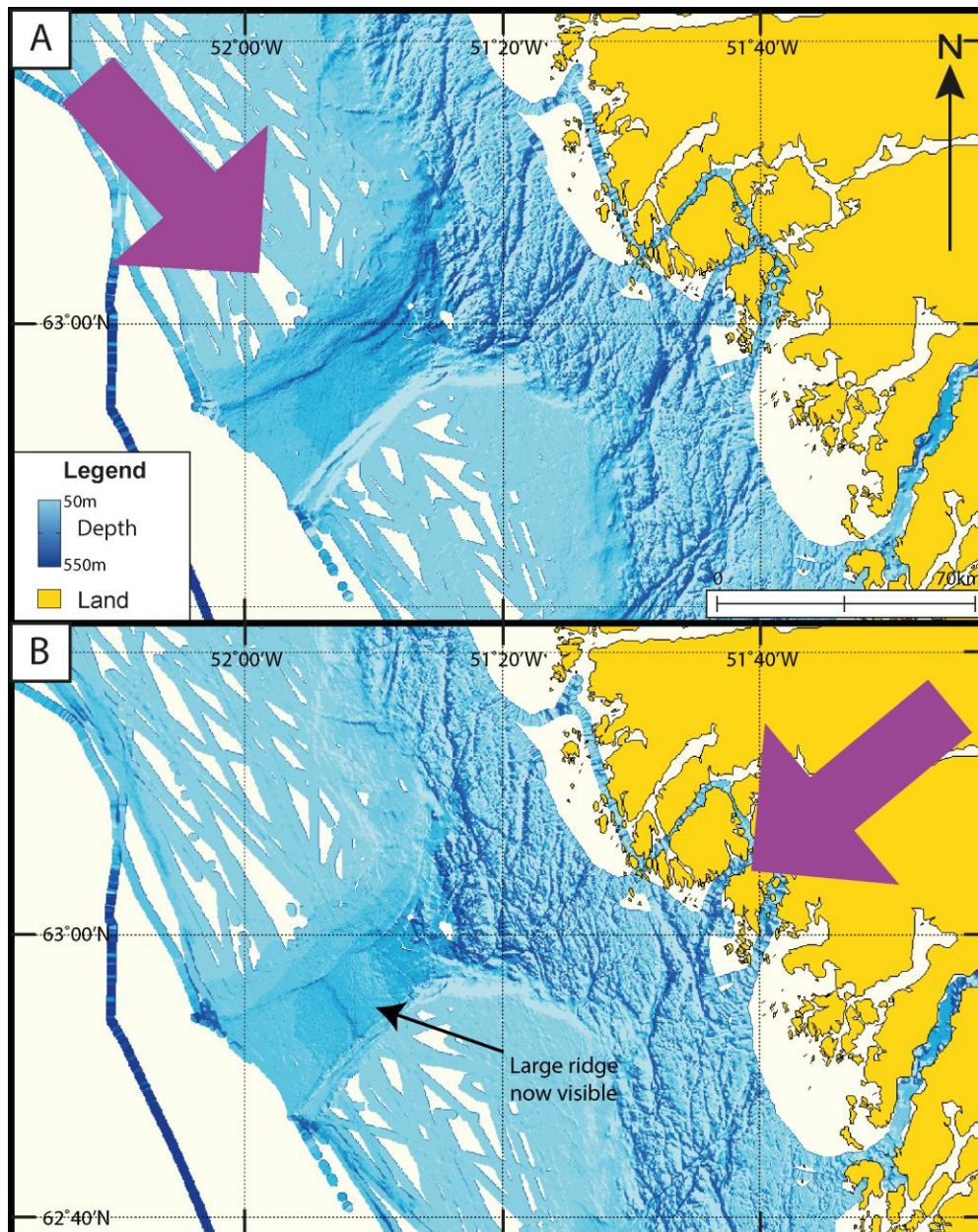


Figure 2.16. (A) Olex bathymetry viewed with an azimuth of 315° (from NW). (B) Same as (A) but viewed with an azimuth 45° (from NE). Channels are not as obvious but a large subdued feature appears. Arrows indicate direction of light source.

To overcome azimuth-bias, the DEM was illuminated first from the northeast and then from the northwest when identifying landforms. This technique enabled the impartial and accurate identification of submarine landforms. The Olex software package also provides tools for 3D visualization, measuring distances and drawing bathymetric profiles. These tools were also useful for identifying and describing features. Landform dimensions, such as length, height and width, were measured digitally within the Olex software package.

3. Geomorphology of the continental shelves of Southeast and Southwest Greenland

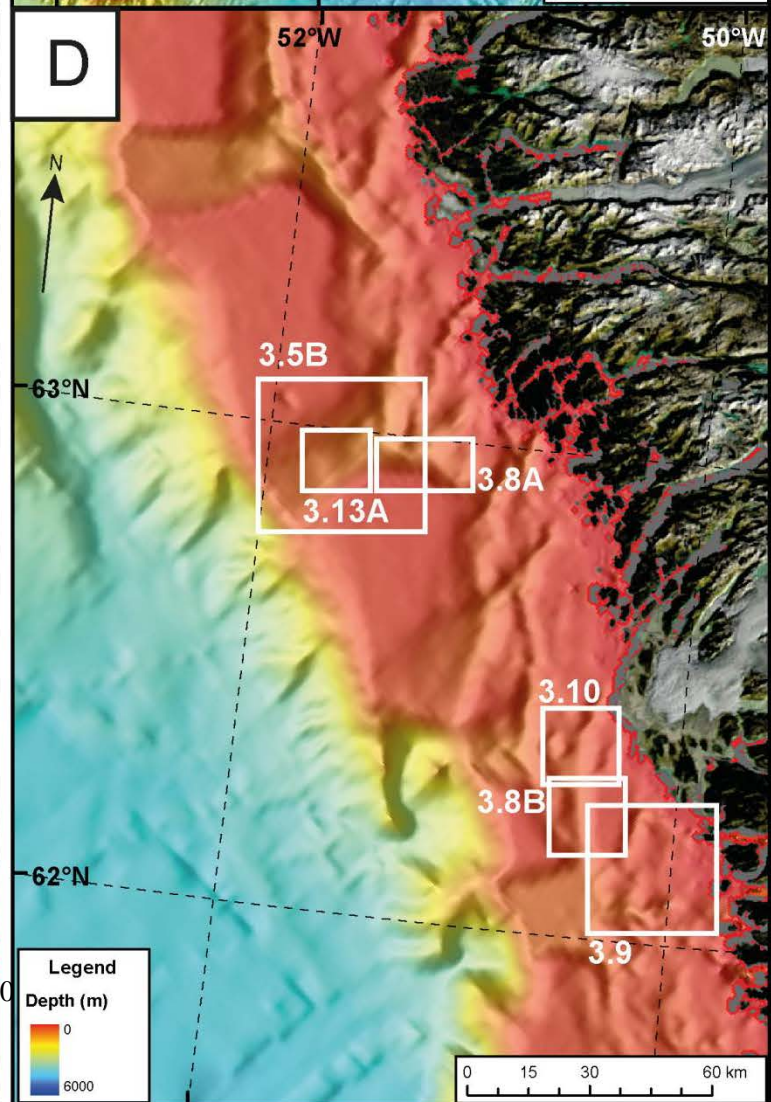
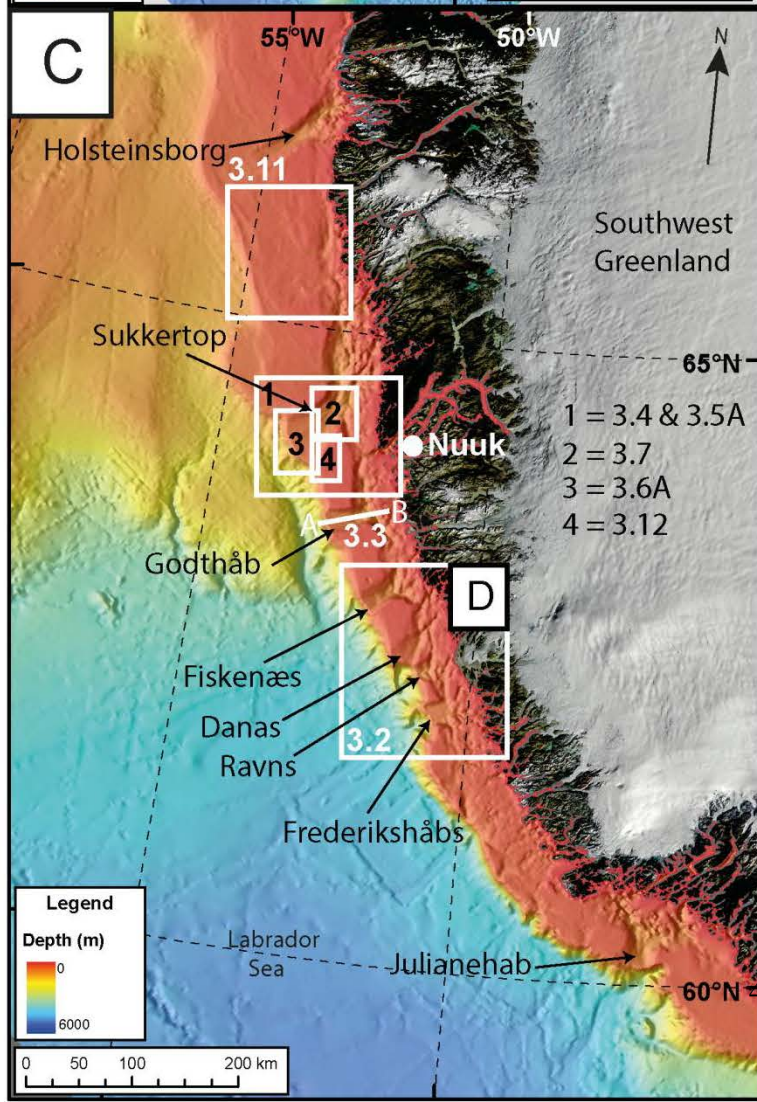
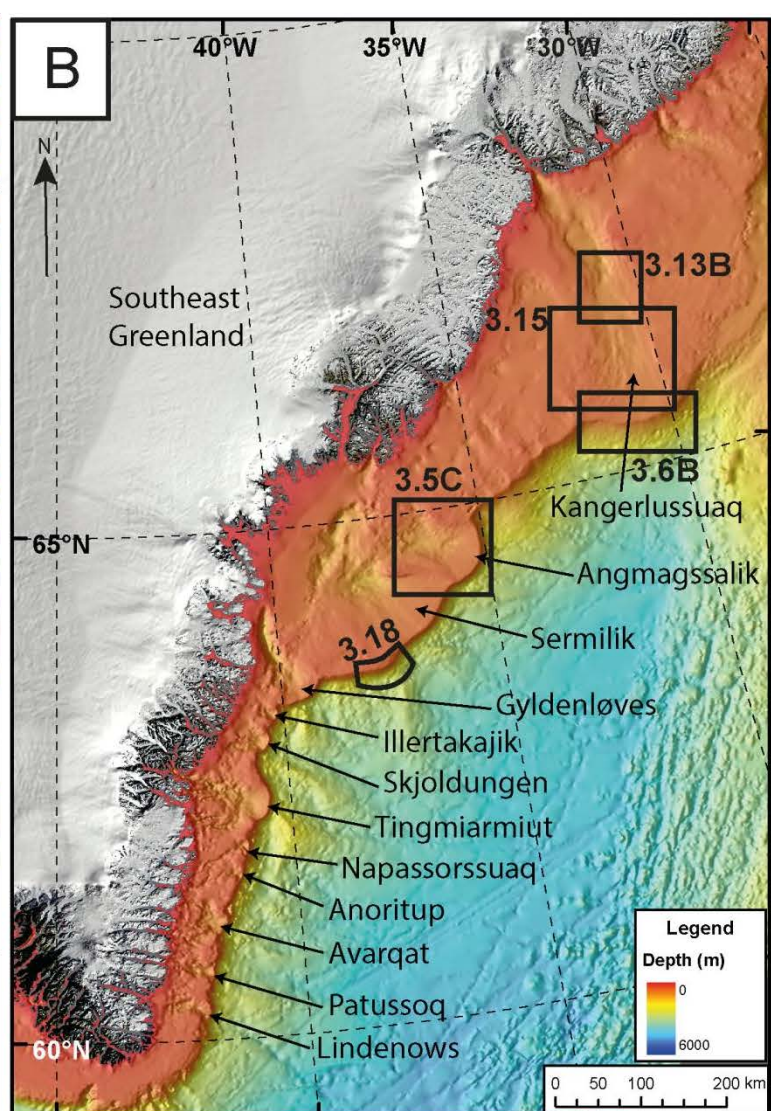
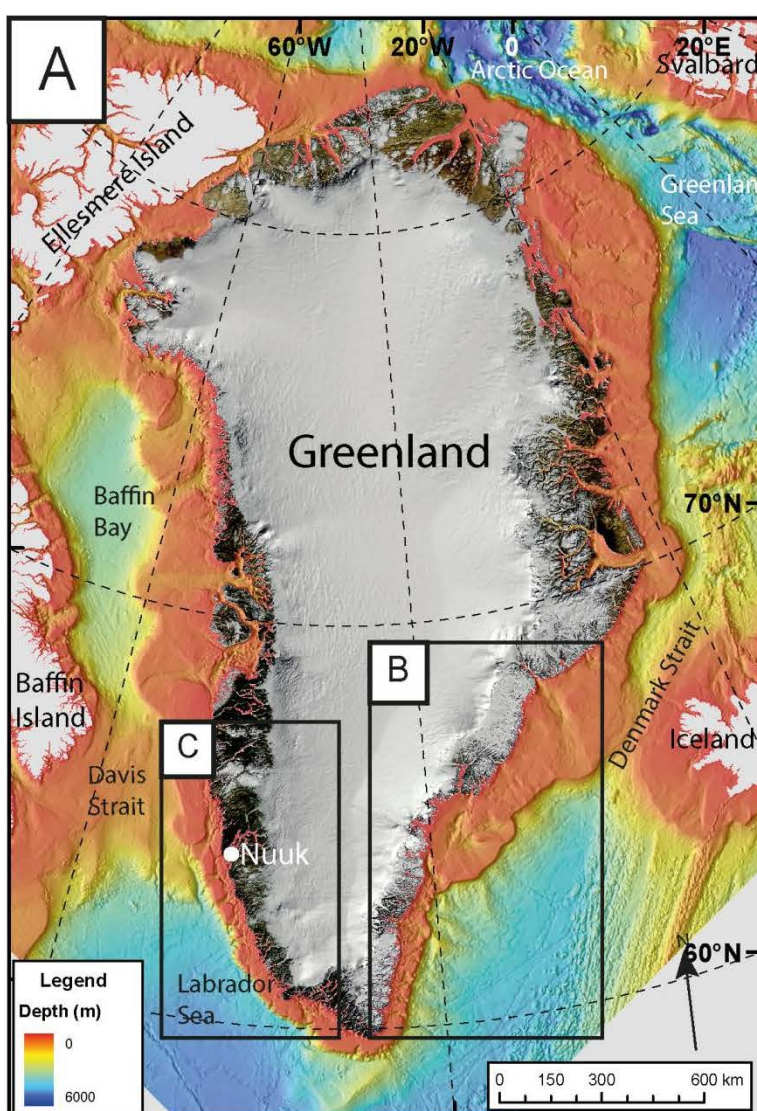
3.1. Introduction

The systematic analysis of the Olex, multi-beam and IBCAO data from the Southern Greenland continental margin resulted in a number of morphological zones and features being identified (Fig. 3.1). The large-scale morphology of the continental shelf of Southern Greenland has a consistent form. Where the Olex resolution is relatively high (Section 2.7.1), the inner continental shelf has a noticeably different bathymetry to the outer continental shelf (Fig. 3.2). The inner shelf has a shallow, rugged topography and is dissected by steep groove- and channel-like depressions. In contrast, the outer shelf has a much smoother bathymetry and consists of alternate troughs and banks (Fig. 3.2). The banks are wide and relatively shallow with depths of 50 - 100 m below sea level. The relatively narrow troughs dissect the banks before terminating at the continental shelf edge. The troughs have depths of up to 500 m on the outer continental shelf although they are often much deeper towards the inner continental shelf, reaching depths of up to 1000 m. The two regions are separated by a white, dashed line in Figure 3.2.

The difference between the two regions is interpreted as differences between the underlying substrate. The rugged inner shelf of Southern Greenland is interpreted as predominantly hard crystalline bedrock, similar to that mapped onshore in Greenland (Roberts et al., 2010). The opaque, acoustic basement identified by seismic reflection profiles in this area confirms this interpretation (Fig. 3.3) (Brett and Zarudzki, 1979; Nielsen et al., 2005). This region was termed the 'strandflat' by Holtedahl (1970) who likened its bathymetry to the inner continental shelf of the Norwegian continental margins. The near-horizontal strandflat can be explained by many factors including periglacial, subaerial and marine erosion. However, the width of the platform around the edge of the Greenland continent suggests that the strandflat has been at least partially shaped by glacial erosion (Benn and Evans, 2010). The smooth outer shelf is interpreted as largely sedimentary substrate deposited at a prograding margin. This substrate is thought to have formed by the net long-term transfer of material from erosional to depositional zones by glacial processes over successive Quaternary glaciations (Lykke-Andersen, 1998). Seismic reflection profiles confirm that this region is composed of sediments of probably Quaternary age (Fig. 3.3) (Roksandić, 1979; Nielsen et al., 2005).

An example of each type of morphological feature observed on the Southern Greenland continental margin is described in this chapter. For most of the features, an interpretation is offered. Where the interpretations cannot be based on one individual feature (e.g. channels, gullies), the spatial distribution of each landform type will be described in Chapter 4 to interpret these features more conclusively.

Figure 3.1. Next page. (A) A 250 m resolution MODIS mosaic of Greenland (Kargel et al., 2012) overlaid onto the IBCAO Version 3.0 surrounding Greenland. The main study areas are enlarged in (B), (C) and (D). The locations of the subsequent figures are shown in black and white boxes. The troughs identified are also labelled.



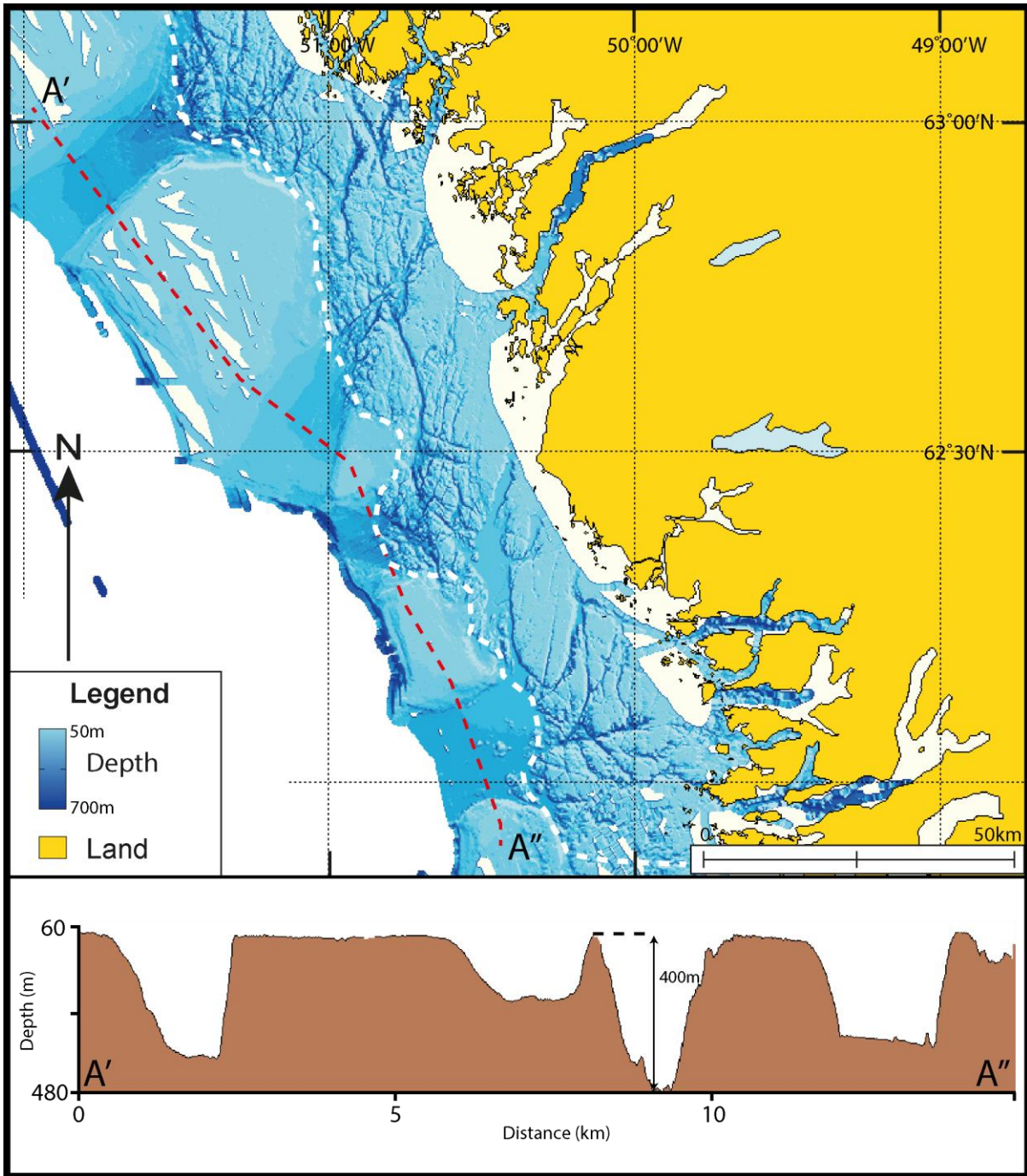


Figure 3.2. Typical morphology of the continental shelf of Southern Greenland shown by Olex data. The inner shelf is characterised by a rugged, dissected topography (strandflat) whilst the outer shelf is characterised by a smoother topography with alternate banks and troughs. White line shows the boundary between the two areas. Location in Figure 3.1C.

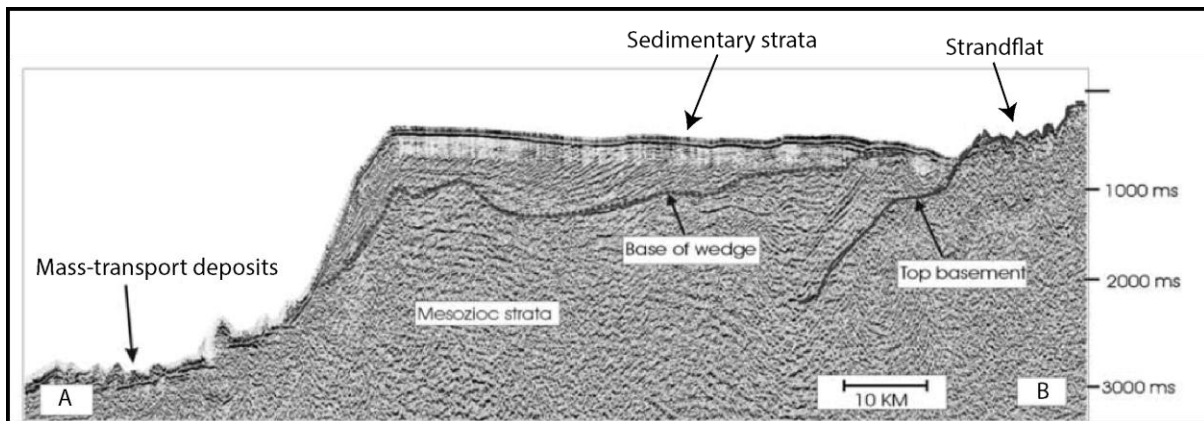


Figure 3.3. Seismic profile along the long axis of Godthåb Trough. This shows that the outer continental shelf consists of a thick prograding wedge of Quaternary sediments. This wedge overlies crystalline bedrock which is exposed on the inner continental shelf. Location in Figure 3.1C. Adapted from Nielsen et al., (2005).

3.2. Cross-shelf troughs

3.2.1. Description

The Olex and IBCAO data show that a number of large cross-shelf troughs dissect the continental margins of Southern Greenland (Figs. 3.1, 3.2). These features are relatively steep-sided, flat-bottomed, elongated depressions that sometimes widen towards the continental shelf edge. All the troughs identified in the study area are composed of a single trunk, but some have several tributaries which converge to a central trough on the inner- or mid- shelf. The tributary troughs are often orientated parallel to the coastline.

Twelve troughs have been identified on the continental shelf of Southeast Greenland and eight on the continental shelf of Southwest Greenland (Batchelor and Dowdeswell, In Press). Many troughs widen and shallow towards the continental shelf edge. For example Sukkertop Trough in Southwest Greenland has a relatively narrow, deep cross-profile on the inner continental shelf but becomes more subdued towards the shelf edge (Fig. 3.4). In addition, the walls of some troughs have breaks in slope. For example, the cross profiles B and D in Figure 3.4 show that the southeast bank of Sukkertop Trough has a number of steps on the side of the bank.

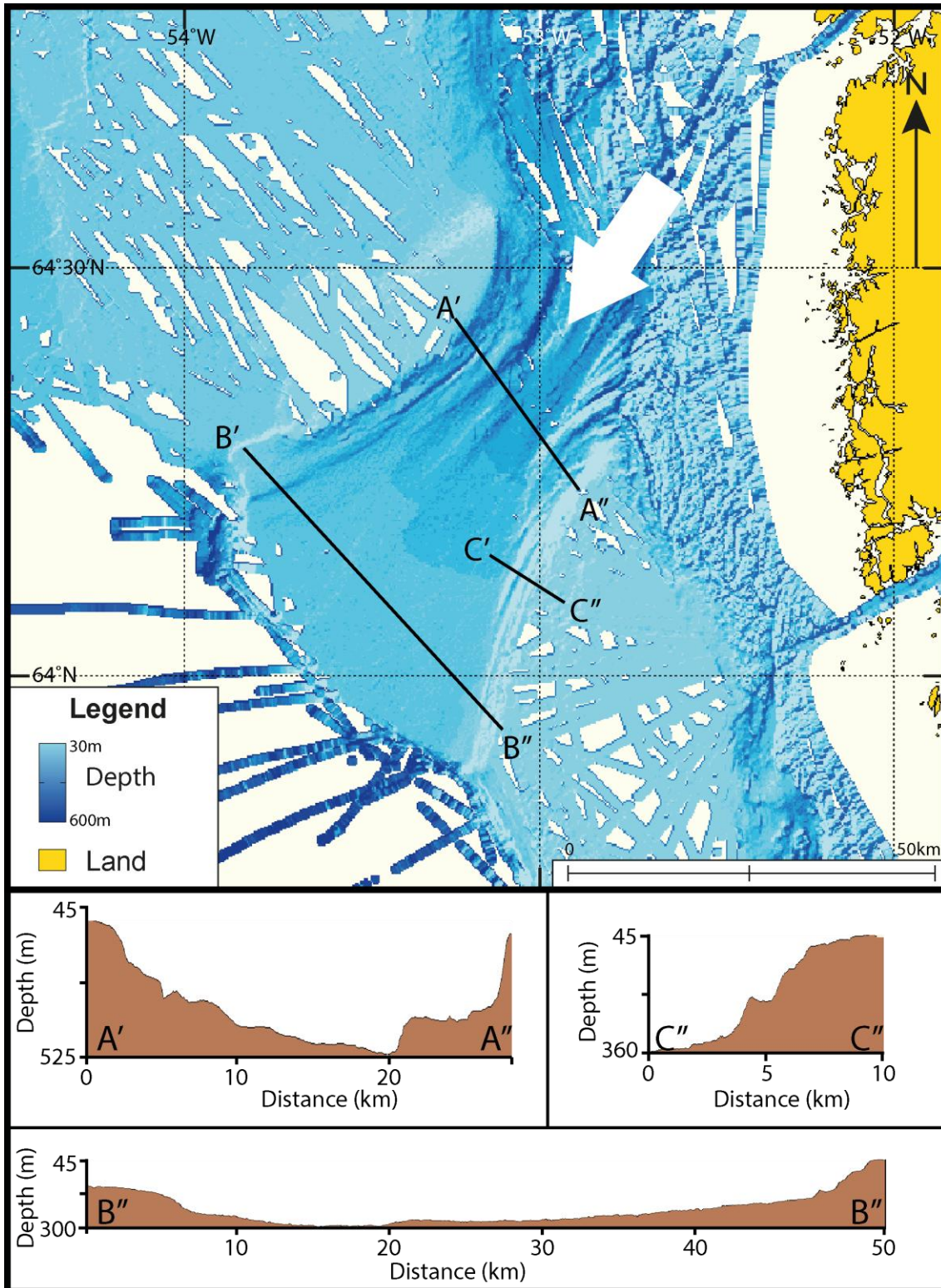


Figure 3.4. An example of a typical cross-shelf trough, Sukkertop Trough in Southwest Greenland in the Olex data. It has a length of 100 km, a maximum width of 50 km and a maximum depth of 600 m. Profiles B and C show that the trough widens and shallows towards the continental shelf edge. Profile D shows that the banks of the trough are stepped. Location in Figure 3.1C.

The deepest sections of troughs usually occur at the initiation of the trough between the strandflat and the outer shelf (Fig. 3.5). These sections are sometimes associated with the convergence of two or more tributary troughs. The maximum depths in these deepest areas range between 360 and 1000 m with an average depth of 586 m. The trough long profiles show that the majority of troughs identified on the Southern Greenland continental margin have reverse slopes that shallow seawards (Fig. 3.5). The average slope angle is 0.28° and ranges from 0.63° to 0.06° . Frederikshåbs Dyb in Southwest Greenland is the only trough with a normal sloped long profile.

3.2.2. Interpretation

The cross-shelf troughs identified in the Olex and IBCAO data are interpreted as evidence for glacial erosion by palaeo-ice streams that drained the Greenland Ice Sheet during Quaternary glacial periods (Batchelor and Dowdeswell, In Press). The Olex data show that the cross profiles of the troughs are commonly U-shaped or parabolic (Fig. 3.4). Theoretical and observational studies have related this form to the action of glacial erosion (Harbor, 1992). The variance in the cross profiles may be the result of differences between glaciological, geological or non-glacial factors which vary initially, during and after glacial erosion (Harbor, 1992). The seaward increase in width is probably due to ice emerging from the constraints of fjords and spreading on the outer shelf where topographic control is lost (Fig. 3.4)

Similar U-shaped troughs have been identified on the continental shelf of Greenland (e.g. Kangerlussuaq, Scoresby Sund, Uummannaq and Egedesminde troughs) (Batchelor and Dowdeswell, In Press). These troughs have been the subject of previous investigations which combined bathymetric data with seismic reflection profiles and sediment cores (e.g. Dowdeswell et al., 2010, In Press; Ó Cofaigh et al., 2013a, 2013b). The investigations identified the presence of elongate lineations, extensively deformed till in the troughs, and voluminous sediment accumulations on the adjacent continental slopes. From this evidence, it was interpreted that the troughs were formerly occupied by ice streams when the Greenland Ice Sheet reached the shelf edge. It is therefore inferred that the troughs identified in this study were also former locations of palaeo-ice streams during periods when the Greenland Ice Sheet extended to the shelf edge.

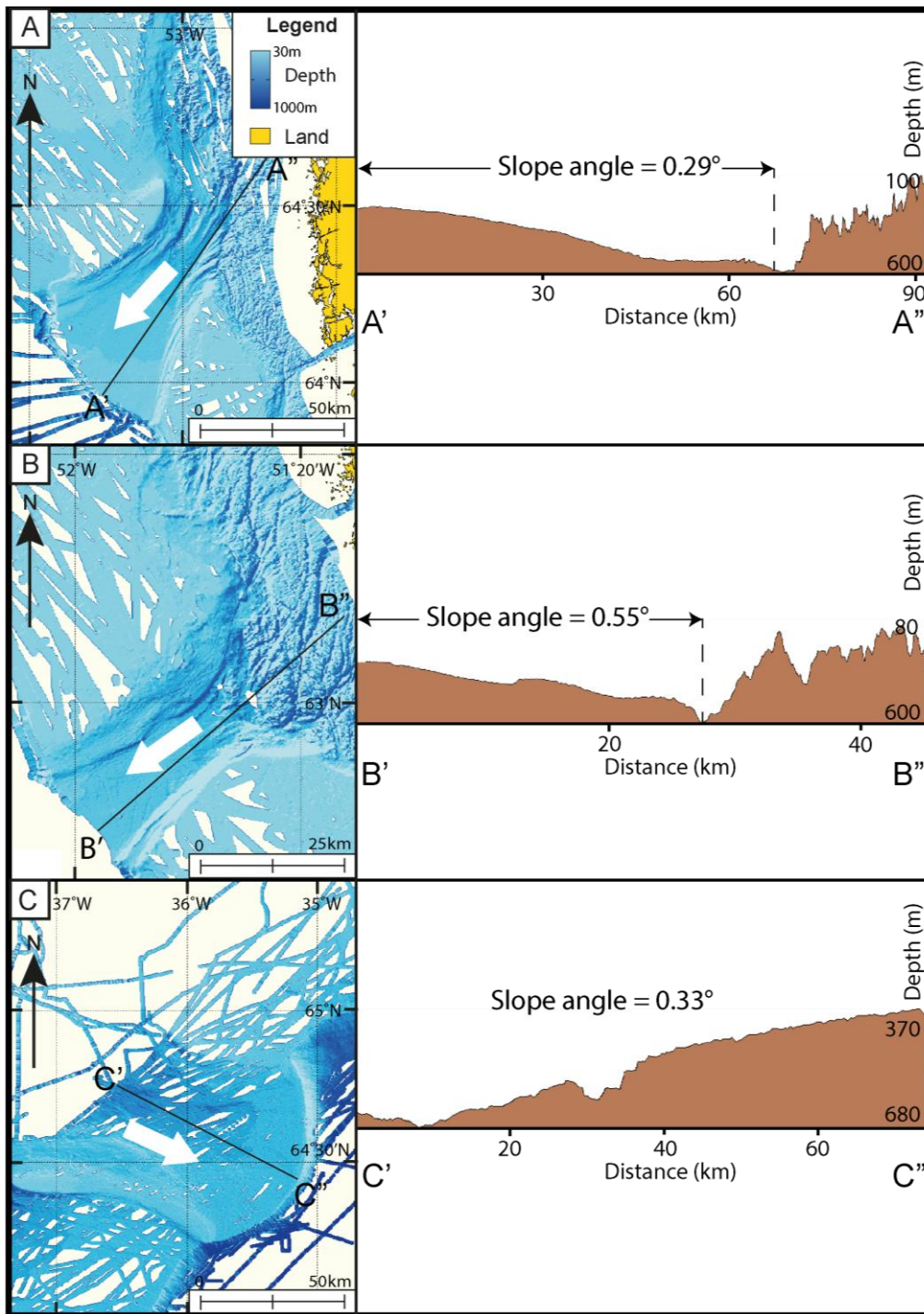


Figure 3.5. Bathymetric long-profiles of three typical cross-shelf troughs in Southern Greenland. (A) Sukkertop Trough, (B) Fiskenaes Trough, and (C) Angmagssalik Trough. Profiles A, B and C show that all troughs shallow towards the shelf edge. White arrows indicate the inferred direction of palaeo-ice flow. Note the highly rugged topography of the inner continental shelf of (A) and (B) in the long-profiles. This area is interpreted as hard crystalline bedrock. Location in Figures 3.1B, 3.1C and 3.1D.

The reverse long profiles indicate that the cross-shelf troughs of Southern Greenland were repeatedly overdeepened by glacial erosion during the Quaternary (ten Brink and Schneider, 1995). Results from models suggest that the reverse slopes of Antarctic troughs are a result of the time-transgressive effects of glacial erosion and sedimentation related to the position of the ice grounding line over successive glacial cycles (ten Brink and Schneider, 1995). The reverse slopes of the Southern Greenland cross-shelf troughs are therefore likely to have been formed by multiple glaciations when ice extended to the shelf edge. Kuijpers and Nielsen (2013) suggest that this happened five times.

3.3. Outward bulging bathymetric contours beyond cross-shelf troughs

3.3.1. Description

The IBCAO data show that a number of Southern Greenland cross-shelf troughs (Kangerlussuaq, Angmagssalik, Sermilik, Gyldenløves, Skjoldungen and Tingmiarmiut troughs in Southeast Greenland and Sukkertop trough in Southwest Greenland) are associated with outward bulging bathymetric contours beyond their trough-mouths (Fig. 3.6). These features were also identified and described in detail by Batchelor and Dowdeswell (In Press). The lack of Olex data on the continental slopes of Southern Greenland means that the Olex data do not add to the information gained from the IBCAO data.

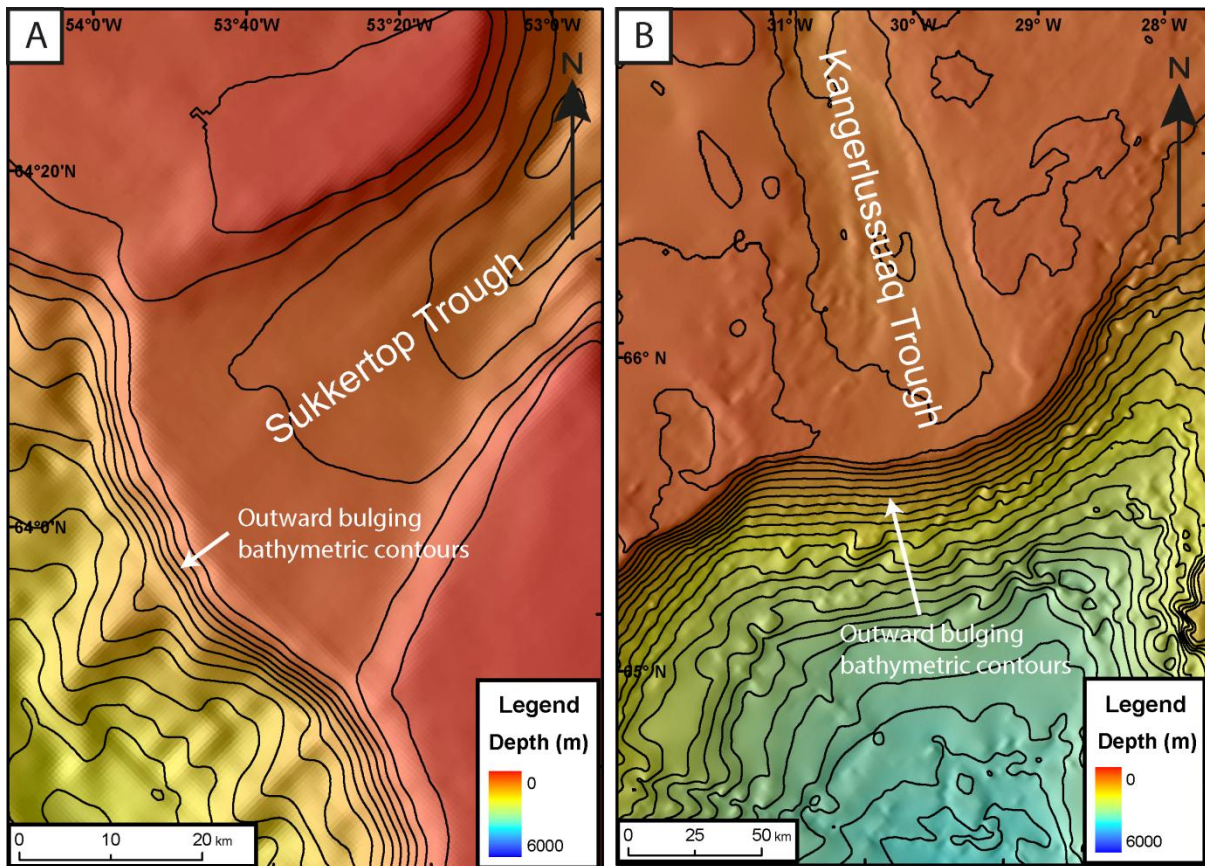


Figure 3.6. The outward bulging bathymetric contours on the continental slope offshore of (A) Sukkertop Trough, location in Figure 3.1C and (B) Kangerlussuaq Trough, location in Figure 3.1B.

3.3.2. Interpretation

The outward bulging bathymetric contours imply that the continental shelf has prograded in a seaward direction and that trough-mouth fans (TMFs) have built up on the upper-slope beyond some cross-shelf troughs (Dowdeswell et al., 1996; Laberg and Vorren, 1996; Batchelor and Dowdeswell, In Press). Where TMFs have been investigated, they are found to be composed primarily of glacial debris flows and turbidite deposits (Vorren et al., 1988, 1989; Dowdeswell et al., 1996; Elverhøi et al., 1997; Vorren and Laberg, 1997; King et al., 1996; Ó Cofaigh et al., 2003). This suggests that the continental slopes offshore of some troughs in Southern Greenland experienced rapid delivery of glacial sediments when fast-flowing ice streams reached the shelf edge on multiple occasions (Vorren et al., 1998; Dowdeswell and Siegert, 1999). Large TMFs have also been identified on the continental slopes of the Western Greenland margin, offshore of the Ummannaq and Egedesminde

troughs (Ó Cofaigh et al., 2013a, 2013b; Dowdeswell et al., In Press), and the Eastern and Northeastern Greenland margins, offshore of the Norske, Dove Bugt, and Scoresby Sund troughs (Dowdeswell et al., 1994, 1997; Evans et al., 2009).

The spatial distribution and implications of the locations of the TMFs will be discussed in Section 4.3.1.

3.4. Elongate streamlined lineations

3.4.1. Description

Lineations

On the inner continental shelf of some troughs, there are a number of elongate, streamlined lineations that converge to the main trough trunks (Fig. 3.7). Nearer the margins of the troughs, these features curve around the trough sides. The elongate lineations have lengths of up to 65 km, widths of up to 1.5 km and heights of around 20 – 40 m with a maximum of 90 m. They have length to width or elongation ratios between 8 and 20. The features are initially prominent on the inner shelf but gradually taper in an offshore direction.

Drumlinised features

Numerous oval-shaped features are observed in the Olex data on the inner continental shelf of Southern Greenland (Fig. 3.8). These protuberances are much shorter than the elongate streamlined lineations with average lengths of 1.5 km, average widths of 0.5 km and average heights of about 90 m. They have elongation ratios of between 2 and 5. Some features have symmetrical long axes but most of the hills have asymmetric long axes with blunt-nosed landward faces and a streamlined tail that tapers towards the outer continental shelf. The features are orientated in the direction of the trough or tributary trough long axis and when they are observed they usually occur abundantly (Fig. 3.8).

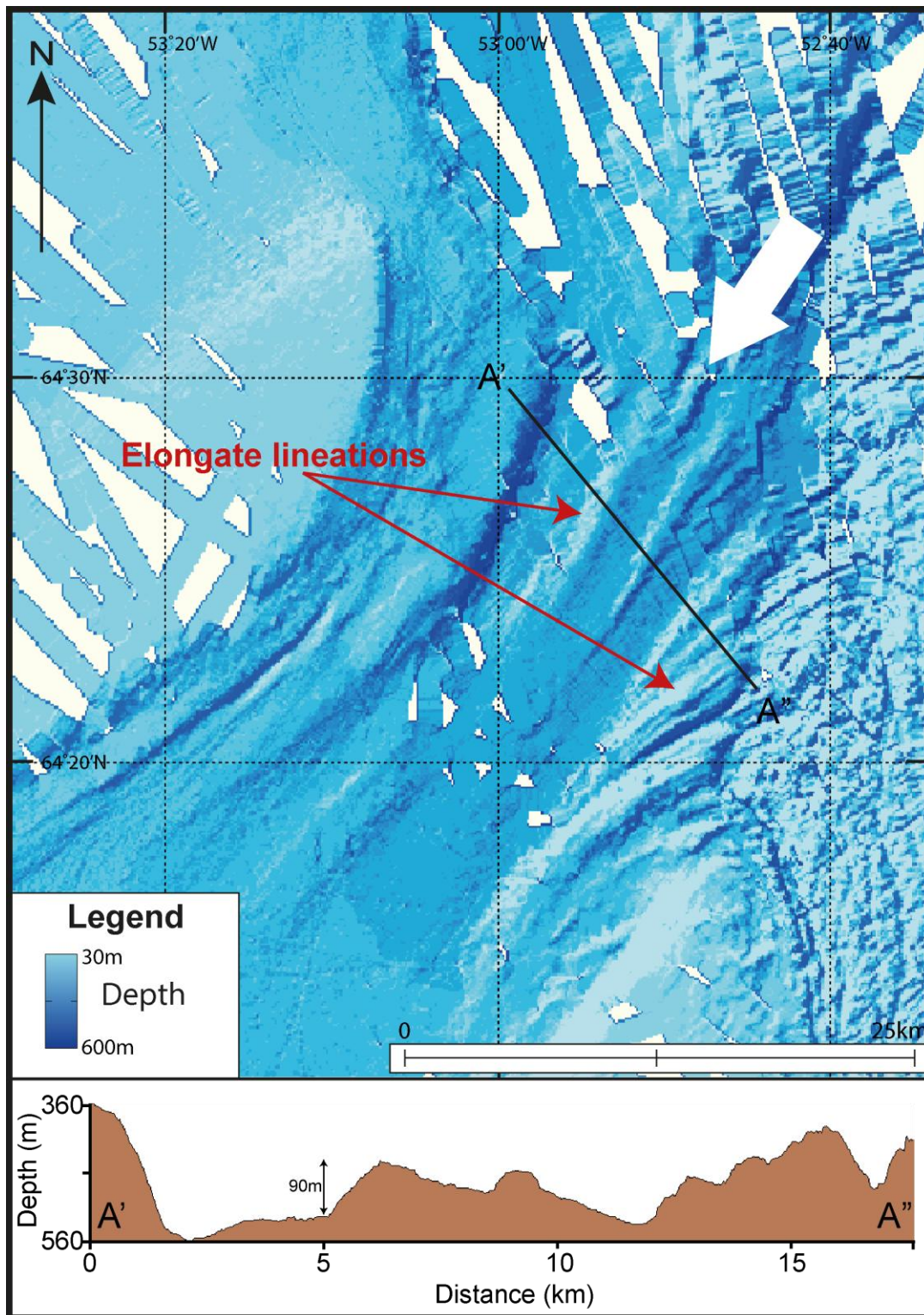


Figure 3.7. Streamlined lineations on the inner continental shelf of Sukkertop Trough, Southwest Greenland. These features are elongate and strongly convergent towards the main trunk of the trough. White arrow indicates direction of inferred palaeo-ice flow. Location in Figure 3.1C.

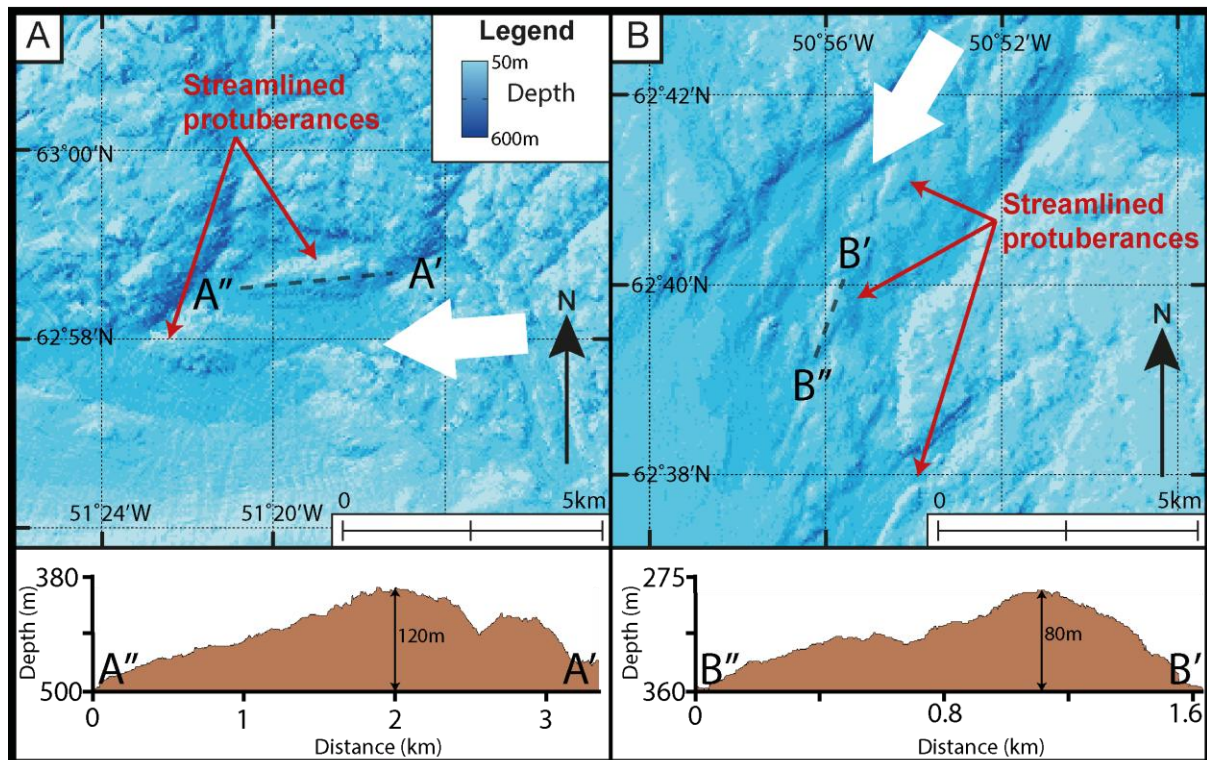


Figure 3.8. Oval-shaped protuberances and their associated long-profiles. These features are identified on the inner continental shelf. Profiles A and B show that they taper seawards. White arrow indicates direction of inferred palaeo-ice flow. Location in Figure 3.1D.

3.4.2. Interpretation

Lineations

The streamlined lineations are interpreted as crag-and-tails with an upstream rock core ‘crag’ and a downstream tapering sedimentary tail (Benn and Evans, 2010). Although the form of these features is similar to mega-scale glacial lineations (MSGSL) (Clark, 1993), they are not as elongate and do not consist wholly of deformable till. The seismic reflection profiles discussed in Section 3.1 suggest that the ‘heads’ of the crag-and-tails are associated with hard bedrock and that the ‘tails’ consist of sedimentary material which tapers towards the outer shelf (Brett and Zarudzki, 1979; Roksandić, 1979). Crag-and-tails are recognised as a product of sustained periods of ice streaming around an obstacle. The bedrock component of the crag-and-tails probably acted as an area of high friction. The tails are thought to have either been protected from erosion or formed by the melting and release of entrained debris into the subglacial lee-side cavity. Similar features have been identified on the inner continental shelf

of Uummannaq Trough at 70° N in West Greenland (Ó Cofaigh et al., 2013b; Dowdeswell et al., In Press).

Drumlinised features

The oval-shaped features are interpreted as evidence for sustained subglacial erosion. The elongation ratios and size of the landforms are similar to whaleback and rock drumlin landforms identified in other high-latitude marine and terrestrial regions (Roberts and Long, 2005). Furthermore, the location of the landforms on the inner shelf concurs with the observations of other studies who found similar landforms in similar inner shelf areas (Wellner et al., 2001; Lowe and Anderson, 2002; Evans et al., 2005; Anderson and Oakes-Fretwell, 2008; Graham et al., 2009).

The location of these features on the inner shelf suggests that they are associated with the strandflat region and consist of hard crystalline bedrock (Brett and Zarudzki, 1979; Roksandić, 1979). Whalebacks and rock drumlins are formed by the erosive streamlining of bedrock protrusions by glacial abrasion to produce positive upstanding landforms (Bennett and Glasser, 2009). Whalebacks are distinguished from rock drumlins as the former have been smoothed and rounded on all sides by ice and are therefore approximately symmetrical. Rock drumlins have pronounced asymmetry with steeper up-ice faces and gently tapering down-ice sides which suggests spatially variable glacial erosion (Bennett and Glasser, 2009).

3.5. Channels

3.5.1. Description

Many channels are identified on the inner continental shelf of Southern Greenland from the Olex data (Fig. 3.9). The largest of these channels have lengths of up to 30 km, widths of up to 3 km and depths of up to 500 m. Some channels may be longer but they lie outside the coverage of the Olex data. Numerous smaller channels with widths and depths typically of an order of magnitude smaller also exist. The small channels generally converge into large channels which, in turn, generally feed into the deepest sections of cross-shelf troughs (Fig. 3.9).

On the continental shelf of Southwest Greenland channels have a dendritic pattern. In some cases channels exist as singular features (Fig 3.9). The gradients of the channel long profiles

are variable. Most channels have net downhill gradients but do not have constant gradients. Instead the long profiles are undulating and have significant uphill gradients (Figs. 3.9, 4.2).

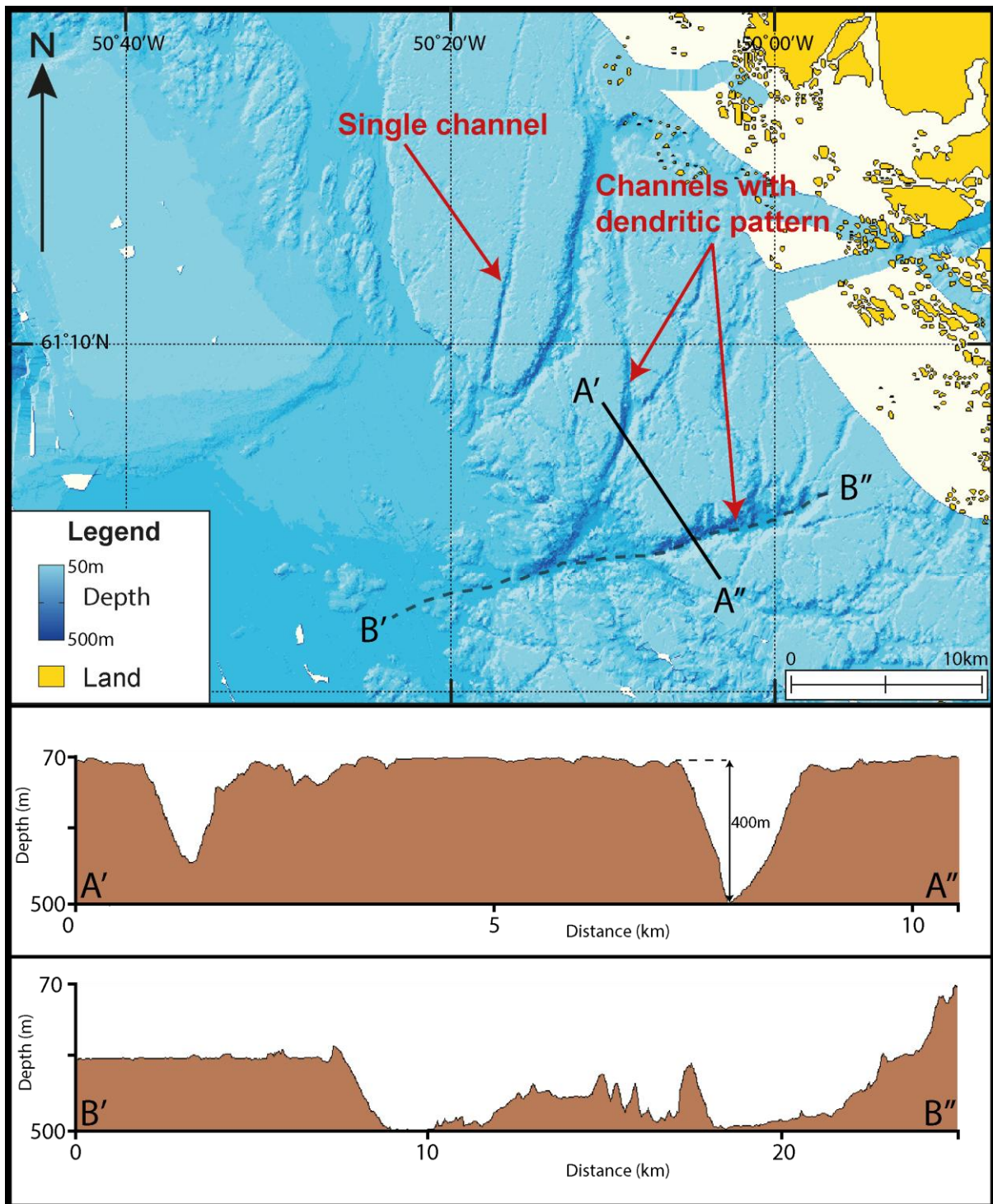


Figure 3.9. Multiple channels are identified on the inner continental shelf of Southern Greenland. Profile A shows that these channels are very large and V-shaped. Profile B shows that this channel has an undulating long-profile. Location in Figure 3.1D.

3.5.2. Interpretation

The channels observed in the Olex bathymetry are interpreted as evidence for fluvial and/or glacial meltwater erosion preceding, during or following a Quaternary glacial period when ice extended onto the continental shelf. It is thought that they were formed in one or more of the following environments:

Subglacially (beneath the ice)

Laterally (along the ice margin)

In proglacial locations (in front of the ice) either preceding or following a glacial period and sometimes by the outburst of ice-dammed lakes

The differences between channel dimensions and spatial distributions provide evidence for the environment in which they were formed. This will be discussed in more detail in Section 4.1.1.

3.6. Meandering submarine channel

3.6.1. Description

A channel of very different nature to the channels identified in Section 3.5.1 is located on the inner shelf of Southwest Greenland onshore of Frederikshåbs Dyb in the Olex data. This channel is about 11 km in length, 15 m deep and 400 m in width (Fig. 3.10). It has a meandering thalweg and is highly sinuous, with a sinuosity index (Equation 3.1) of 1.53. The channel flows down a continuous, smooth slope with an angle of 12.8°.

$$\textit{Sinuosity index} = \textit{distance measured along channel/straight line distance} \quad (\text{Eq. 3.1})$$

3.6.2. Interpretation

The sinuous channel is interpreted as a turbidity-current channel. Turbidity currents can be initiated by meltwater draining from receding ice sheet and tidewater glacier margins. The dense and probably sediment-rich water flows down-slope eroding a channel. A similar submarine channel was identified by Dowdeswell et al. (In Press) in Rink Fjord, West Greenland.

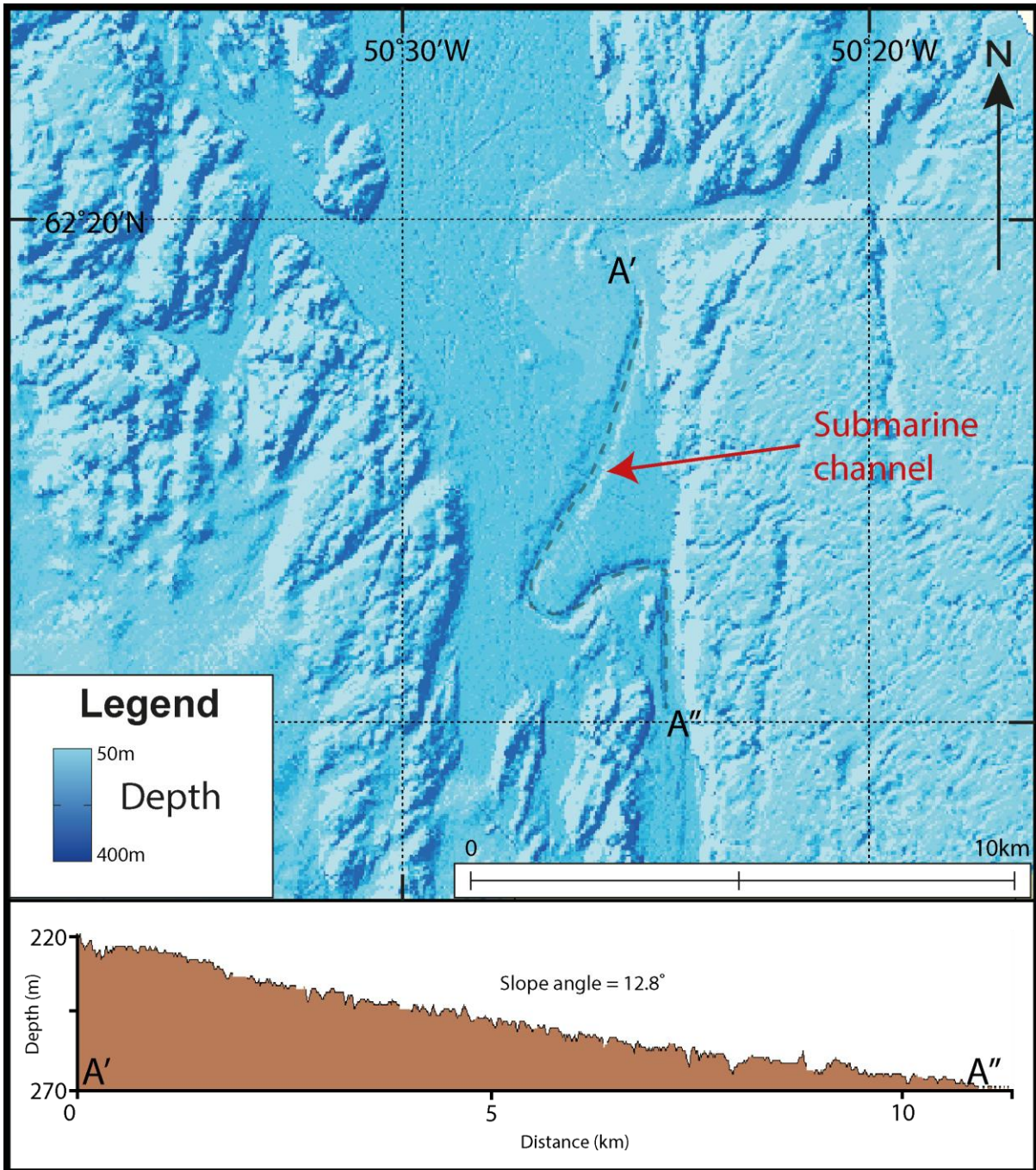


Figure 3.10. A highly sinuous submarine channel with a meandering thalweg in a tributary trough of Frederikshåb Trough. The thalweg is located on the outside of the bend in Profile A, similar to a subaerial river channel. Location in Figure 3.1D.

3.7. Long sinuous ridges transverse to inferred ice flow direction

3.7.1. Description

Three long sinuous ridges are identified on the outer continental shelf in the Olex data (Fig. 3.11). These ridges are between 20 and 30 km long, 1.4 and 2.5 km wide and have heights of 20 – 25 m. They are orientated parallel to the coastline and curve slightly outwards offshore. The ridges are asymmetric in cross-section with a relatively small onshore slope and a much longer seaward slope (Fig. 3.11). The most central of the three ridges terminates on the shelf edge whilst the ridges north and south of the central ridge terminate a few hundred metres from the shelf edge (Fig. 3.11). A smaller irregularly shaped ridge is also identified about 40 km inshore of the outer ridges. This feature has a height of 30 m, a width of 2 km and a length of 11.5 km.

3.7.2. Interpretation

The ridges are interpreted as terminal moraines formed by the deposition of sediment at the margin of an ice sheet at the maximum extent of ice advance. High resolution seismic surveys have previously identified these features and have termed them the Outer Hellefisk Moraine System (Brett and Zarudzki, 1979; Kelly, 1985). They closely follow the shelf edge for over 150 km and possibly further north (Brett and Zarudzki, 1979). These locations on relatively shallow banks, rather than in cross-shelf troughs, suggest that they were formed at an ice margin between major fast-flowing ice streams. Terminal moraine ridges have been observed in inter-ice-stream glaciated margins around Svalbard (Ottesen and Dowdeswell, 2009) and are thought to have formed wherever an ice sheet grounding zone remains quasi-stable for long periods of time and/or where sediment fluxes to the ice sheet margin are high.

A number of processes can deposit sediment at the margin of an ice sheet. These include the slumping or falling of supraglacial debris into the water down the ice calving front, the meltout of englacial and subglacial debris below the water, the squeezing out of unfrozen deformation till from beneath the ice, and the transporting of material by meltwater streams (Benn and Evans, 2010). Oscillating ice margins can result in the moraines being modified by ice-push or thrusting. This perhaps caused the crest to form at the summit of the ridge and suggests that the development of these features was not constrained by an overlying ice-shelf, which would have restricted vertical accommodation space (Dowdeswell and Fugelli, 2012).

The outward curve of the ridges probably reflects the form of the calving front of the ice when it last extended to the outer continental shelf.

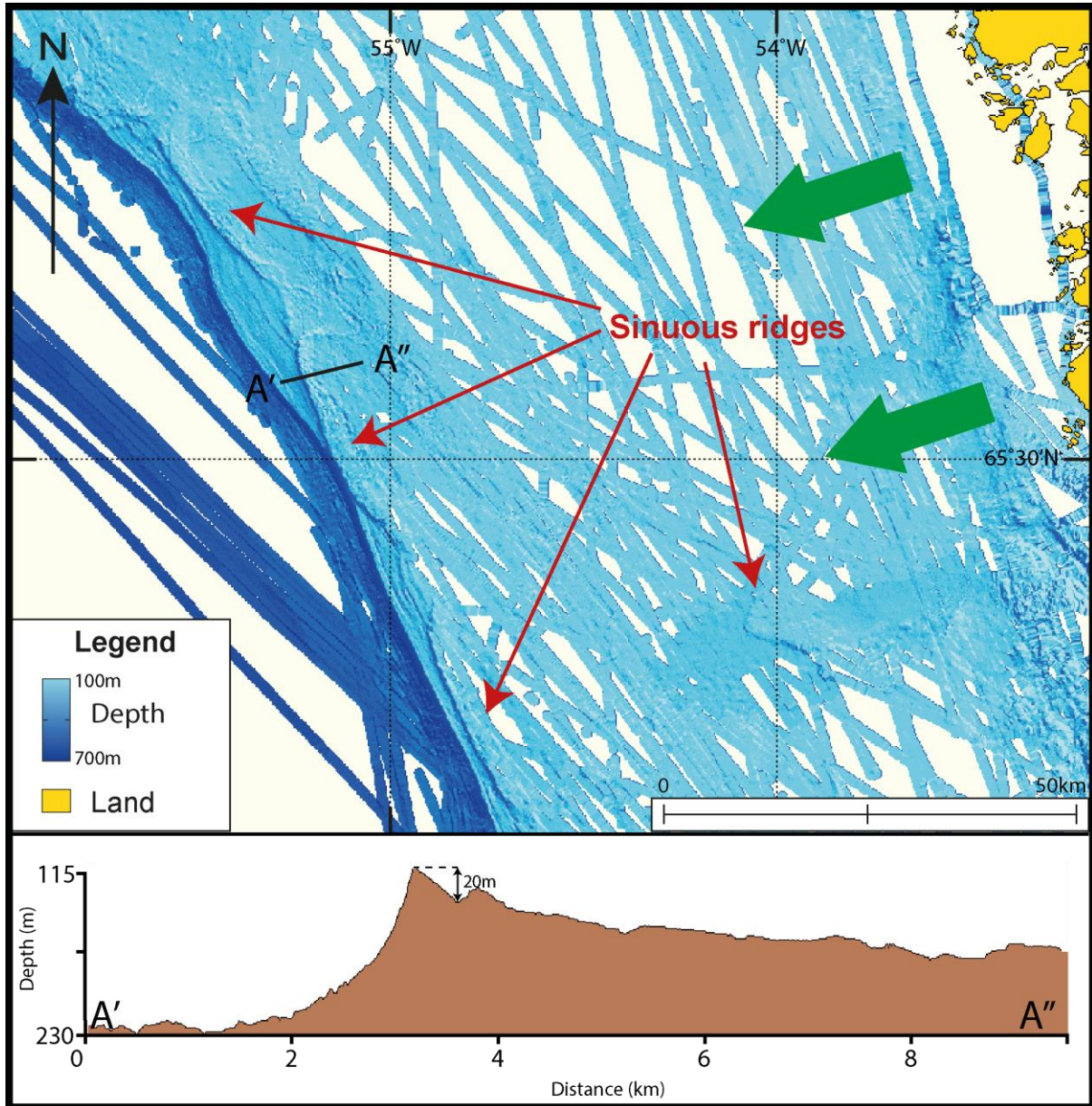


Figure 3.11. Three, long sinuous ridges and one smaller irregularly shaped ridge identified on Tovqussaq Bank, Southwest Greenland. Green arrows indicate inferred direction of palaeo-ice flow. Location in Figure 3.1C.

3.8. Long ridges parallel to inferred ice flow direction

3.8.1. Description

On the shallow banks immediately adjoining many cross-shelf troughs in Southern Greenland there are a number of long ridges that run parallel to the direction of the trough long axis (Fig. 3.12). These features are relatively subdued and are not always visible in the Olex data. The cross profiles, however, show that they have heights of around 30 m and widths of around 60 m.

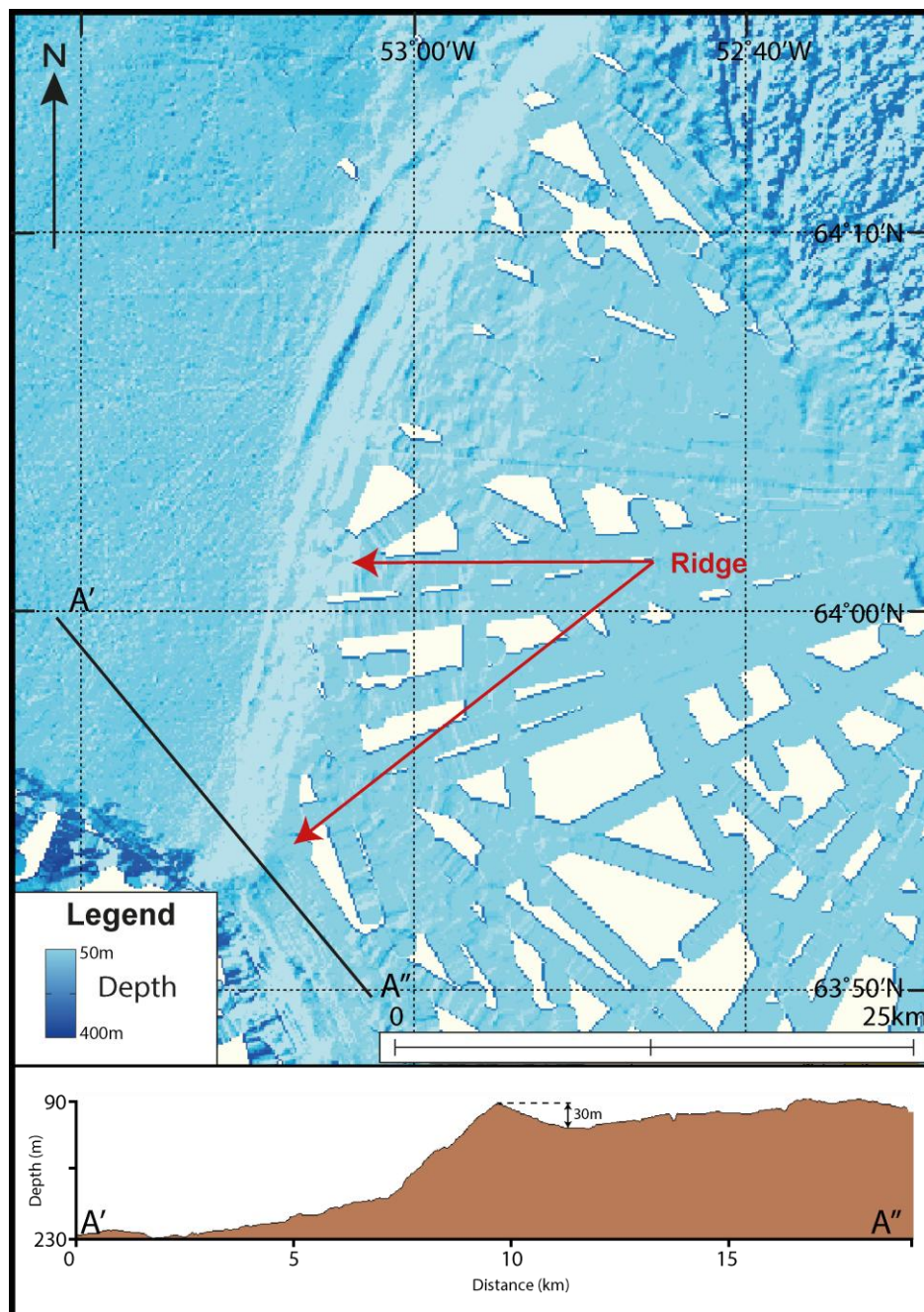


Figure 3.12. A long ridge on the southern bank of Sukkertop Trough, Southwest Greenland. Location in Figure 3.1C.

3.8.2. Interpretation

These features are also interpreted as evidence for the deposition of sediment around the edge of an ice mass. However, because these landforms are orientated parallel to the trough long axis, they are interpreted as lateral moraines rather than terminal moraines. Lateral moraines are depositional ridges that mark the border zone between areas of fast and slower flowing ice and have been used to support evidence for the former existence of ice streams (Stokes and Clark, 1999). Lateral moraines have been identified in terrestrial settings such as the Canadian Arctic (Stokes and Clark, 2003), and in numerous marine locations along the Norwegian and Svalbard continental margins (Ottesen et al., 2005, 2007).

3.9. Wide subdued ridges

3.9.1. Description

In the Olex data, two large but subtle ridges are observed in two cross-shelf troughs. One is situated in Fiskenæs Trough, Southwest Greenland and the other in Kangerlussuaq Trough, Southeast Greenland (Fig. 3.13). The ridge in Fiskenæs Trough is 8.7 km in width, 8 km in length (perpendicular to inferred direction of ice flow) and 60 m in height (Fig. 3.13A). The volume of this ridge is 4.2 km³. The feature is orientated perpendicular to the trough long axes and spans the width of the trough floor. It has an asymmetrical character, with a slightly steeper seaward facing slope of 0.68° and a slightly gentler onshore facing slope of 0.63° (Fig. 3.13A). The ridge in Kangerlussuaq Trough is 15 km in width, 40 km in length and 65 m in height (Fig. 3.13B). The volume of this ridge is 39 km³. The ridge in Kangerlussuaq Trough is also asymmetrical with a steeper seaward slope (0.22°) and a gentler onshore slope (0.07°) (Fig. 3.13B). The ridge in Kangerlussuaq Trough, however, differs from the ridge in Fiskenæs Trough because it is longer than it is wide.

3.9.2. Interpretation

The large subdued ridges are interpreted as grounding-zone wedges (GZWs) (Powell and Domack, 2002; Dowdeswell and Fugelli, 2012). The features' size and relative angles of their seaward and onshore facing slopes mean that they are similar to GZWs described on the continental shelves of other high-latitude regions (Fig. 3.14) (e.g. Shipp et al., 1999; Ottesen et al., 2005; Mosola and Anderson, 2006; Dowdeswell and Fugelli, 2012; Dowdeswell et al., In Press). These landforms are thought to have formed by the deposition of sediment at the

grounding-zones of quasi-stable ice streams during more general periods of retreat (Dowdeswell and Fugelli, 2012). The relatively subdued nature of the GZW indicates that a floating ice shelf was probably present beyond the grounding-zone (Dowdeswell and Fugelli, 2012). Upward accommodation space would have been limited by the roof of the water-filled cavity into which the sediment was deposited. Many processes are attributed to the deposition of sediment including the lodgement of sediments from the base of the ice stream, deposition from sediment-laden subglacial meltwater, melt-out from the base of the ice streams, rain-out of IRD, debris flows and suspension settling from meltwater plumes (Dowdeswell and Fugelli, 2012; Bjarnadóttir et al., 2013).

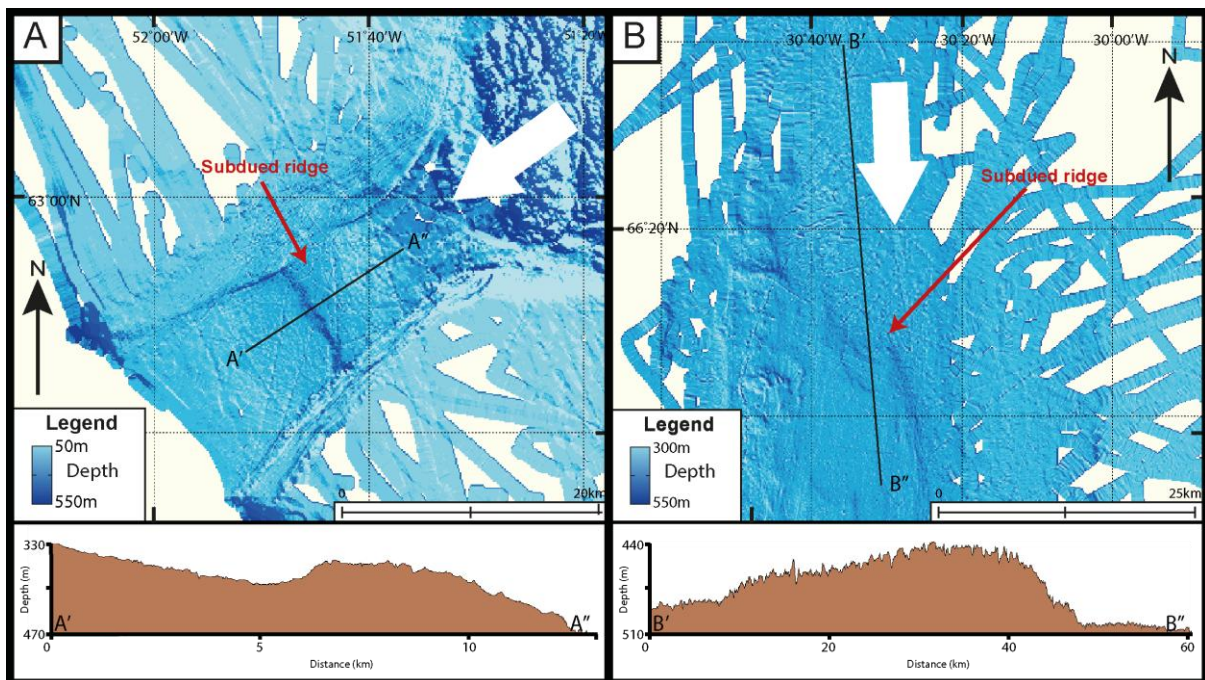


Figure 3.13. The large subducted ridges identified in Fiskenaes Trough, Southwest Greenland and Kangerlussuaq Trough, Southeast Greenland. These features have asymmetric long axes with steeper offshore facing slopes and gentler onshore facing slopes. White arrows indicate inferred direction of palaeo-ice flow. Location in Figures 3.1B and 3.1D.

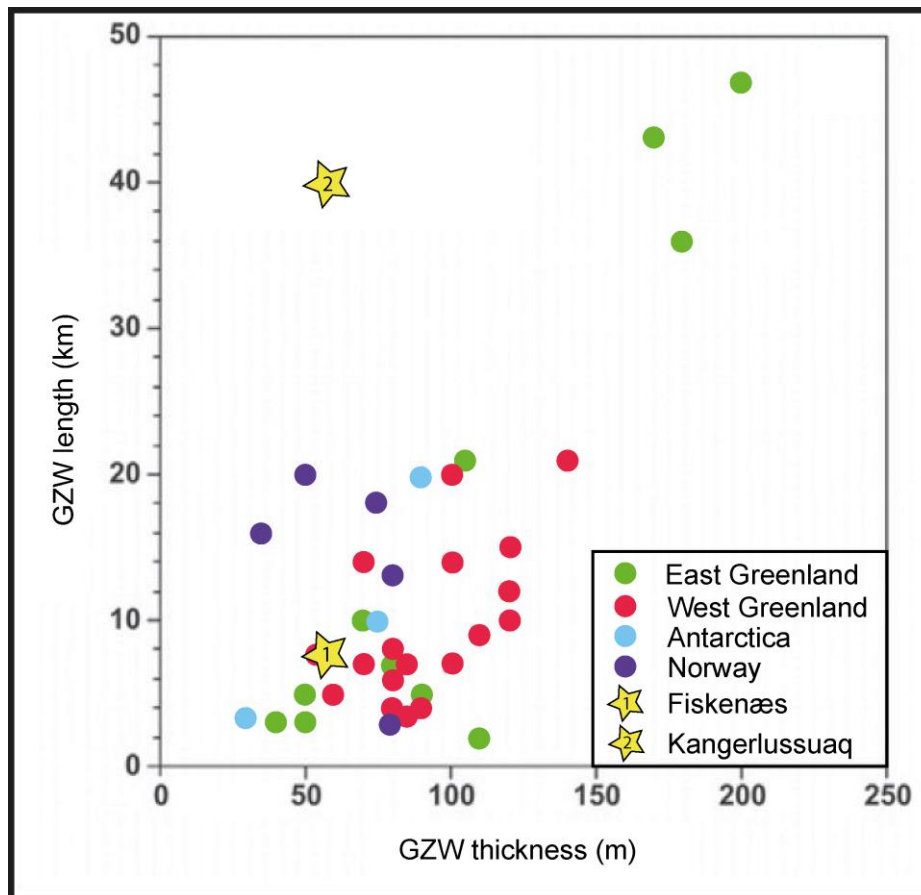


Figure 3.14. Scatter plots of GZW thickness and length data from high-latitude continental shelves of east and west of Greenland, west of Norway and the Barents Sea, and around Antarctica (Heroy and Anderson, 2005; Ottesen et al., 2005, 2008; Mosola and Anderson, 2006; Graham et al., 2010; Rebesco et al., 2011; Dowdeswell and Fugelli, 2012). The GZWs identified in this thesis are displayed with yellow stars (1 and 2). Adapted from Dowdeswell and Fugelli (2012).

3.10. Curvilinear depressions or ploughmarks

3.10.1. Description

In some areas that are covered by multi-beam data (Fig. 2.2) and where there is relatively high Olex data resolution, numerous irregular curvilinear depressions are identified in the sedimentary sea floor (Fig. 3.15). These features are linear and curvilinear, have widths of a few tens of metres, depths of 10 – 25 m, and lengths of up to 20 km. The depressions are U-shaped in cross-section and often have berms, of a few metres in height, either side of the

main depression. Where the depressions occur, they are abundant features and cover areas of 1260 and 770 km² on the outer-shelf of Kangerlussuaq Trough and the mid-shelf of the Heimland Bank, Southeast Greenland, respectively. Further discussion about the spatial distribution and orientation of these features will take place in Section 4.2.2.

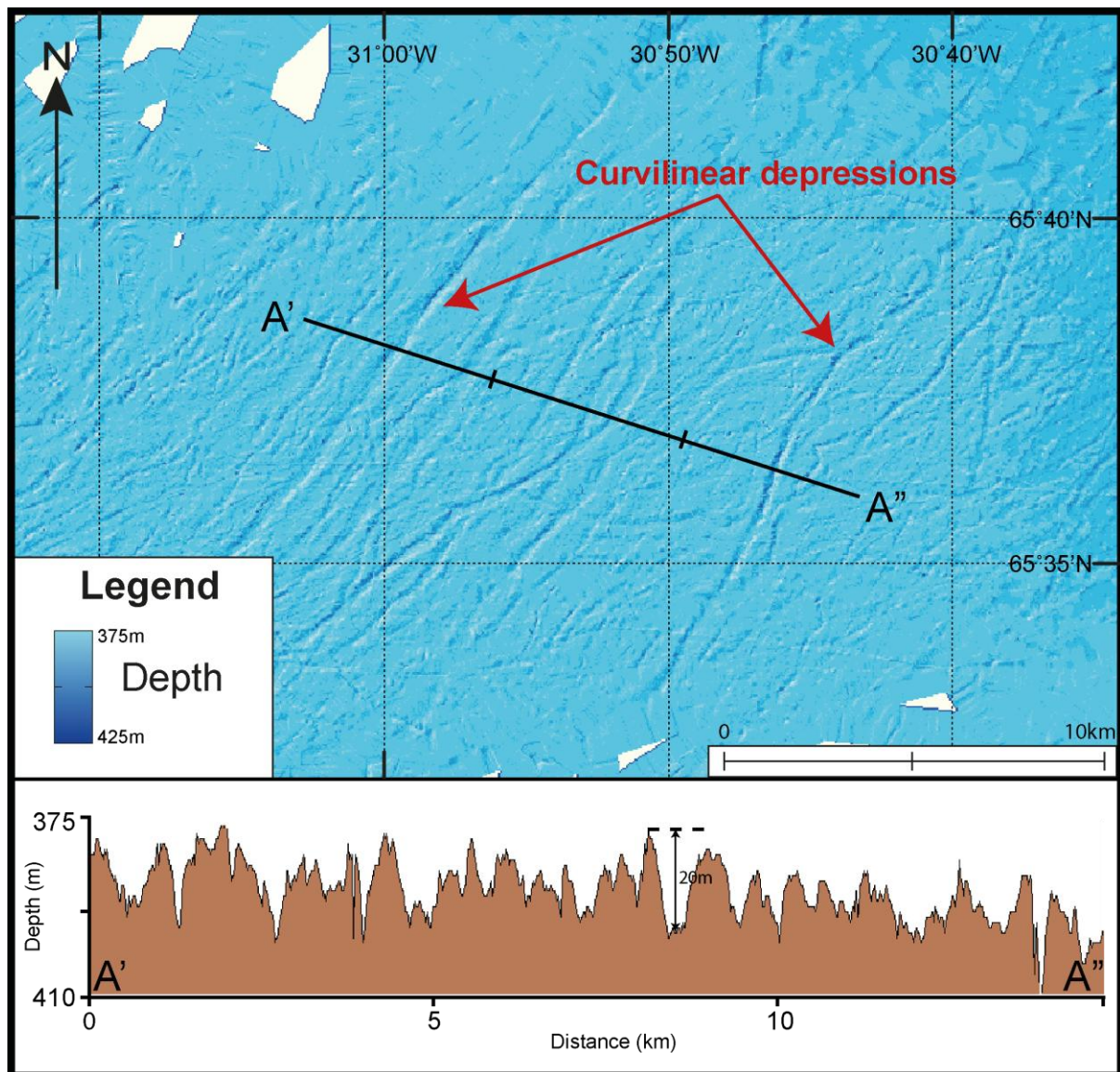


Figure 3.15. Example of irregular curvilinear features or ploughmarks on the outer continental shelf of Kangerlussuaq Trough. Location in Figure 3.1B.

3.10.2. Interpretation

These features are interpreted to have formed by the ploughing action of iceberg keels on the sea floor as they drift in the ocean (Dowdeswell et al., 1993). Similar iceberg ploughmarks have been identified on high-latitude continental shelves, including offshore of Greenland, and provide information on the former dimensions and drift tracks of icebergs (e.g. Brett and Zarudzki, 1979; Dowdeswell et al., 1993; Syvitski et al., 2001; Kuijpers et al., 2007). Further interpretation based on the spatial distributions of these landforms will be made in Section 4.2.2.

3.11. Features on the continental slope and rise

The continental slope and rise of Southern Greenland have a wide range of geomorphological features. An overview of the main types of features is shown in Figure 3.16 where IBCAO and multi-beam data were combined to allow the wider context of these features to be analysed. Three contrasting sets of features exist on the continental slope and rise which will be described and interpreted in the following sections.

3.11.1. Set 1 - Gullies

3.11.1.1. Description

A number of gully-like features are identified on the upper continental slopes of Southwest Greenland in the multi-beam data (Fig. 3.17). The largest of these features have widths of 1.5 – 3 km and depths of 150 - 350 m. The gullies are highly variable in size. Smaller gullies also exist with widths of 50 – 500 m and depths of around 20 - 50 m. The features extend for up to 14 km in length and have a low sinuosity. The upstream parts of the gullies are usually V-shaped in cross-section, steep-sided and symmetrical. This shape gradually changes to a gentler, U-shaped cross-section further downstream. In some cases, the upstream heads of the gullies bifurcate but downstream there is little or no branching (Fig. 3.17). Similar gullies are identified on the continental slopes of Southeast Greenland in the Olex data (Fig. 3.18).

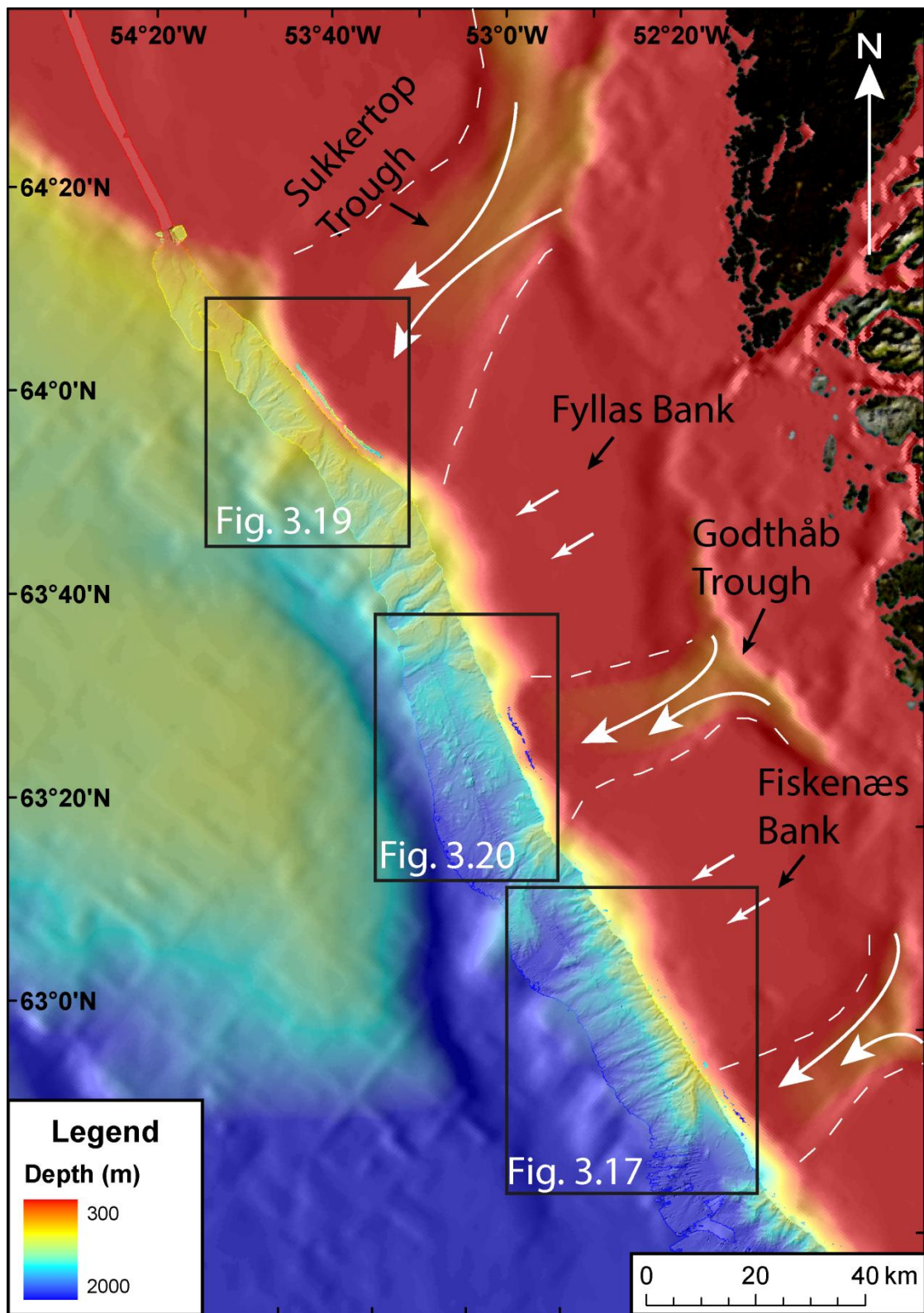


Figure 3.16. The region of Southwest Greenland covered by multi-beam data overlaid onto IBCAO data. The multi-beam data are gridded at a cell size of 100 m. The major banks and troughs discussed in this section are labelled in black and the direction of inferred ice flow during full-glacial periods is labelled with white arrows.

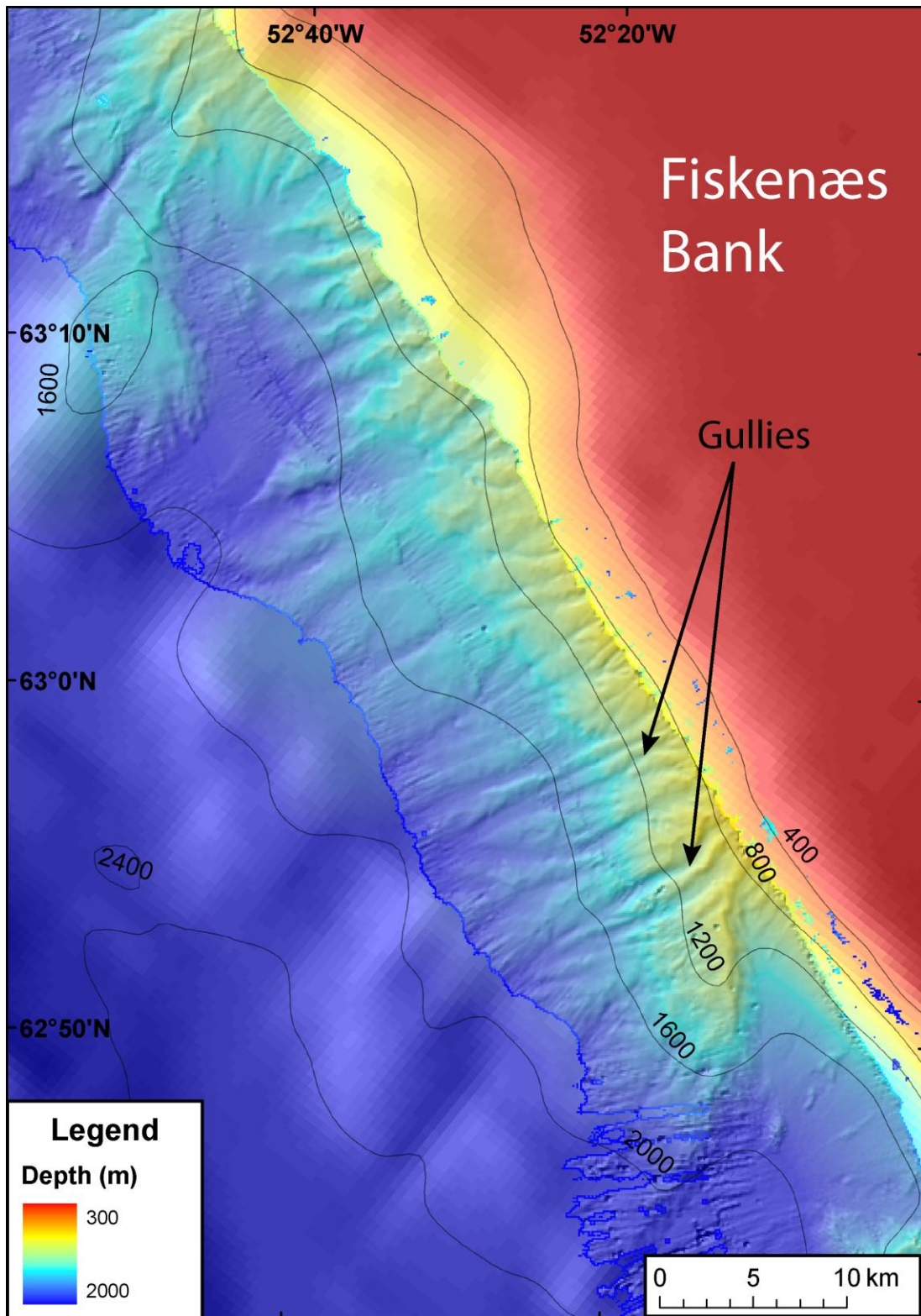


Figure 3.17. Example of the gullies identified in the multi-beam data. These gullies are identified on the continental slope adjacent to Fiskenæs Bank and have widths of 1 – 3 km and depths of 150 – 350 m. The shelf edge is approximated by the 400 m contour. Location in Figure 3.16.

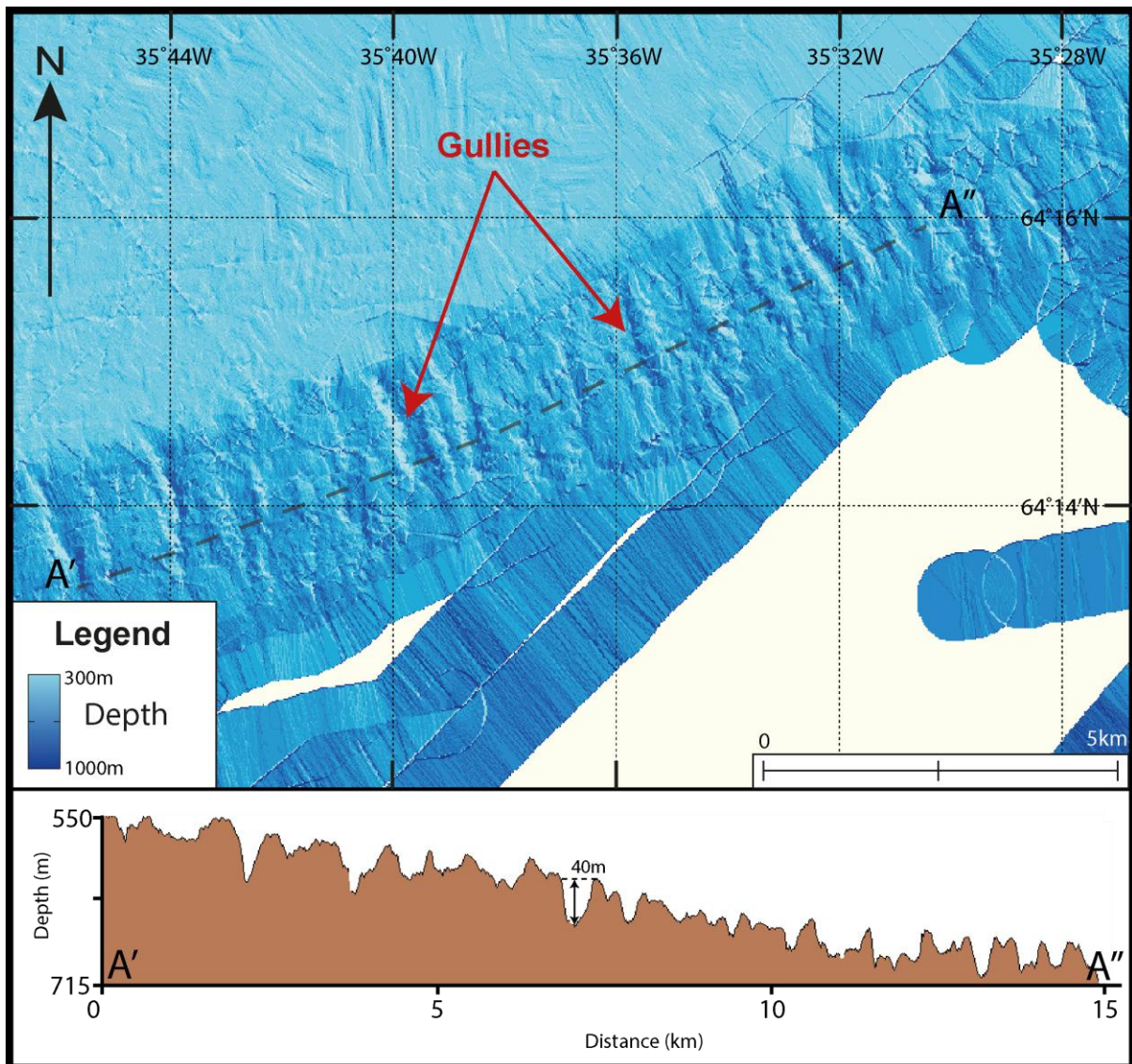


Figure 3.18. Example of some of the gully-like features identified on the continental slopes of Southeast Greenland from the Olex data. These gullies have depths of 20 – 50 m and widths of 50 – 150 m. Location in Figure 3.1B.

3.11.1.2. Interpretation

The steep-sided, symmetrical gullies are interpreted as evidence for high-energy gravity-driven erosion processes occurring on the continental slopes of Southern Greenland. Gullies incise many high-latitude (Vanneste and Larter, 1995; Shipp et al., 1999; Dowdeswell et al., 2004, 2006, 2008; Laberg et al., 2007; Noormets et al., 2009; Gales et al., 2012, 2013) and mid-latitude continental margins (Micallef and Mountjoy, 2011; Piper et al., 2012; Vachtman

et al., 2012). There are a number of hypotheses for gully formation. These include mass flows, subglacial meltwater discharge and dense bottom water overflow.

The gullies identified in Southwest Greenland have symmetrical V-shaped cross-sections, low sinuosity and lack of extensive branching. These gullies are therefore similar to the Type *I* gullies identified on the Antarctic continental slopes by Gales et al. (2013). Type *I* gullies are thought to have been caused by the high erosive power of active fluid flow (Gales et al., 2013). The cascading of dense bottom water is a more passive process and is probably not able to produce such distinctive V-shaped cross-sections with low sinuosity (Piper and Normark, 2009; Gales et al., 2013). The spatial distribution of gullies will be analysed in Section 4.3.2 to further investigate the glaciological implications of these features.

3.11.2. Set 2 – Dendritic channel system and elongate depression with sidewall escarpment

3.11.2.1. Description

On the continental slope of Southwest Greenland, a dendritic channel system dissects a number of sediment mounds (Fig. 3.19). Smaller channels originate on the upper continental slope offshore of Sukkertop Trough, at a depth of about 1000 m. These channels coalesce to form large channels down-slope at a depth of 1200 m. The large channels probably extend further down-slope but there is a lack of multi-beam data coverage in this area (Fig. 3.19). The smaller channels have widths of about 1000 m and depths of 70 m. The large, down-slope channels have widths of over 1500 m and depths of over 120 m (Fig. 3.19). The channels dissect large sediment mounds. The mound labelled in Figure 3.20 has a length of 18 km and a maximum width of 7 km.

An elongate depression downslope of prominent vertical sidewall escarpment is also identified from the multi-beam data and labelled in Figure 3.19. The escarpment has a height of 60 – 70 m. The depression beneath the escarpment has a smooth floor with a width of about 4 km.

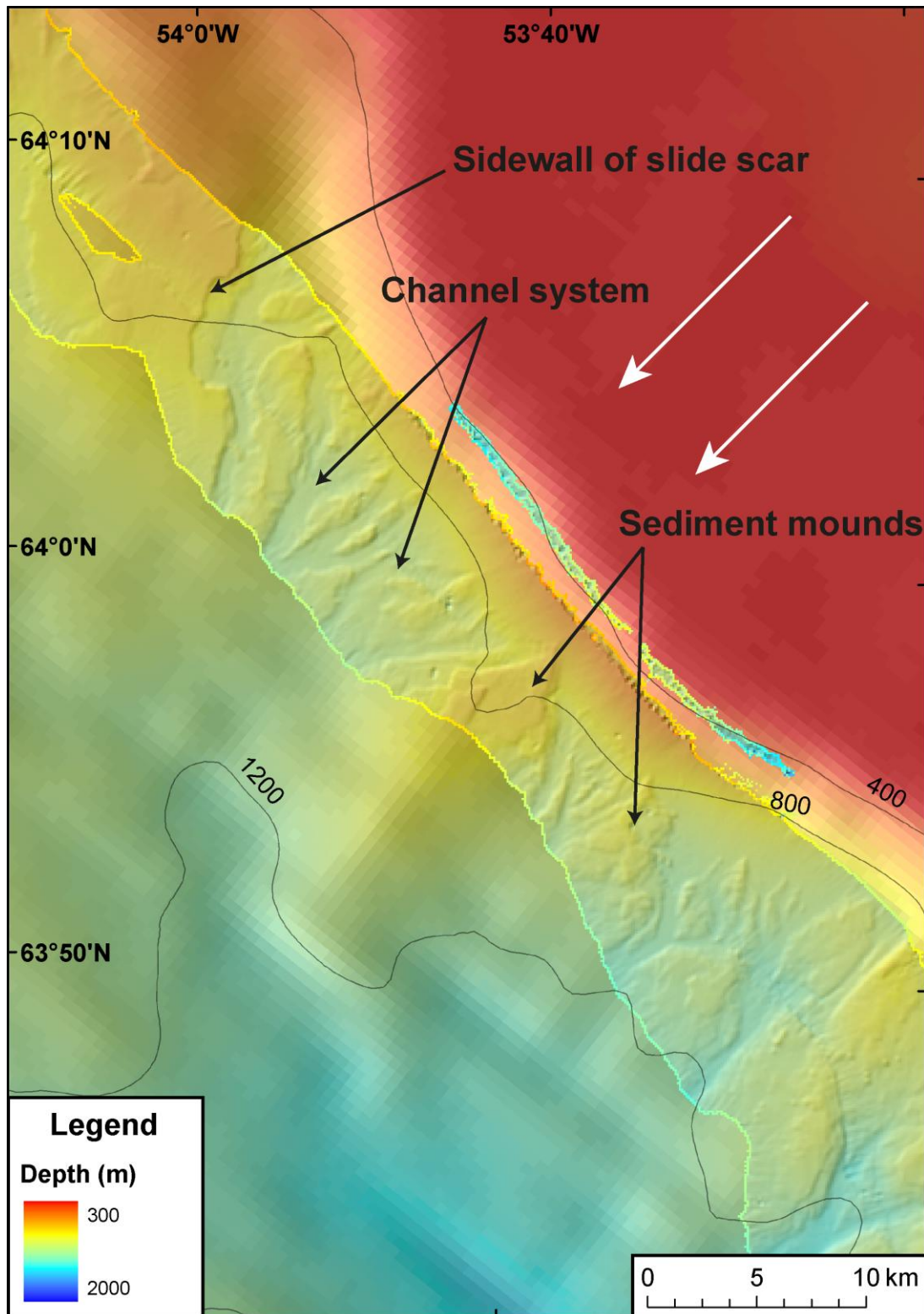


Figure 3.19. A dendritic channel system dissects a number of sediment mounds on the continental slope adjacent to Sukkertop Trough. A prominent sidewall escarpment with a height of 70 m is also identified above an elongate depression. White arrows indicate inferred direction of ice flow during full-glacial periods. Location in Figure 3.16.

3.11.2.2. Interpretation

The dendritic channel system that dissects a number of sediment mounds is interpreted as evidence for down-slope flowing turbidity currents. The sediment mounds are probably composed of finer material delivered to the base of the continental slope by the turbidity currents (Dowdeswell et al., 2004). A similar set of features were identified on the continental slope offshore of Marguerite Trough, Antarctic Peninsula (Dowdeswell et al., 2004). Further discussion is needed to determine the mechanisms that could have caused the turbidity currents. This will take place in Section 4.3.2.

The elongate depression down-slope of a prominent sidewall escarpment is interpreted as a slide scar. This feature was probably formed by the removal of a slab of sediment by translational slide from the upper to the lower continental slope (Baeten et al., 2013). Translational slides involve the displacement of material along one or more discrete shear surfaces (Baeten et al., 2013). The slide scar indicates that potentially unstable and failure-prone segments of the shelf edge have collapsed at some time in the past (Laberg and Vorren, 2000; Noormets et al., 2009). The preconditions for the formation of an unstable shelf edge could have resulted from the rapid deposition of glacially derived or glacially influenced debris at the shelf edge by the Greenland Ice Sheet when ice extended onto the continental shelf edge (Laberg and Vorren, 1996; Laberg and Vorren, 2000; Ó Cofaigh et al., 2005; Vanneste et al., 2006; Noormets et al., 2009). The exact mechanism triggering debris flows is not known and the mechanism probably varies with location.

3.11.3. Set 3 - Wide flat-floored valleys with blocky terrain

3.11.3.1. Description

Wide, flat-floored valleys with ‘blocky’ terrain are identified on the continental slope offshore of several large troughs in Southwest Greenland (Fig. 3.20). The widths of the flat-floored valleys are 34, 15 and 20 km on the slopes offshore of Godthåb, Fiskenes and Frederikshåbs troughs, respectively

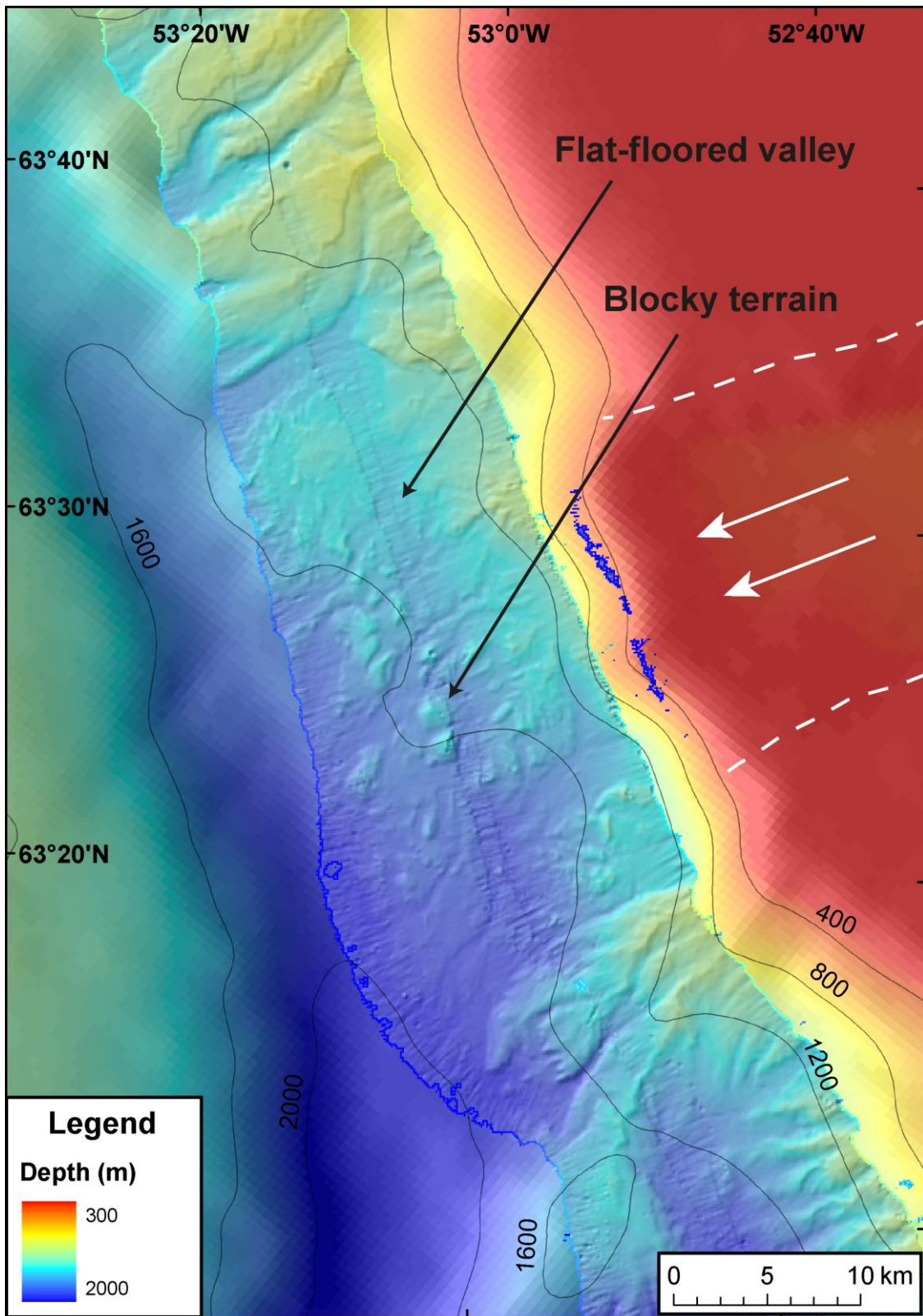


Figure 3.20. Blocky terrain in a wide, flat-floored valley at the bottom of the continental slope. The valley is 34 km in width. The margins of the Godthåb Trough are labelled with dotted white lines and white arrows indicate the direction of inferred palaeo-ice flow. Location in Figure 3.16.

3.11.3.2. Interpretation

The wide, flat-floored valleys are thought to have been formed by large subglacial meltwater outburst flows (Fig. 3.20). Similar features have been identified on the Laurentian and Northeast fans on the Eastern Canadian continental margin (Piper et al., 2007; Piper and Normark, 2009; Piper et al., 2012).

The blocky terrain is interpreted as evidence of debris flows that have resulted in the accumulation of mass-transport deposits at the base of the continental slope (Piper et al., 2012). This terrain is also identified in the seismic profile in Figure 3.3. Similar blocky terrain has been observed in the lower parts of the Hinlopen Slide, north of Svalbard, and the Traenadjupet Slide offshore of Northern Norway (Laberg and Vorren, 2000; Vanneste et al., 2006).

Further interpretation of these sets of features depends on the analysis of the spatial distributions of the slide scars, gullies and blocky terrain. This will be discussed in Section 4.3.2.

3.12. Flat and featureless sea floor

3.12.1. Description

Some areas of the sea floor appear flat and apparently featureless even when the resolution of the Olex data is relatively high. The best example is the floor of Frederikshåbs Trough, Southwest Greenland (Fig. 3.21). The featureless sea floor in Frederikshåbs Trough has an area of 340 km². It should be noted that the linear features on the floor of the trough are not real features and were probably caused by poor bathymetric depth measurements by ships collecting Olex data (Section 2.4.3).

3.12.2. Interpretation

These featureless sections of the sea floor were investigated using seismic reflection profilers in the 1970s (Roksandić, 1979). The seismic profiles show that Frederikshåbs Trough and its tributaries are asymmetrically shaped valleys that are filled with a well-stratified sedimentary sequence characterised by an even-layered parallel seismic facies composed of clay, silt and sand (Roksandić, 1979). The maximum thickness of the seismic facies is about 270 – 290 m

(Roksandić, 1979). The sequence is interpreted as sedimentation of fine-grained sediment by glacial and glaciofluvial meltwater sources following ice retreat across the continental shelf.

Similar acoustically stratified facies were identified by Dowdeswell et al. (In Press) in Rink Fjord and Karrat Isfjord, West Greenland. This smooth sea floor was also interpreted as fine-grained basin fill derived largely from meltwater sedimentation.

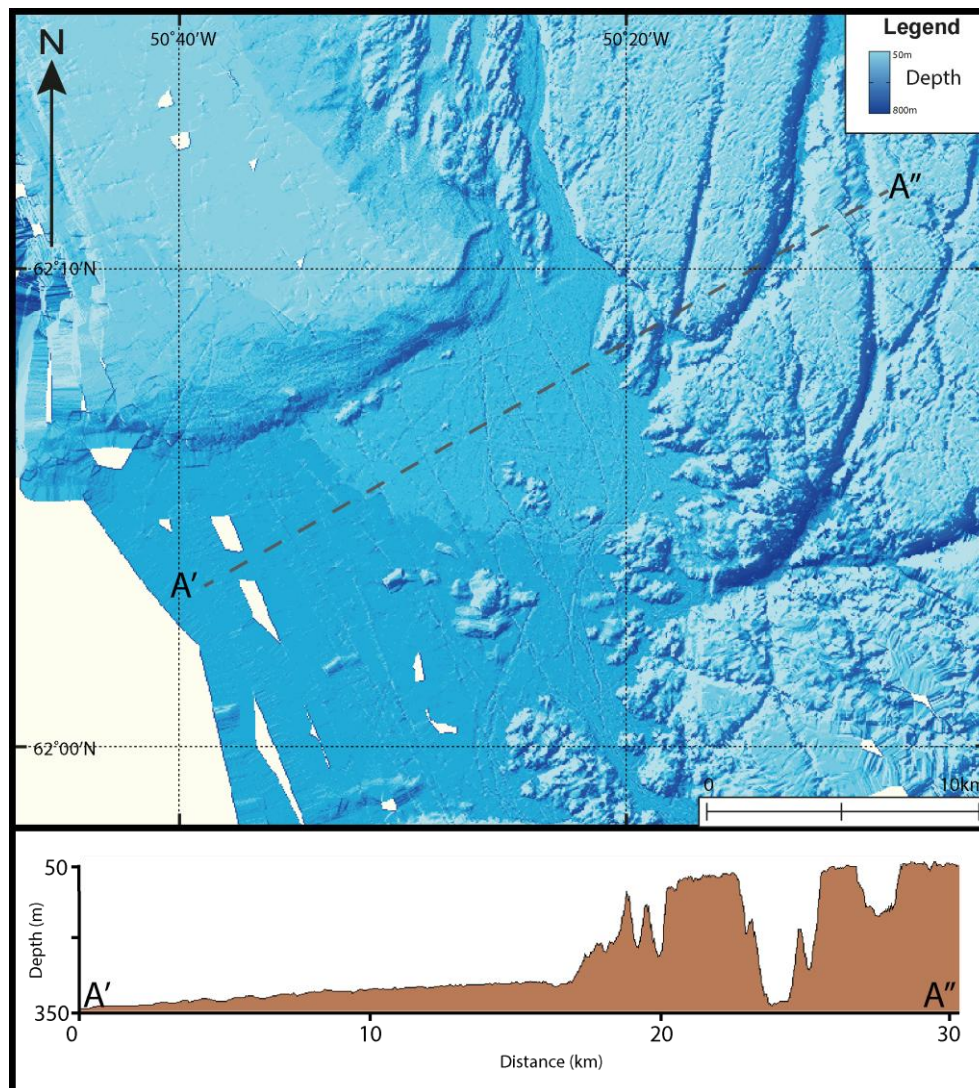


Figure 3.21. The flat, featureless sea floor of Frederikshåbs Trough. It covers an area of 340 km². Location in Figure 3.1D.

3.13. Summary

This chapter has described and interpreted the individual morphology of a number of features identified in the Olex, multi-beam and IBCAO data. The interpretations made in this chapter will be used in the next chapter to describe the locations and spatial distributions of the landforms identified. Where possible, the glaciological implications of the landform distributions will be discussed.

4. Synthesis and identification of submarine landform assemblages on the Southern Greenland continental margin

This chapter describes the spatial distribution of the landforms identified in Chapter 3 in order to make more conclusive interpretations about the geomorphology of the continental margins of Southern Greenland. These landform assemblages are discussed in an order based on the location of these features on the continental margin and the substrate that they were formed in. The landform assemblages therefore fall into one of three categories. These are:

- Bedrock-dominated inner shelf
- Sedimentary outer shelf
- Continental slope

Schematic maps (e.g. Fig. 4.2, 4.4) show that the spatial distribution of landforms and the types of submarine landforms change from the inner- to the outer- continental shelf and onto the continental slope. The locations of the schematic maps can be found in Figure 4.1.

4.1. Bedrock-dominated inner shelf

4.1.1. Meltwater channels

A number of bedrock channels are cut into the strandflat in Southwest Greenland (Figs. 4.2, 4.3). Where the resolution of the Olex data is relatively high, these channels are easily identified. In Southeast Greenland some very large channels are observed but their extent and morphology is difficult to describe as the resolution of the Olex data in these regions is poor.

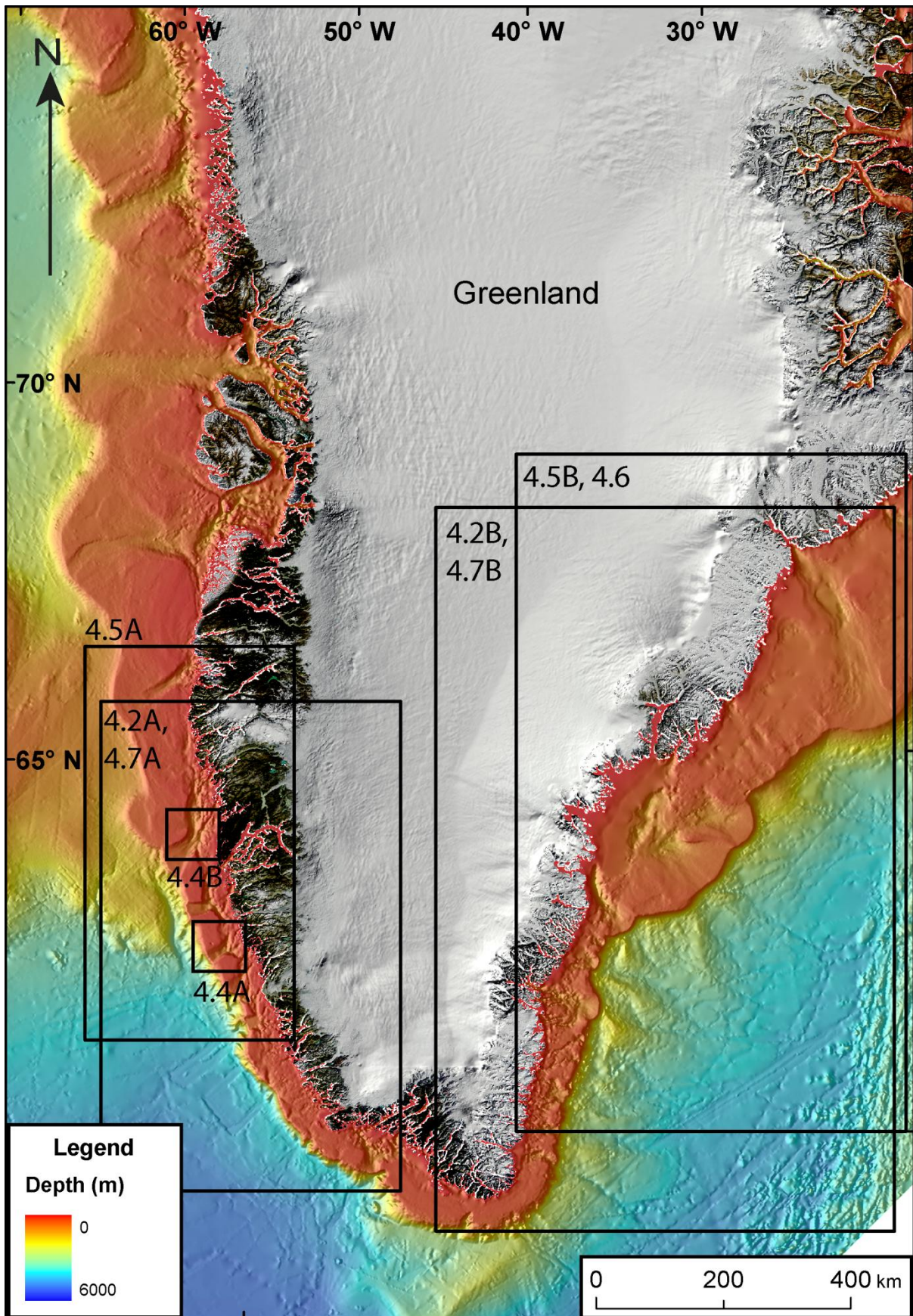


Figure 4.1. Map of the continent and continental margins of Greenland with the locations of subsequent figures in black boxes.

The proximity of the Greenland Ice Sheet means that the channels were probably eroded, at least partially, by meltwater. Figures 4.2 and 4.3 show that the channels are located on the inner shelf where the substrate consists of hard bedrock (Fig. 3.2). Meltwater channels cut into bedrock are common features on formerly glaciated continental shelves in both hemispheres (e.g. Ó Cofaigh et al., 2002; Lowe and Anderson, 2003; Graham et al., 2009; Nitsche et al., 2013). Channels are not identified on the outer shelf where the substrate is sedimentary and softer (Fig. 4.2). A similar absence of channels on the sedimentary outer shelf is also observed in Antarctica (e.g. Ó Cofaigh et al., 2002). This suggests that, if subglacial meltwater existed at the base of the Greenland Ice Sheet in areas where the bed was sedimentary, the majority of it flowed through the topmost soft sediment layer or through a distributed system (Tulaczyk et al., 1998; Boulton et al., 2007a,b). A channelised meltwater system may have formed when meltwater production exceeded the flux that can be discharged through the basal sediment layer but it is thought that such a system would exist only temporarily (Clark and Walder, 1994; Tulaczyk et al., 1998).

It is inferred that the Greenland Ice Sheet extended over these channels during Quaternary glacial periods. However, the environment in which these channels were formed and whether or not they contained water during glacial periods is uncertain. The next section therefore investigates the morphology of the bedrock channels and discusses their likely formation and role during glacial periods.

4.1.1.1. Subglacial channels

The morphology and dimensions of the channels described in Section 3.5.1 is similar to the channels observed on the inner shelf of Dotson, Getz B, Pine Island Bay troughs, West Antarctica, and Marguerite Bay and Palmer Deep, Antarctic Peninsula (Lowe and Anderson, 2003; Domack et al., 2006; Anderson and Oakes-Fretwell, 2008; Graham et al., 2009; Nitsche et al., 2013). These deep, V-shaped channels are eroded exclusively into bedrock substrate and are thought to have formed beneath an ice sheet during multiple large subglacial meltwater discharge events, such as subglacial lake outburst, or by constant, steady-state meltwater erosion over successive glacial phases (Graham et al., 2009).

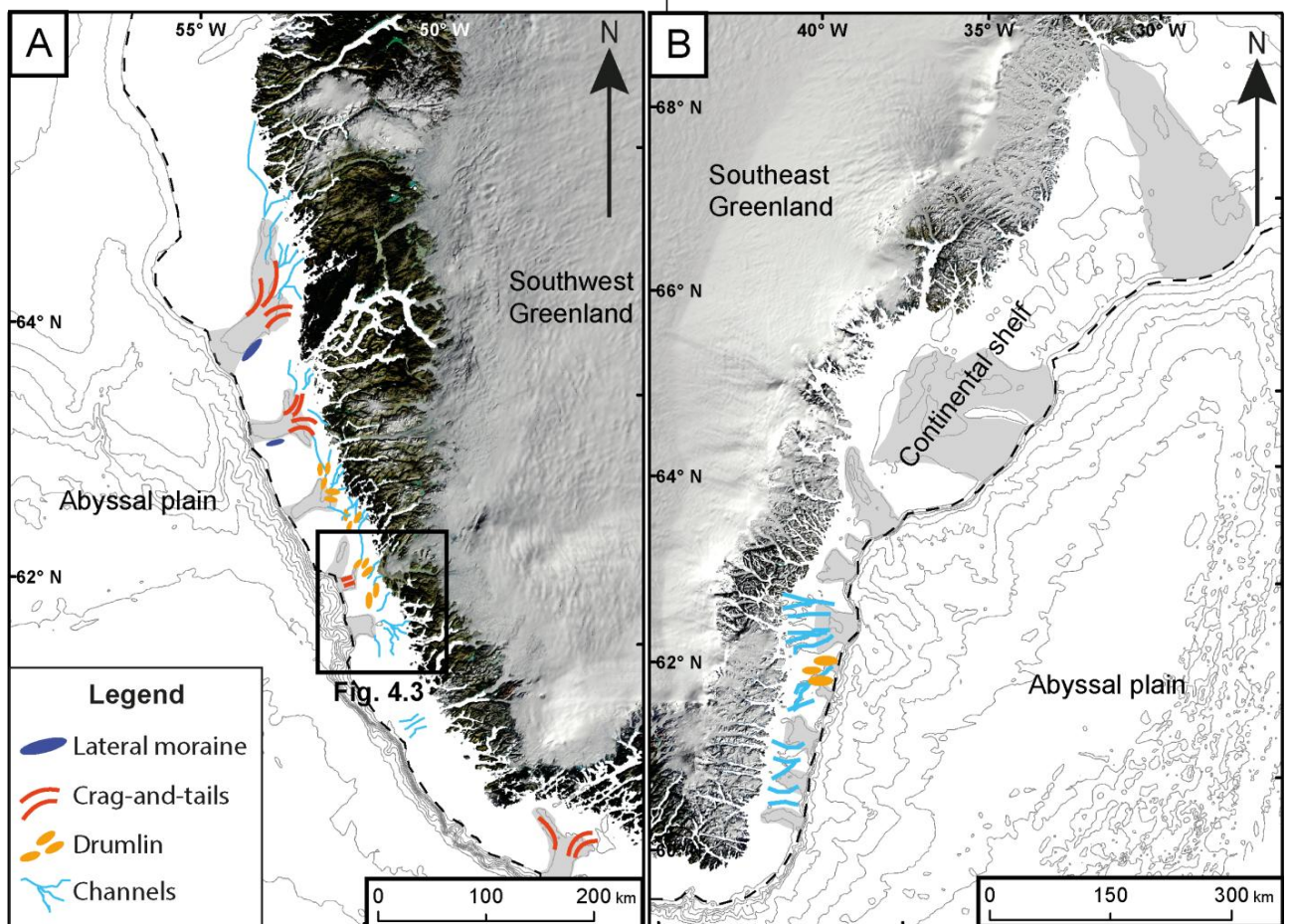


Figure 4.2. The distribution of landforms on the bedrock-dominated inner shelf. Meltwater channels and drumlins are exclusively situated on bedrock substrate. Crag-and-tails are usually located at the transition between bedrock and sedimentary substrate. More channels are identified on the inner shelf of Southwest Greenland than Southeast Greenland, but this is probably due to better Olex data resolution in the southwest. Location in Figure 4.1.

In addition, flow in water-filled subglacial channels is driven by gradients in water pressure as well as bed elevation. Water pressure gradients are determined primarily by the glacier surface slope (Shreve, 1972). As a consequence, water in subglacial channels can flow uphill. Undulatory long profiles of meltwater channels as they cross topographic barriers are therefore an important criterion for distinguishing subglacial meltwater channels from meltwater channels formed in subaerial environments (Benn and Evans, 2010). The long profiles of channels identified in Southern Greenland are also undulatory (Fig. 4.3). This

suggests that pressurised subglacial meltwater has been, at least partially, responsible for the erosion of the channels observed on the inner continental shelf of Southern Greenland.

4.1.1.2. Proglacial channels

In proglacial environments, powerful streams draining a glacier may cut distinct channels or gorges as the water flows away from the ice margin. Channels and gorges cut by proglacial streams can reach impressive dimensions (e.g. Kleman et al., 2001). In areas formerly occupied by glacier ice, however, it is difficult to determine the relative contribution of subglacial and subaerial erosion. For example, the channels could be pre-existing fluvial channels that were subsequently filled by subglacial meltwater, which further eroded the channels. It is likely that the inner continental shelf of Southern Greenland was exposed to the atmosphere before the inception of ice cover on Greenland seven million years ago (Larsen et al., 1994). Therefore fluvial processes may well have eroded parts of the channels that are identified in the bathymetry today. Whether or not fluvial erosion alone would have the power to erode such large features is unclear.

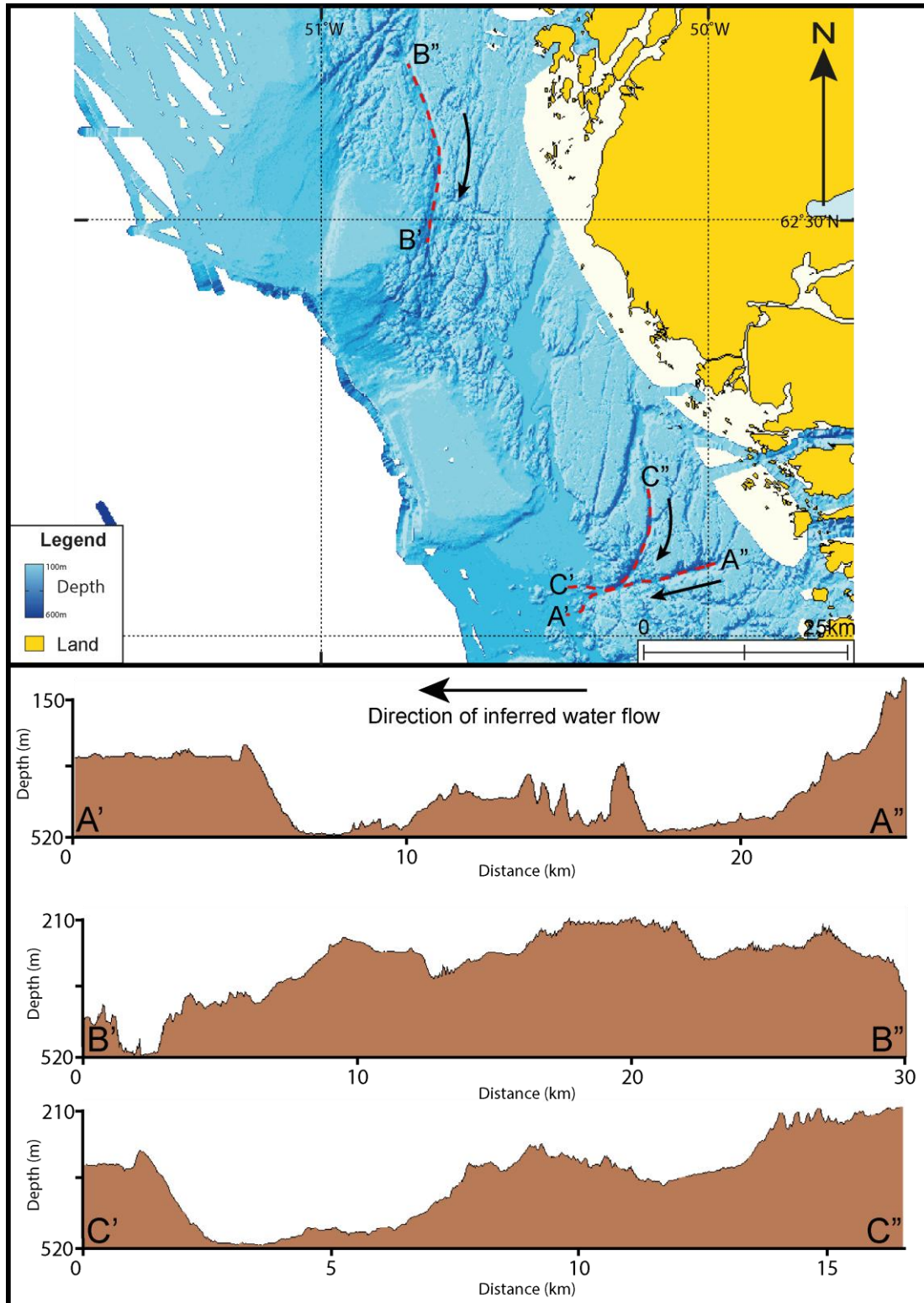


Figure 4.3. Long profiles of three channels identified on the inner shelf of Southwest Greenland. Their undulatory nature suggests that water that flowed through these channels was influenced by water pressure gradients as well as elevation gradients. Arrows indicate inferred water flow direction. Location in Figure 4.2.

4.1.2. Streamlined landforms assemblages

4.1.2.1. Description

The cross-shelf troughs contain a number of geomorphological features that are indicative of the former presence of active ice flow on the continental shelf of Southern Greenland (Fig. 4.2). The distribution of landforms identified on the inner shelf of Fiskenæs Trough and Sukkertop Trough, Southwest Greenland is shown in Figure 4.4. On the inner shelf of Fiskenæs Trough (Fig. 4.4A) a number of channels and drumlins are eroded into the crystalline bedrock. Both the channels and the drumlins are orientated in the direction of the trunk zone of the trough. Due to the poor coverage of data, no landforms were identified on the outer shelf of Fiskenæs Trough. In Sukkertop Trough, however, a number of crag-and-tails were identified (Fig. 4.4B). These landforms are situated on what is inferred to be the boundary between the hard crystalline bedrock on the inner shelf and the sedimentary substrate on the outer shelf. The crag-and-tails are also orientated in the direction of the main trough long axis but are much more elongate than the drumlins identified in Figure 4.4A.

4.1.2.2. Interpretation

Similar landform assemblages illustrated in Figure 4.4 have been identified on formerly glaciated inner continental shelves in other parts of the Arctic and Antarctic (Ó Cofaigh et al., 2002; Lowe and Anderson, 2003; Anderson and Oakes-Fretwell, 2008). This landform assemblage has been interpreted as evidence for the onset zones of fast-flowing palaeo-ice streams (Ó Cofaigh et al., 2002; Anderson and Oakes-Fretwell, 2008; Graham et al., 2009; Livingstone et al., 2012a).

The streamlined landforms show a clear increase in elongation ratios (from drumlins with an elongation ratio of between 2 and 5, to crag-and-tails with an elongation ratio of between 8 and 20) at the transition between crystalline bedrock and sedimentary substrate on the outer shelf. This is thought to be a result of palaeo-ice stream acceleration (Canals et al., 2000; Wellner et al., 2001, 2006; Ó Cofaigh et al., 2002; Ottesen et al., 2005). Crag-and-tails are thought to reflect a long 'pressure shadow' under the ice in the lee of the bedrock 'crag'. This suggests that the ice-stream that filled these troughs had a high sliding velocity (Benn and Evans, 2010). The fan shape arrangement of the crag-and-tail landforms demonstrates a convergent pattern of palaeo-ice flow (Clark, 1993; Stokes and Clark, 1999, 2001). Finally, the lateral moraines (Fig. 4.2, 4.4B) are interpreted to have been produced at the shear zone

between areas of fast and slower flowing ice. The lateral moraines therefore locate the abrupt transition between the fast-flowing palaeo-ice streams in the troughs and passive ice on the banks (Stokes and Clark, 1999).

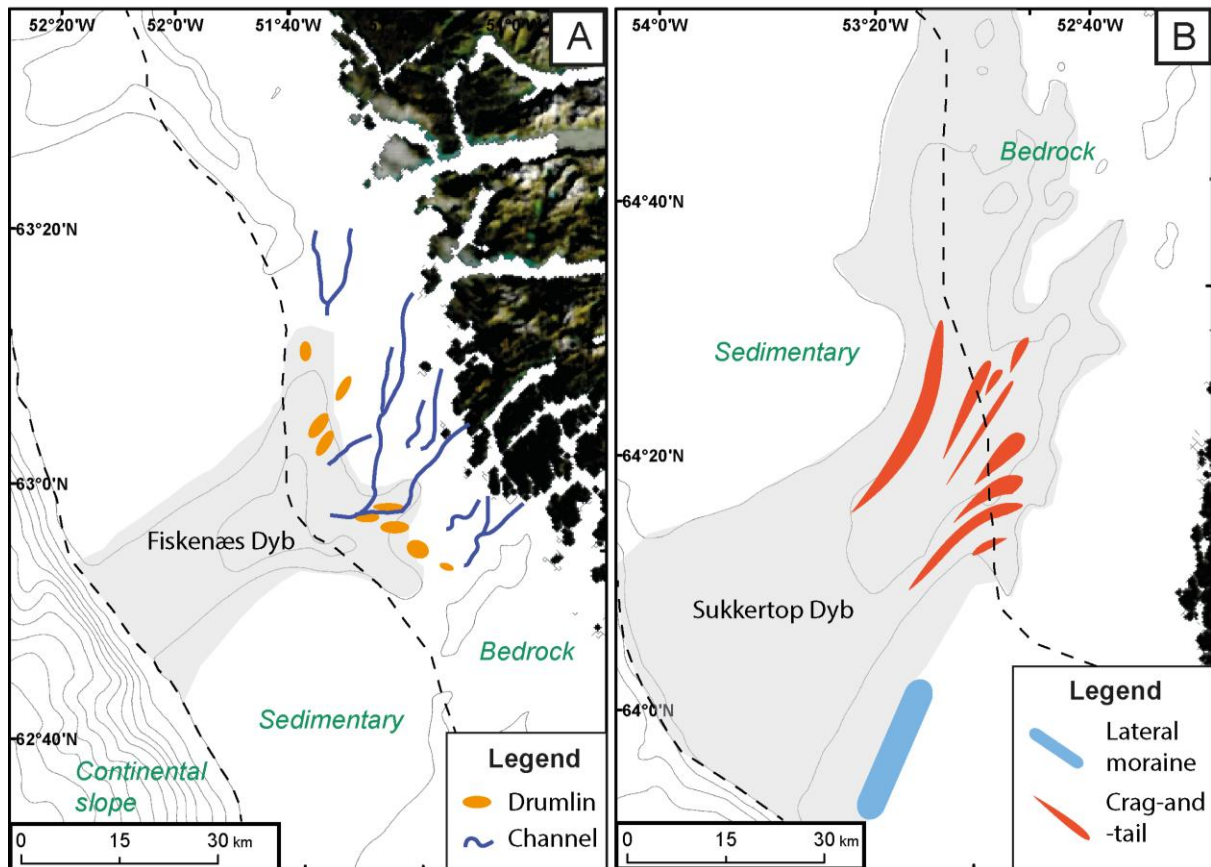


Figure 4.4. (A) A number of drumlins and channels are identified on the inner continental shelf of Fiskenaes Trough. These features are confined to bedrock substrate. (B) At the transition between bedrock and sedimentary substrate, crag-and-tails are identified in Sukkertop Trough. These have 'crag' consisting of bedrock and sedimentary 'tails'. Green labels show the regions of the continental shelf. Location in Figure 4.1.

Despite the relatively high resolution of Olex data in many of the troughs of Southern Greenland, landforms such as MSGs, which are indicative of ice streaming (Clark, 1993; Stoke and Clark, 1999), have not been identified in this study. This, however, also does not preclude their existence. It is thought that these features do exist on the outer parts of the troughs but, due to their subdued nature, they may have been covered by post-glacial sedimentation from either hemipelagic or meltwater sources. In particular, it is inferred that meltwater was abundant during the deglaciation of the Greenland Ice Sheet in Southwest Greenland and the rain-out of fine-grained sediment could have buried subtle features on the outer continental shelf. This process is thought to have buried streamlined landforms in Rink Fjord, West Greenland (Dowdeswell et al., In Press). The existence and quantity of meltwater produced during deglaciation will be discussed in Section 5.3.2.

4.2. Sedimentary outer continental shelf

4.2.1. Distribution of moraines and GZWs

4.2.1.1. Description

The distribution of moraines and GZWs identified in this study is shown in Figure 4.5. Two sets of terminal moraine systems were identified on Tovqussaq Bank (Fig. 4.5A). The outer system has been termed the Outer Hellefisk Moraine System by previous studies (Brett and Zarudzki, 1979; Kelly, 1985). These studies indicate that the Outer Hellefisk Moraine System covers a large area of the outer shelf of Southwest Greenland. This thesis, however, is the first study to identify bathymetric evidence of the existence of these moraines. The Outer Hellefisk moraines are, in fact, relatively subdued features between 20 and 25 m high and around 2 km wide and consist of three individual ridges located at the shelf edge (Fig. 3.12).

Unlike the moraines, which are found on relatively shallow banks, GZWs are located in cross-shelf troughs (Fig. 4.5). They occupy the sedimentary mid-shelf areas of Fiskenæs and Kangerlussuaq troughs. Again, this is the first evidence collected for the existence of these features in these locations.

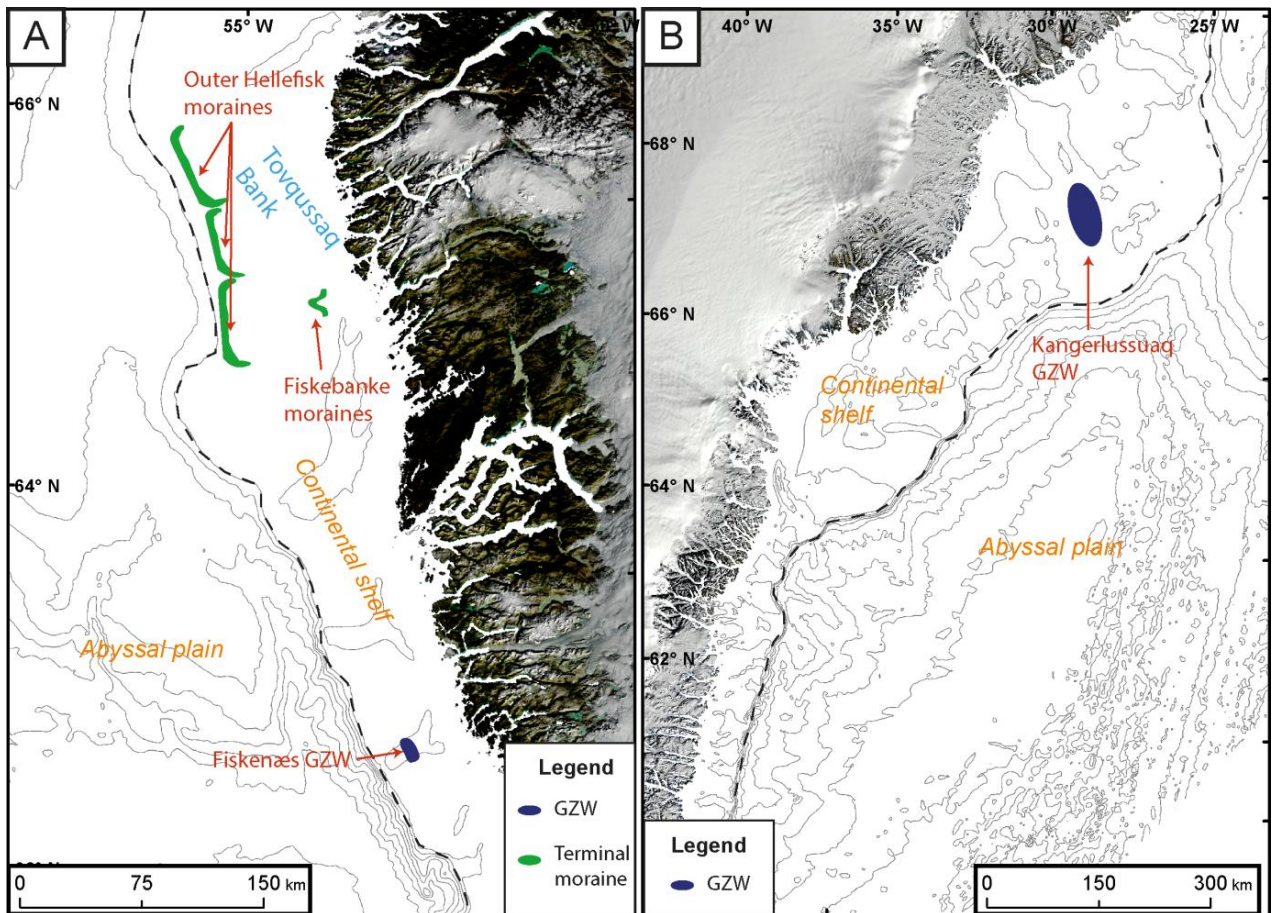


Figure 4.5. Distribution of moraines and GZWs identified on the continental shelf of Southern Greenland. The moraines are located on the banks of the outer shelf whilst the GZWs are located in the mid shelf areas of cross-shelf troughs. Location in Figure 4.1.

4.2.1.2. Interpretation

Terminal moraines

The terminal moraines suggest that the Greenland Ice Sheet extended 100 km across the continental shelf during at least one Quaternary glacial period. The morphology of the Outer Hellefisk moraines is interpreted to reflect the form of the ice front when it was located at the edge of the continental shelf. The presence of these moraines on the shallow banks between ice streams is important because it indicates that ice extended across the shelf not only in troughs, but on the inter-ice stream shallow banks between them. The moraines have crests on their summits which suggest that their development was not constrained by an overlying ice-shelf (Dowdeswell and Fugelli, 2012). This indicates that the ice that extended to the edge

of the continental shelf during one or more glacial periods had a grounded, vertical calving front.

A smaller ridge is identified inshore of the Outer Hellefisk moraines (Figs. 3.12, 4.5A). This ridge is thought to belong to the Fiskebanke moraines identified by Brett and Zarudzki (1979) and Kelly (1985). The ridge suggests the ice margin had a still-stand during a more general period of retreat. In addition, the fact that the ridge is observable in the bathymetry suggests that the moraine has not been overridden by subsequent ice advance.

GZWs

The two GZWs imply that deglacial retreat of the Greenland Ice Sheet across some areas of the Southwest and Southeast Greenland shelf was episodic and punctuated by a still-stand, rather than a single catastrophic collapse (Dowdeswell et al., 2008; Ó Cofaigh et al., 2008). The large volumes of the ridges (4 km³ and 40 km³) and their locations in troughs, suggest that during the still-stand the ice streams located in these troughs deposited large amounts of sediment to the grounding-zone.

The absence of such features in other parts of the Southern Greenland continental shelf implies that retreat of the Greenland Ice Sheet from the continental shelf was a rapid, and possibly catastrophic, event (Fig. 4.5) (Dowdeswell et al., 2008; Ó Cofaigh et al., 2008). GZWs are, however, subdued features and are sometimes difficult to identify in bathymetric data (Bjarnadóttir et al., 2013). Therefore, more GZWs may well exist on the continental shelf of Southern Greenland but still remain unidentified.

4.2.2. Iceberg keel ploughing

Southeast Greenland

Iceberg ploughmarks are identified on vast areas of the sedimentary outer continental shelf surrounding Southeast Greenland in water depths of up to 490 m (Fig. 4.6). Similar ploughmarks were also identified by Johnson et al. (1975), Syvitski et al. (2001) and Dowdeswell et al. (2010). The ploughmarks were probably produced soon after full-glacial periods when the ice margin was retreating from the shelf edge. This is because, today, within 50 km of exiting Kangerlussuaq and Helheim fjords, the East Greenland Current directs all icebergs southwestward, preventing icebergs exiting the fjords from reaching the outer shelf (Andrews et al., 1997). Therefore it is likely that the iceberg ploughmarks were produced by

a palaeo-calving ice margin that calved directly into the main cross-shelf troughs (Syvitski et al., 2001). The northeast-southwest orientation of the ploughmarks adds support to this interpretation (Figs. 3.16, 4.6). Alternatively, icebergs could have been derived from north of Southeast Greenland, from Scoresby Sund for example (Dowdeswell et al., 1993), and travelled south in the East Greenland Current. This means that the possibility that the icebergs came from East and Northeast Greenland cannot be ruled out.

The high density of iceberg ploughmarks suggests that iceberg calving rather than surface melting acted as the dominant process of mass loss during the initial deglaciation of the Greenland Ice Sheet in the southeast.

Iceberg ploughmarks in water depths of more than 300 m are indicative of calving from fast-flowing outlet glaciers (Dowdeswell and Bamber, 2007). In contrast, floating ice shelves produce tabular icebergs with relatively shallower keels. This means that, during deglaciation, the ice sheet that retreated from the continental shelf of Southeast Greenland probably had a grounded, vertical calving front rather than an extensive floating ice shelf for at least some period of time.

Southwest Greenland

In Southwest Greenland, no iceberg ploughmarks were identified. This could be due to the poor Olex coverage on the banks of the outer shelf. Brett and Zarudzki (1979) identified iceberg ploughmarks on the outer shelf of Egedesminde Trough at 68° N, but south of this area, they confirmed that there were no iceberg ploughmarks (Brett and Zarudzki, 1979). This suggests that large numbers of deep-keeled icebergs were not produced during the deglaciation of the Greenland Ice Sheet in the southwest. Therefore, surface melting may have been the dominant mechanism of mass loss in Southwest Greenland. Further discussion about the contrast in initial deglaciation between Southeast and Southwest Greenland will be discussed in Section 5.3.2.

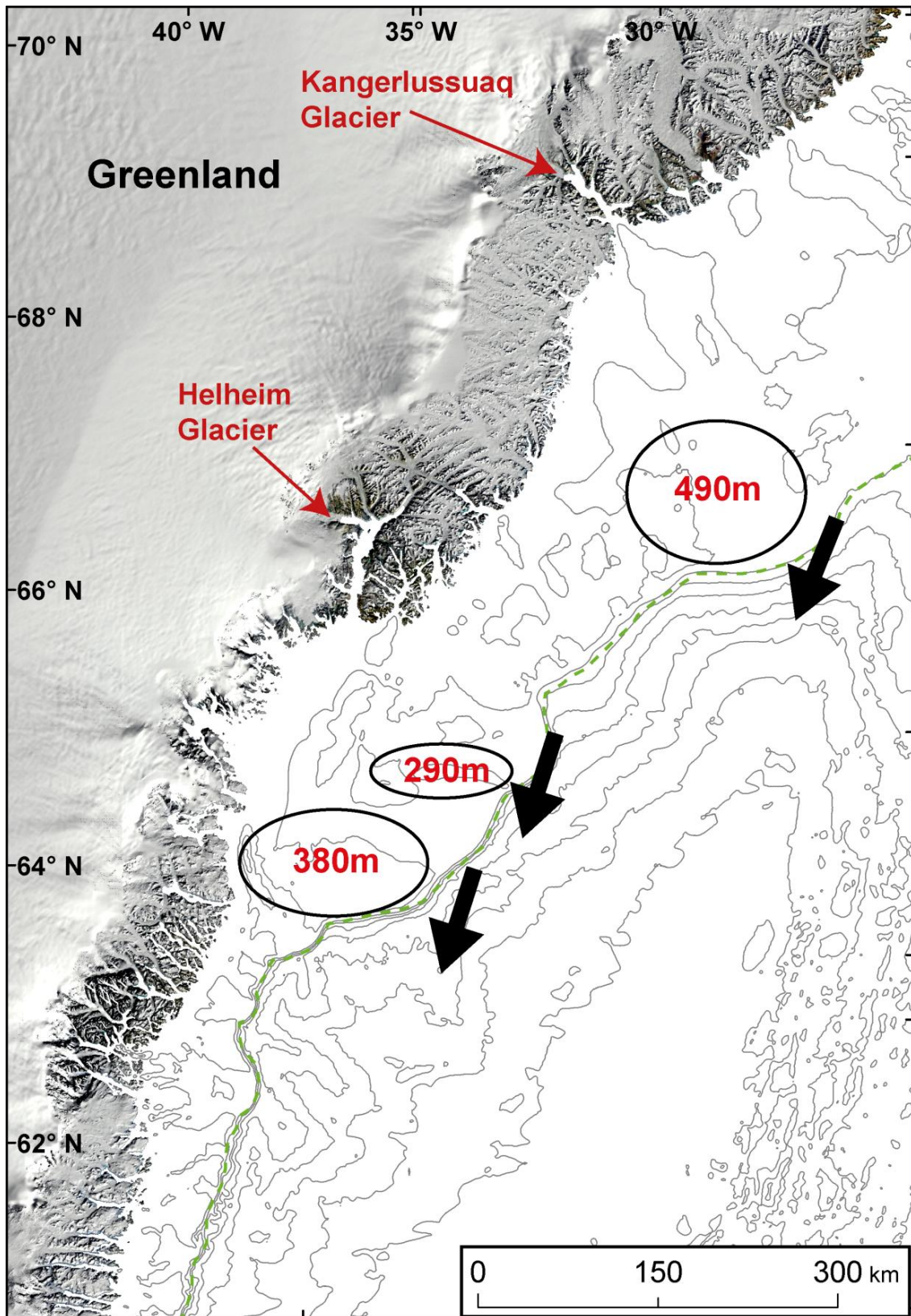


Figure 4.6. The locations and maximum depths of iceberg ploughmarks identified on the continental shelf of Southeast Greenland. Green dotted line shows location of continental shelf edge. Location in Figure 4.1.

4.3. Continental slope

4.3.1. Distribution of the presence and absence of TMFs

4.3.1.1. Description

The continental slopes of the Southern Greenland continental margin exhibit a range of geomorphological features from large TMFs to small gullies (Figs. 3.7, 4.7). At the largest scale, Batchelor and Dowdeswell (In Press) divide the continental slopes of the Arctic margins that exhibit outward bulging of bathymetric contours into two types. Type 1 slopes possess gradients of $< 4^\circ$. Type 2 slopes possess gradients of $> 4^\circ$. Continental slopes that are not associated with outward bulging bathymetric contours are classified as Type 3 (Batchelor and Dowdeswell, In Press). They suggest that Type 1 slopes are probably associated with TMFs. Type 2 slopes are probably too steep to support a TMF but are likely to be associated with prograding sedimentary prisms (Fig. 3.3).

In Southern Greenland, only the continental slopes offshore of Kangerlussuaq Trough and Sukkertop Trough are associated with Type 1 slopes (Fig. 3.7). These TMFs have slope gradients of 1.8° and 3.5° , respectively. Sermilik, Angmagssalik, Gyldenløves, Skjoldungen and Tingmiarmiut troughs in Southeast Greenland have outward bulging bathymetric contours but have fairly steep slopes of 6.0° , 8.8° , 11.3° , 10.4° and 9.7° , respectively (Fig. 4.7). These are classified as Type 2 slopes. The other twelve cross-shelf troughs in the study area are classified as Type 3 slopes. These slopes possess steep slope gradients of between 5.7 and 13.1° and have no outward bulging bathymetric contours.

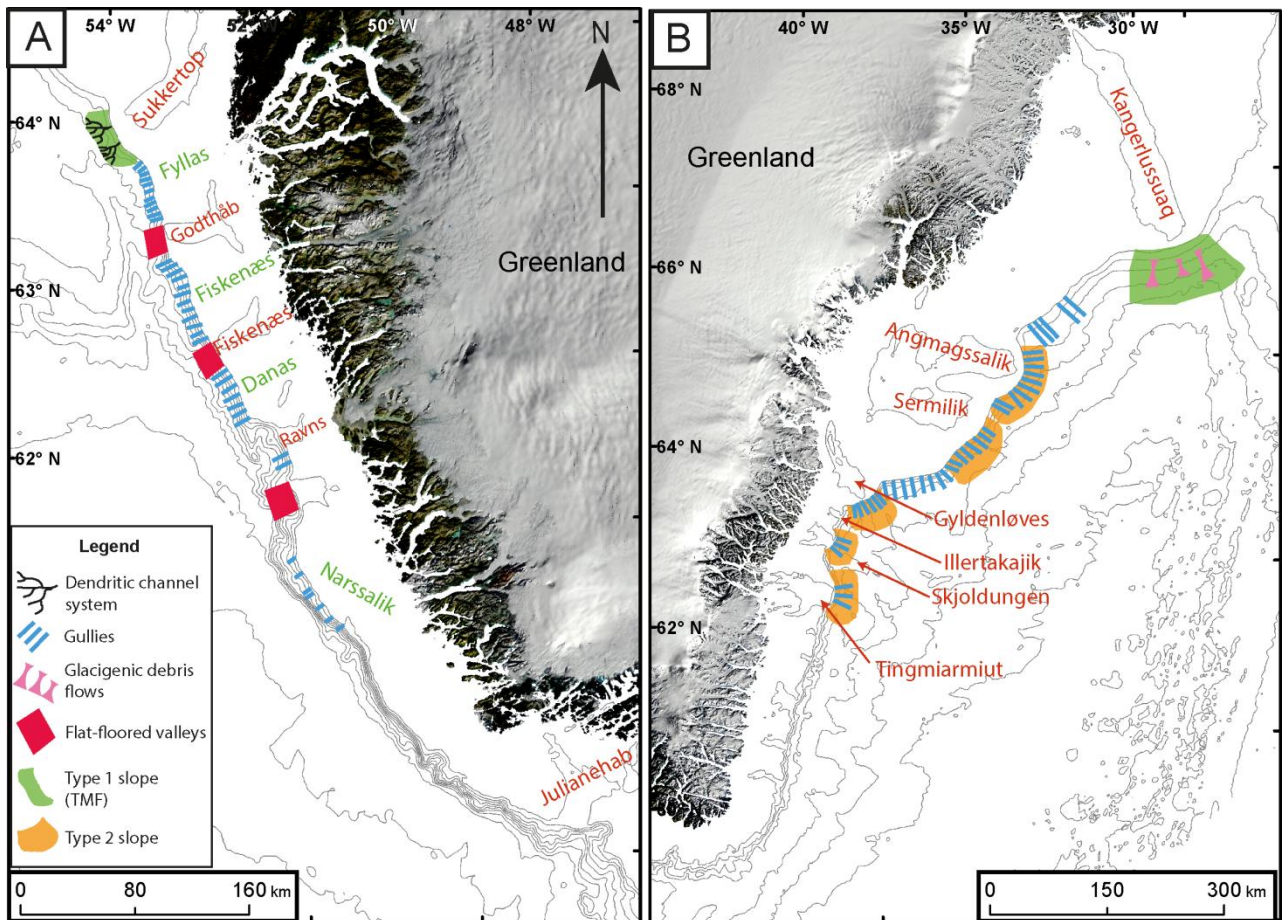


Figure 4.7. The distribution of geomorphic features on the continental slopes of (A) Southwest Greenland and (B) Southeast Greenland. Names of the troughs are labelled in red and names of the banks are labelled in green. Location in Figure 4.1.

4.3.1.2. Interpretation

Type 1 slopes

The large TMFs identified on the continental slopes offshore of Sukkertop and Kangerlussuaq troughs suggest that the upper-slopes have experienced rapid delivery of glacial sediments over successive glaciations when fast-flowing ice streams reached the shelf edge (Dowdeswell et al., 1996; King et al., 1996; Vorren et al., 1998; Dowdeswell and Siegert, 1999). The gentle slopes offshore of the troughs allow the build-up of large volumes of sediment.

Type 2 slopes

The outward bulging of bathymetric contours observed on the Type 2 slopes imply that shelf progradation has occurred as a result of ice streams extending to the shelf break (Fig. 4.7) (Batchelor and Dowdeswell, In Press). These slopes, however, are characterised by gradients that are considerably steeper than 4° and are, consequently, probably too steep to support the build-up of sediment to form large TMFs (Ó Cofaigh et al., 2003; Piper and Normark, 2009). On steeper slopes, glacial debris flows have a tendency to accelerate, entrain water and transform into erosive turbidity currents, producing submarine channel-levee complexes (Figs. 3.19, 4.8) (Piper and Normark, 2009). TMFs therefore do not develop because sediment by-passes the upper continental (e.g. Wilken and Mienert, 2006; Dowdeswell et al., 2004; Tripsanas and Piper, 2008; Piper et al., 2012).

Type 3 slopes

The steep gradients of Type 3 continental slopes offshore of Godthåb, Fiskenæs, Danas, Ravns, Frederikshåbs and Julianehåb troughs in Southwest Greenland and Ilertakajik, Napassorsuaq, Anoritup, Avarqat, Patussoq and Lindenow in Southeast Greenland suggest that slope failure may be at least partially responsible for the lack of TMFs in these locations (Fig. 4.7). This interpretation is supported by seismic data from the slope beyond Godthåb Trough (Fig. 3.3). The seismic profile in Figure 3.3 demonstrates that sediment accumulation on the continental slope beyond Godthåb Trough is largely absent and that a steep, prograding glacial-sedimentary prism is instead present on the upper-slope with mass-wasting deposits at the base of the slope (Nielsen et al., 2005). This is also probably the reason why the TMF offshore of Sukkertop Trough is smaller than the TMF offshore of Kangerlussuaq Trough (Fig. 3.6).

The lack of slope progradation could also be due to the igneous bedrock geology and texture of the shelf sediments of the Southern Greenland continental margin (Ó Cofaigh et al., 2004). This could result in relatively low sediment entrainment and delivery rates to the upper-slope (Ó Cofaigh et al., 2004). However, the presence of a TMF on the slope of Kangerlussuaq Trough (Section 3.3.2, Fig. 3.7), suggests a relatively high sediment supply to this part of the Southern Greenland margin during the Quaternary. Elsewhere in Southeast Greenland, the lack of TMF development may be due to the limited palaeo-ice stream drainage basin areas and limited amount of ice flowing through the troughs. This interpretation is backed up by the lack of Type 1 and Type 2 slopes on the six smallest troughs in Southeast Greenland, which

have inferred palaeo-drainage basins of 3,000 to 5,000 km² (Fig. 4.7) (Batchelor and Dowdeswell, In Press). The five larger troughs on Southeast Greenland have larger palaeo-ice drainage basins between 5,000 and 30,000 km² and have Type 2 slopes (Fig. 4.7). The largest trough, Kangerlussuaq, and the only trough associated with a Type 1 slope, is inferred to have had a palaeo-drainage basin of around 60,000 km² (Figs. 3.7, 4.7) (Batchelor and Dowdeswell, In Press). This suggests that larger troughs have greater ice flux which deposits larger volumes of sediment at the shelf edge.

In Southwest Greenland, although Sukkertop is one of the largest troughs with an inferred palaeo-drainage basin of 20,000 km², Godthåb Trough has a larger palaeo-drainage basin of 25,000 km² and no TMF (Batchelor and Dowdeswell, In Press). The other troughs in Southwest Greenland have palaeo-drainage basins of between 7,000 and 18,000 km² and all have Type 3 slopes even though the size of these drainage basins is no smaller than the troughs of Southeast Greenland which have Type 2 slopes. It is possible that glacial sedimentary depocentres, such as small TMFs or glacial-sedimentary prisms, did develop on the continental slopes offshore of troughs in Southwest Greenland, but were subsequently removed from the slope by slope failures.

Piper et al. (2012) suggest that the slope failure beyond cross-shelf troughs of the Eastern Canadian margin may be due to the abundance of subglacial meltwater. Erosional undercutting of upper-slope sediments by meltwater channels can result in slope failure and the deposition of blocky mass transport deposits (e.g. Piper et al., 2007; Piper et al., 2012). This process is thought to be important for the Southwest Greenland margins as other evidence (bedrock channels, gullies, and turbidity current-channels) suggests that large amounts of subglacial and deglacial meltwater were produced when the Greenland Ice Sheet last extended to the shelf edge. The importance of meltwater will be further discussed in Section 5.3.2.

4.3.2. Spatial distribution of gullies, dendritic channel systems, blocky mass-transport deposits and glacial debris flows

4.3.2.1. Description

At a smaller-scale there is considerable variation in the continental slope morphology of Southern Greenland (Fig. 3.16). This reflects the complexity of glacial and mass failure processes on the continental margin (Ó Cofaigh et al., 2003) and may provide insights into

the larger-scale morphology of the continental slopes. The continental slopes of Southern Greenland were divided into three sets of features in Section 3.11 and the spatial distribution of these landform sets is displayed in Figure 4.7.

Gullies or subglacial meltwater channels incise large areas of the continental slopes of Southern Greenland (Fig. 3.17, 3.18, 4.7). The distribution of gullies is not uniform and heavily gullied sections alternate with gully-free areas. In Southwest Greenland gullies occur on slopes with gradients between 4.9 and 9.5°. The multi-beam data show that gullies cluster mainly on the slopes offshore of Fyllas, Fiskenæs and Danas banks (Fig. 4.7A). In contrast, there is almost no evidence of gullying on the slopes offshore of cross-shelf troughs in Southwest Greenland. The TMF offshore of Sukkertop Trough has a well-developed turbidity current channel system and evidence of translational sediment slides (Fig. 3.19) whilst the steeper slopes offshore of Godthåb and Fiskenæs troughs have wide, flat-floored valleys with blocky mass-transport deposits at the base of their continental slopes (Figs. 3.17, 3.20, 4.7A).

The gullies on the continental slopes of Southeast Greenland have a slightly different distribution (Fig. 3.19, 4.7). Like Southwest Greenland, gullies occur on a range of slope gradients between 2.0 and 11.3°. Unlike Southwest Greenland, gullies in Southeast Greenland can be identified on slopes offshore large cross-shelf troughs as well as bank areas (Fig. 4.7). Gullies in these areas have also been identified by other studies. According to Johnson et al. (1975), the gullies that incise the continental slope of Southeast Greenland coalesce down-slope into at least eight major submarine canyons which traverse the continental rise and reach the base level of the basin sea floor. Unfortunately, these landforms are outside the Olex data coverage. No features were identified on the TMF offshore of Kangerlussuaq Trough but Dowdeswell et al. (2010) identified glacigenic debris flows in seismic profiles (Fig. 4.7). Glacigenic debris flows were not identified in this study as they are subdued features and are not always identifiable in bathymetric data. No evidence of blocky mass-transport deposits were identified in Southeast Greenland (Fig. 4.7).

4.3.2.2. Interpretation

The contrasting geomorphology identified on the slopes of Southern Greenland is explained well by the conceptual model proposed by Piper et al. (2012) which is based on the geomorphology of the Eastern Canadian continental margin (Fig. 4.8).

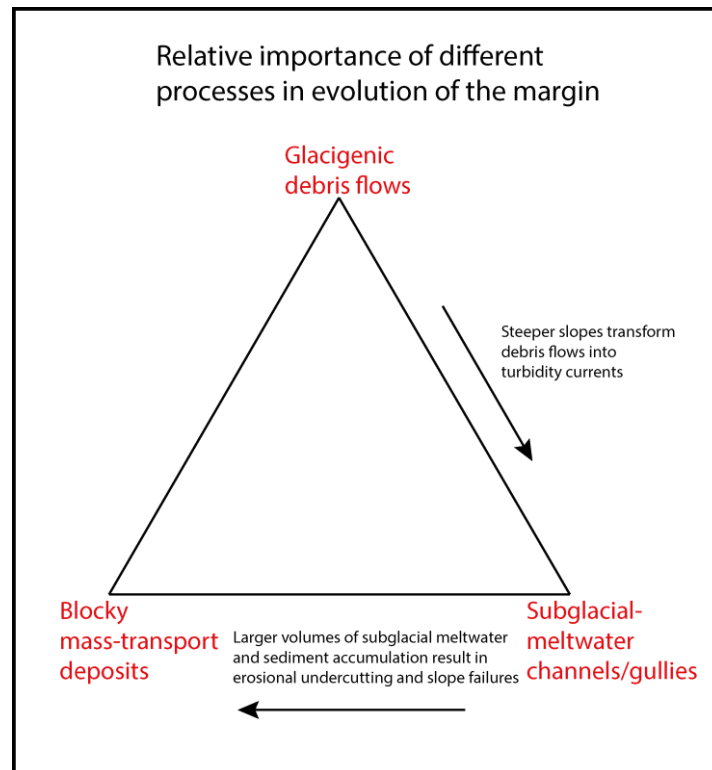


Figure 4.8. Diagram showing the relative importance of different processes in the development of the continental slopes influenced by glaciological processes. Adapted from Piper et al. (2012).

The gradient of the upper continental slope is an important control on the presence of glacigenic debris flows (Fig. 4.8) (Piper and Normark, 2009). On gentle slopes, sediment transported by palaeo-ice streams is able to build-up and episodic failures result in viscous debris flows. This explanation is consistent with the results of this study, as the glacigenic debris flows identified by Dowdeswell et al. (2010) are only found on the TMF offshore of Kangerlussuaq Trough where the upper-slope gradient is 2° (Figs. 3.7, 4.7).

Glacigenic debris flows are, however, absent from the TMF offshore of Sukkertop Trough (Fig. 4.7). This is because the slope gradient of this TMF is about 4° . On steeper slopes, glacigenic debris flows accelerate and entrain water, transforming the slope failures into turbidity currents (Fig. 4.8) (Piper and Normark, 2009). This process is likely to have produced the dendritic channel system identified on the continental slope offshore of Sukkertop Trough. Furthermore, it is inferred that this process restricts the volume of sediment retained on the slope (Wilken and Mienert, 2006; Dowdeswell et al., 2004; Tripsanas and Piper, 2008; Piper et al., 2012). This accounts for the less well-developed TMF

offshore of Sukkertop Trough in comparison to the much larger and gentler sloped TMF offshore of Kangerlussuaq (Fig. 3.7). A similar hypothesis was suggested to explain the dendritic channels system and lack of TMF offshore of Marguerite Trough, Antarctic Peninsula (Dowdeswell et al., 2004) and the extensive turbidite system offshore of the Kejser Franz Josef margin, Northeast Greenland (García et al., 2012).

The transformation of glacial debris flows into turbidity currents might also account for the development of gullying on the continental slopes offshore of the shallow banks on the continental shelf (Figs. 4.7, 4.8). However, it is inferred that these areas of the shelf received relatively little sediment during full-glacial periods due to the presence of slow-moving ice (Dowdeswell and Elverhøi, 2002; Ottesen and Dowdeswell, 2009). Therefore, it is thought that the gullying is related to erosion by turbidity currents triggered as a result of sediment-laden meltwater sourced from beneath the full-glacial ice margin grounded at the shelf edge (Fig. 4.8) (Powell, 1984; Jaeger and Nittrouer, 1999; Wellner et al., 2001, 2006; Ó Cofaigh et al., 2003). Subglacial meltwater is able to entrain sediment at the base of glaciers and may produce a hyperpycnal flow, which travels along the continental slope, when discharged at the grounding line (Noormets et al., 2009). The critical sediment concentration needed for meltwater to initiate hyperpycnal underflows in seawater is $1 - 5 \text{ kg m}^{-3}$ (Parsons et al., 2001; Mulder et al., 2003). This implies that subglacial meltwater was present beneath relatively slow-moving ice when it last reached the shelf edge. Further discussion about the formation of this subglacial meltwater will take place in Section 5.3.2 where it is suggested that surface melting allowed water to reach the base of the ice sheet.

The wide, flat-floored valleys with blocky mass-transport deposits offshore of several large cross-shelf troughs in Southwest Greenland suggest that much larger subglacial discharges occurred offshore of large ice streams than offshore of inter-ice stream areas (Fig. 4.7) (Piper et al., 2012). The width of these valleys indicates that these discharges were highly erosive. Sedimentological evidence from Eastern Canada suggests that the beds of these valleys are armoured with coarse-grained material which prevents further erosion by smaller turbulent flows (Piper and Normark, 2009). This explains why no gullying is identified offshore cross-shelf troughs in Southwest Greenland. Gullies might have previously existed on the continental slopes but since the coarse-grained sediment was deposited, no gullies have been able to form.

In contrast, no wide valleys were identified offshore of the cross-shelf troughs of Southeast Greenland (Fig. 4.7). This suggests that the style of subglacial meltwater supply to the continental slopes offshore of the cross-shelf troughs of Southern Greenland was spatially variable. Further discussion about the formation of subglacial meltwater and the contrast between Southwest and Southwestern Greenland is presented in Section 5.3.2.

The interpretation of the evidence could also explain why no significant TMFs exist on the continental slopes of Southwest Greenland. As mentioned in Section 4.3.1, the discharge of subglacial meltwater has been proposed to exert a major control on the slope architecture beyond cross-shelf troughs (Piper et al., 2012). Glacigenic debris may have accumulated on the slopes of Southwest Greenland during Quaternary glaciations, yet was subsequently removed and re-deposited on the down-slope by mass failures initiated by large subglacial meltwater outburst flows (Fig. 4.8).

4.4. Summary

In this chapter, the locations and spatial patterns of the landforms identified in the bathymetric data have been described. These descriptions have enabled the interpretation of the processes that were responsible for the formation of these features. The next chapter combines these glaciological interpretations to investigate the palaeo-glaciological implications of such findings and attempts to determine a chronology based on the results of this thesis and other literature. Where possible, comparisons between Southeast and Southwest Greenland will be made.

5. Palaeo-glaciological implications and chronology

The palaeo-glaciological implications of the geomorphology of the continental shelf and slopes of Southern Greenland, mapped in Figures 4.2, 4.5, 4.6 and 4.7, will be discussed in this chapter. Based on a review of the literature, this chapter also aims to attempt to construct a tentative chronology of glaciological events and, where possible, provide a comparison between Southeast and Southwest Greenland. This chapter is split into the following three sections:

- Extent of LGM Greenland Ice Sheet in Southern Greenland
- Dynamics of LGM Greenland Ice Sheet in Southern Greenland
- Greenland Ice Sheet retreat since the LGM in Southern Greenland

5.1. Extent of the LGM Greenland Ice Sheet in Southern Greenland

5.1.1. Southwest Greenland

The Outer Hellefisk moraines at 65° N (Figs. 3.11, 4.5) suggest that ice on the shallow banks of the continental shelf reached the shelf edge (Fig. 5.1). The moraines are easily identifiable in the bathymetry which suggests that these features were produced relatively recently (Fig. 3.11). This agrees with the work of recent studies which suggest that the Outer Hellefisk moraines date to the LGM and the Fiskebanke moraines to the Younger Dryas (Fig. 1.4) (Weidick et al., 2004; Roberts et al., 2009, 2010). A marine limit of 140 m in the Sisimiut area (Fig. 1.2) supports these views. The high marine limit implies a strong glacio-isostatic rebound caused by a large change in ice-load (Bennike et al., 2011). A large change in ice-load may have been caused by the retreat of a major ice sheet, perhaps from the continental shelf edge. Finally, there is now strong evidence in the form of both submarine landforms and radiocarbon dates to suggest that the Greenland Ice Sheet reached the western shelf edge at 68° and 70° N during the LGM (Section 1.2.1) (Ó Cofaigh et al., 2013a, 2013b; Dowdeswell et al., In Press). If the Greenland Ice Sheet could extend up to 360 km in this region, it could be argued that it also extended up to 100 km across the shelf of Southwest Greenland (Fig. 5.1).

The shelf moraines have yet to be directly dated so the arguments made in this study are tentative. The precise age of the Outer Hellefisk moraines and whether the Greenland Ice

Sheet extended to the shelf edge of Southwest Greenland therefore remains, to some extent, an open question.

The geomorphology of the continental slopes of Southwest Greenland also suggests that the Greenland Ice Sheet probably extended to the shelf edge during the LGM. The processes related to the erosion of gullies and channel systems identified on the slopes imply that an ice sheet was present on the shelf edge. They are also easily identified which indicates that they too were formed relatively recently (Fig. 5.1). Again, this evidence is not unequivocal due to the lack of direct absolute dating and these interpretations are tentative.

5.1.2. Southeast Greenland

The gullies identified on the continental slope of Southeast Greenland are also easily identified which indicates that they were formed relatively recently and that the Greenland Ice Sheet extended to the continental shelf edge during the LGM (Figs. 3.18, 5.1). Other studies generally support this assertion (Section 1.2.1).

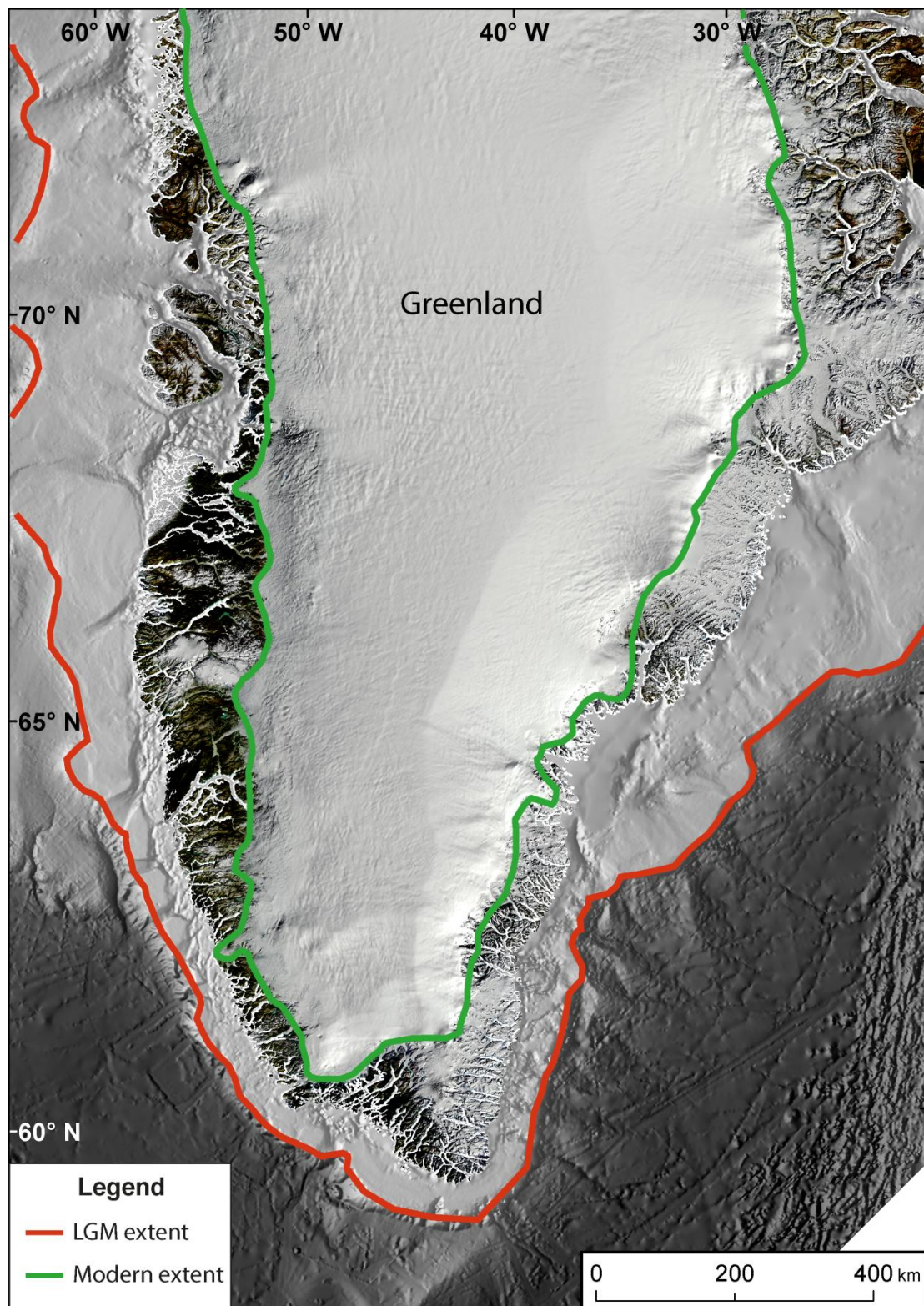


Figure 5.1. Map showing the inferred extent of the Greenland Ice Sheet over Southern Greenland during the LGM. The evidence acquired in this thesis, and the literature, suggests that the ice sheet reached the continental shelf edge of Southern Greenland. Red line represents the inferred extent at the LGM and the green line represents the modern extent.

5.2. Dynamics of the LGM Greenland Ice Sheet in Southern Greenland

5.2.1. Ice streams

The geomorphological evidence acquired in this study suggests that fast-flowing ice streams were located in every trough on the continental shelf of Southern Greenland during the LGM (Figs. 4.4, 5.2, 5.3). Under full-glacial conditions, the largest of these ice streams, which occupied Sukkertop and Kangerlussuaq troughs (Fig. 3.1), supplied large volumes of deformable till to the ice margin. This debris was subsequently remobilised by debris-flow processes on the upper-slope to form large TMFs (Figs. 3.7, 4.7) (Laberg and Vorren, 1995; Dowdeswell et al., 1996).

The magnitude of glacial erosion and sedimentation needed to produce over-deepened cross-shelf troughs imply that ice streams extended to the shelf break of Southern Greenland multiple times (ten Brink and Schneider, 1995). Seismic profiles recording multiple sets of glacial debris flows on the continental slopes beyond cross-shelf troughs on the Southeast and Southwest Greenland margins suggest that this has happened at least five times since the Early Pliocene (Nielsen and Kuijpers, 2013).

5.2.1.1. Subglacial meltwater

The thick ice that occupied cross-shelf troughs in Southern Greenland under full-glacial conditions would probably have allowed pressure-melting at the bed. This would have produced large amounts of subglacial meltwater, lubricated the bed and caused fast ice flow. Some of the evidence in this study, for example bedrock channels (Fig. 4.2), suggests that subglacial meltwater was present beneath the Greenland Ice Sheet in Southern Greenland during the full-glacial periods.

In Kangerlussuaq Trough, bedrock channels and crescentic overdeepenings on the upstream sides of drumlins strongly suggest that subglacial meltwater was produced at the ice-bed interface of the ice stream that occupied this trough (Dowdeswell et al., 2010). The well-defined and extensive network of bedrock channels identified on the inner shelf of Southwest Greenland in this study (Fig. 4.2) also implies that subglacial meltwater existed at the base of the Greenland Ice Sheet. The bedrock channels may have served to discharge subglacial meltwater from the interior of the ice sheet to its margin. This interpretation is, however,

tentative and further work is needed to confirm whether the bedrock channels identified in this study were occupied by subglacial meltwater repeatedly during successive glacial periods.

The gullying on the continental slope offshore of cross-shelf troughs in both Southeast and Southwest Greenland suggests that subglacial meltwater was discharged from the ice margin when it last reached the shelf edge (Figs. 3.17, 3.18, 4.7). However, the steepness of the upper-slopes on which these gullies are formed (Section 4.3.2) means that the gullies could have formed by the transformation of debris flows into erosive turbidity currents (Piper and Normark, 2009). Therefore the gullies might not have necessarily been produced by subglacial meltwater.

5.2.2. Inter-ice stream areas

The Outer Hellefisk moraines (Figs. 3.12, 4.5) indicate that the fast-flowing ice streams of Southwest Greenland were flanked by slower flowing ice which also extended to the continental shelf edge at least once during full-glacial periods (Fig. 5.2). The presence of overconsolidated diamictic sediment from a core to the east of Kangerlussuaq Trough suggests that grounded ice was also active on the shallow shelf of Southeast Greenland (Fig. 5.3) (Mienert et al., 1992). Numerical ice sheet modelling predicts that ice velocities in these regions will be one to two orders of magnitude lower than the ice streams located within the cross-shelf troughs (Dowdeswell and Siegert, 1999).

Overall, this evidence suggests that a dynamic and complex glacial environment with fast-flowing ice streams in troughs, and areas of less dynamic ice, on shallow bank areas, covered the continental margins of Southern Greenland during full-glacial periods, and probably the LGM (Figs. 5.2, 5.3).

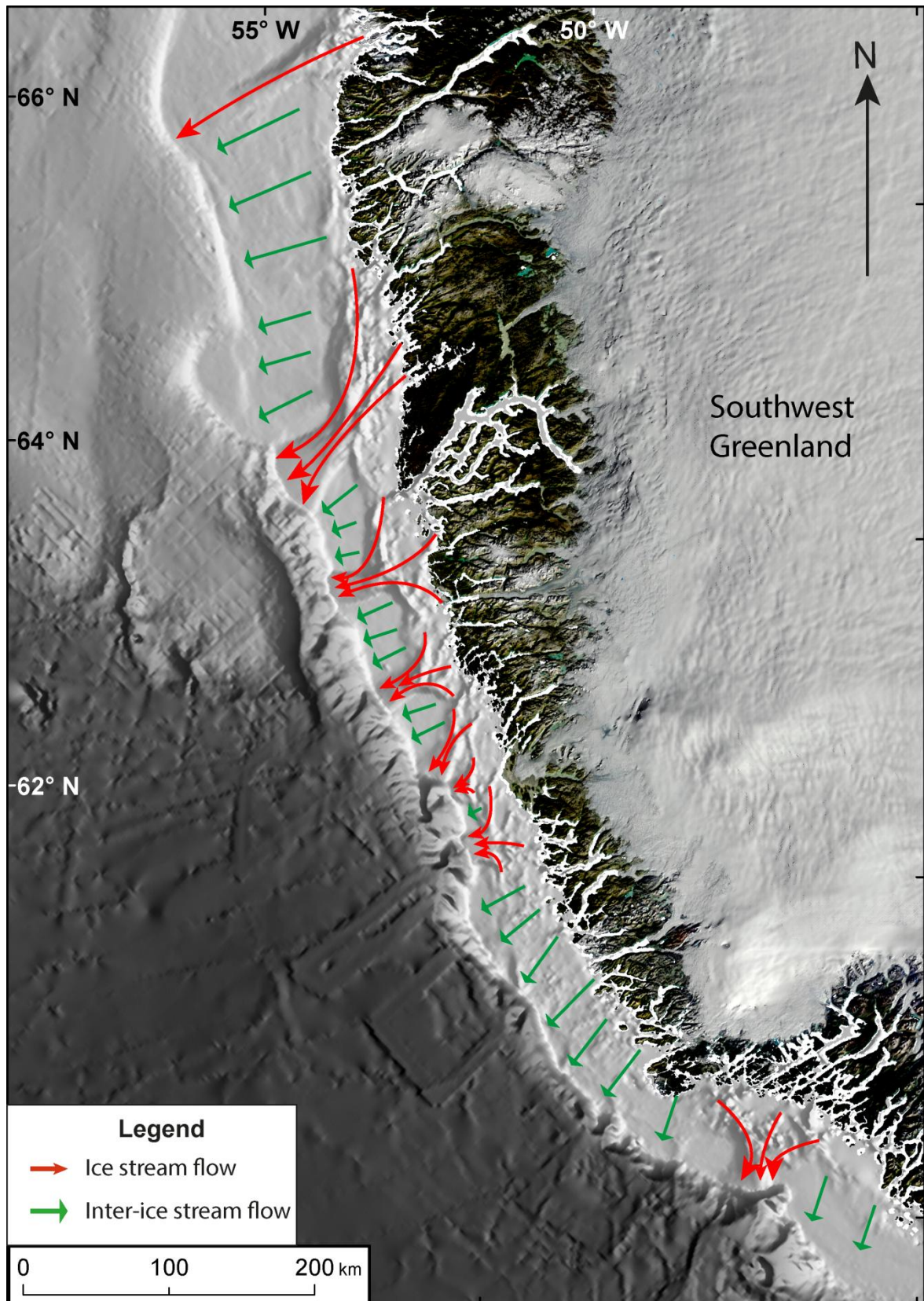


Figure 5.2. Map showing a tentative reconstruction of the locations of ice streams draining the Greenland Ice Sheet during the LGM in Southwest Greenland. The evidence acquired in this thesis suggests that the ice streams were situated in every cross-shelf trough in Southern Greenland.

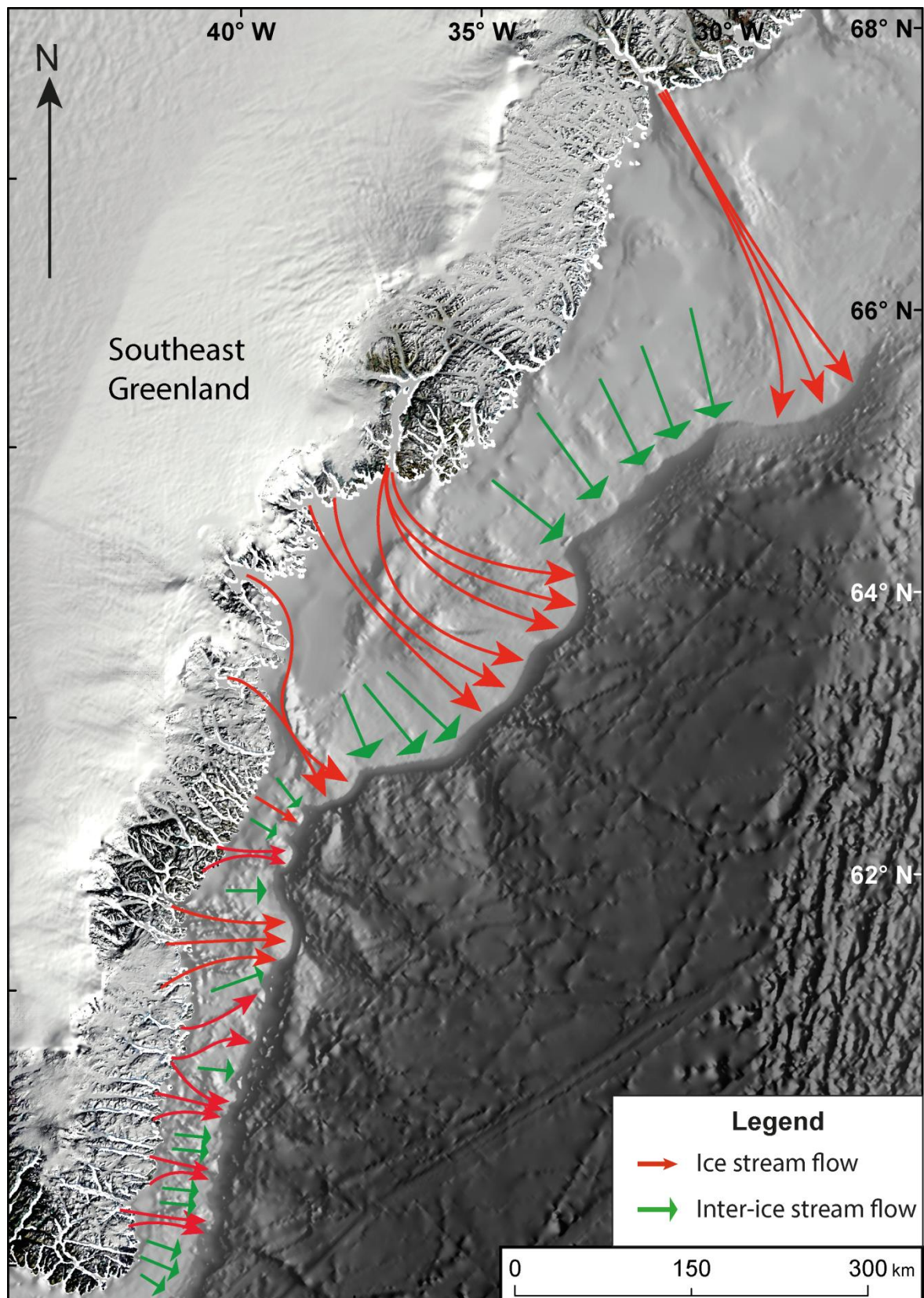


Figure 5.3. Map showing the interpreted locations of ice streams draining the Greenland Ice Sheet during the LGM in Southeast Greenland. The evidence acquired in this thesis suggests that the ice streams were situated in every cross-shelf trough in Southern Greenland.

5.3. Deglaciation of the LGM Greenland Ice Sheet in Southern Greenland

5.3.1. Nature of retreat

Episodic retreat

The presence of GZWs in Fiskenæs and Kangerlussuaq troughs (Fig. 3.13, 4.5) suggest that ice stream retreat in these regions was episodic and punctuated by at least one still-stand (Dowdeswell et al., 2008; Ó Cofaigh et al., 2008). These features were probably deposited after the LGM because their relatively subdued nature means that it is unlikely that they would be identified in the bathymetry if they had been formed earlier. Kangerlussuaq ice stream is thought to have retreated from the continental shelf edge around 17,000 years ago and retreated past the mid-shelf by 15,000 years BP (Section 1.2.3). This means that the ice stream retreated more than 215 km in two thousand years at a rate of at least 105 m yr⁻¹. The GZW in Kangerlussuaq Trough, however, suggests that the ice stream was in a stable position for at least some of this period. When the rates of sediment delivery from modern ice streams are considered, the size of this wedge (40 km³) indicates that it probably took centuries to develop (Dowdeswell and Fugelli, 2012). Therefore, the rate of Kangerlussuaq ice stream retreat was probably up to 200 m yr⁻¹ before and after the still-stand period. This rate is higher than the average rate of retreat of Greenland glaciers between 2000 and 2010, which retreated at a rate of 110 m yr⁻¹ (Howat and Eddy, 2011). However, Kangerlussuaq Glacier retreated at a rate of 630 m yr⁻¹ during this period (Walsh et al., 2012) and it is likely that that rate of ice stream retreat after the LGM, like the rate of modern glacier retreat, is highly variable at shorter timescales.

No streamlined lineations were identified on the surface of the GZWs. This suggests that these features were not overridden by subsequent ice advance after deposition (Dowdeswell et al., 2008). This implies that, during the Younger Dryas and in contrast to Jakobshavn Isbræ, the Kangerlussuaq and Fiskenæs ice streams did not undergo re-advances onto the continental shelf (Section 1.2.3). However, the relatively poor resolution of the bathymetric data means that it was difficult to identify sedimentary streamlined lineations in this study. Subsequent ice stream re-advance over the GZWs therefore cannot be precluded.

The GZWs are both located in troughs that are reverse sloping and deepen towards the inner continental shelf (Fig. 3.5B, 4.5). This indicates that grounding-zones of ice streams can stabilise on reverse sloping beds. In recent decades, the grounding-zones of several marine-terminating Antarctic ice streams and Greenland outlet glaciers have experienced significant acceleration, thinning and retreat (Rignot and Kanagaratnam, 2006; Pritchard et al., 2009; Walsh et al., 2012; Shepherd et al., 2012) and concerns have been raised over the stability of ice stream grounding-zones on reverse sloping beds (Joughin and Alley, 2011). Numerical ice-sheet modelling studies have suggested that ice streams on reverse slopes are inherently unstable and can propagate the rapid collapse of an ice sheet (e.g. Schoof, 2007; Nick et al., 2009; Katz and Worster, 2010). However, GZWs identified in this study indicate that rapid grounding-line retreat does not necessarily occur on reverse slopes.

Catastrophic retreat

The absence of GZWs in other cross-shelf troughs on the continental shelf of Southern Greenland indicates that the retreat of the other Greenland ice streams after the LGM was probably rapid, and possibly catastrophic (Dowdeswell et al., 2008; Ó Cofaigh et al., 2008). In addition, no transverse-to-flow ridges were identified in the cross-shelf troughs. The absence of these features also implies that ice stream retreat was rapid (Dowdeswell et al., 2008; Ó Cofaigh et al., 2008). Transverse ridges are, however, relatively small features with heights of about 2 – 25 m (Shipp et al., 1999; 2002; Ottesen and Dowdeswell, 2009). Therefore, they may exist but were not identified due to the relatively poor resolution of the Olex data.

5.3.2. Mechanisms of retreat

Southeast Greenland - calving

The initial retreat of the Greenland Ice Sheet in Southeast Greenland is thought to have been dominated by calving. Evidence for large amounts of iceberg calving is demonstrated by the density of iceberg ploughmarks on the outer sedimentary shelf of Southeast Greenland in this study (Fig. 4.6). Large iceberg ploughmarks have also been identified on the shelf of Southeast Greenland and in the North Atlantic Ocean at depths of up to 1000 m by Syvitski et al. (2001) and Kuijpers and Werner (2007), respectively. The fresh appearance and the limited sediment infilling of the ploughmarks, combined with the current, relatively warm,

oceanographic conditions, mean that the icebergs were probably produced as the Greenland Ice Sheet margin retreated from the shelf edge after the LGM (Section 4.2.2).

The pronounced increase in IRD concentrations also indicates higher intensities of iceberg calving. Between 17,400 and 16,000 years BP elevated concentrations of IRD were identified in sediment cores from the Labrador Sea and the continental shelf of East and Southeast Greenland (Fig. 1.1) (Nam et al., 1995; Andrews et al., 1997; Knutz et al., 2011). The mineralogy of these deposits are interpreted as evidence of increased iceberg calving from Southeast Greenland during initial deglaciation after the LGM (Jennings et al., 2002; Knutz et al., 2011).

The influence of warm ocean water impinging on the shelf has been proposed as the driver for increased calving and retreat of the LGM ice sheet in Southeast Greenland (Jennings et al., 2006; Knutz et al., 2011). The IRD peaks coincide with enhanced advection of warm subsurface Atlantic water to the Southeast Greenland margin, perhaps under the influence of an early Irminger Current intensification (Kuijpers et al., 2003).

Southwest Greenland - melting

Whilst iceberg ploughmarks have been identified on the outer shelf of Egedesminde Trough, West Greenland (Brett and Zarudzki, 1979; Syvitski et al., 2001; Kuijpers et al., 2007), to the south of Disko Bay (68° N) in Southwest Greenland both this study and the extensive seismic surveys and side-scan sonar records carried out by Brett and Zarudzki (1979) did not find any evidence of iceberg ploughmarks. This suggests that large icebergs were not produced in large numbers during the deglaciation of the Greenland Ice Sheet in the southwest and that calving did not contribute significantly to ice sheet mass loss.

The initial retreat of the Greenland Ice Sheet Southwest Greenland is thought to have been dominated by melting. The gullying on the continental slope offshore of inter-ice stream areas in Southwest Greenland suggests considerable surface melting occurred when the Greenland Ice Sheet was located at the shelf edge. The gullies are inferred to have been formed by sediment-laden meltwater that was produced and discharged during deglaciation after the LGM (Section 4.3.2; Figs. 3.18, 4.7). Inter-ice stream areas of ice sheets are thought to have produced relatively little basal meltwater during full-glacial periods due to low ice velocities (Dowdeswell and Siegert 1999). Therefore, the meltwater that was produced in these areas was probably caused by surface melting. Recent studies have shown that surface

meltwater is able to reach the base of the Greenland Ice Sheet through water-driven fracture propagation (Zwally et al., 2002; Das et al., 2008; Joughin et al., 2008; Shepherd et al., 2009; Bartholomew et al., 2010). This process could be responsible for the discharge of subglacial meltwater and the formation of gullies offshore of inter-ice stream areas.

The steep Type 3 continental slopes associated with wide, flat-floored valleys offshore of cross-shelf troughs in Southwest Greenland are also thought to have been formed by subglacial meltwater discharge when the Greenland Ice Sheet extended to the shelf edge (Fig. 3.20) (Piper et al., 2012). The size of these valleys suggests that much larger subglacial discharge events occurred offshore of major ice streams compared with offshore of inter-ice stream areas (Section 4.3.2) (Piper and Normark, 2009; Piper et al., 2012). Based on similar features identified on the Eastern Canadian margin, the outburst flows may have been caused in response to increased subglacial meltwater input during deglaciation when surface melting increased as air temperatures in Greenland started to rise. The timing or number of the subglacial outburst events, however, is not known and this interpretation is tentative. Other processes such as subglacial lake drainage could also have produced large outburst floods (Wingham et al., 2006; Bell et al., 2007) although palaeo-subglacial lakes have yet to be identified in Greenland (Livingstone et al., 2012b).

The evidence acquired in this study suggests that melting continued to be the dominant mechanism of mass loss from the Greenland Ice Sheet in the southwest after ice retreated from the shelf edge. The thick, well-stratified sedimentary sequence identified in Frederikshåbs Trough (Fig. 3.21) suggests that substantial amounts of suspended sediment were deposited by glacial meltwater after the Greenland Ice Sheet had retreated from the shelf edge. This is consistent with a recent study from Disko Bay, West Greenland, which interpreted large volumes of unlithified sediment as evidence that subglacial and deglacial meltwater was readily available during ice-sheet retreat (Hogan et al., 2012).

These interpretations are backed-up by the current literature. Geochemical terrestrial sediment proxies from a marine sediment core in Southern Greenland suggest that increased ablation and run-off from the Southern Greenland Ice Sheet began at around 19,000 years BP and ended around 10,000 years BP (Carlson et al., 2008). This is confirmed by cosmogenic exposure dating from the Sisimiut area which suggests that the ice sheet began to thin by about 21,000 years BP and continued to thin until 13,600 years BP (Roberts et al., 2009). The thinning coincides broadly with the period of increased air temperatures over Greenland

during the Bølling Interstadial (Fig. 1.4) (Roberts et al., 2009). The Huy1 and Huy2 ice sheet models predict that maximum volume of the Greenland Ice Sheet was reached 16,500 years ago when high accumulation rates in Greenland are thought to have outweighed the larger ablation from increased temperatures (Simpson et al., 2009). Therefore, in the southwest, the Greenland Ice Sheet may have initially responded in a lagged and non-linear fashion to rising ocean and air temperatures (Carlson and Windsor, 2012). Surface ablation at the margins of the ice sheet and accumulation inland may have increased ice stream velocities which would have allowed the ice sheet to remain at the continental shelf edge during warming temperatures. This system might then have been susceptible to threshold behaviour whereby a small perturbation causes a large, dramatic response. As the relative sea level rose (Section 1.2.3), the thinner areas of the ice sheet would have become vulnerable to buoyant lift-off and retreat by calving (Roberts et al., 2009). The thin ice sheet is then thought to have retreated rapidly at between around 15,000 to 11,000 years BP to reach the present coast by 10,000 years BP (Bennike et al., 2011). This interpretation is consistent with other palaeo-marine-based ice sheets such as the Barents-Kara Ice Sheet which is inferred to have collapsed catastrophically after the LGM and raises concerns about the response of the marine-based West Antarctic Ice Sheet to future climate change.

6. Conclusions

6.1. Review of the main findings

The aims of this thesis were to investigate the geomorphology of the continental margins of Southern Greenland in order to improve our understanding of the extent, dynamics and deglacial retreat of the Greenland Ice Sheet during and after the LGM. A summary of the main results follows in this chapter.

- The continental shelf of Southern Greenland is dissected by a number of deep, narrow cross-shelf troughs. Twenty troughs were identified on the shelf Southern Greenland (Figs. 3.1, 3.2). These troughs and the streamlined, elongate landforms within them are interpreted as evidence that fast-flowing ice streams drained the Greenland Ice Sheet during the LGM in Southern Greenland (Figs. 4.2, 4.3, 5.2, 5.3).
- A number of features on the continental slope (gullies, slide scars, glacial debris flows) and moraines on the outer continental shelf (Outer Hellefisk) indicate that the Greenland Ice Sheet extended to the continental shelf edge of Southeast and Southwest Greenland during the LGM (Figs. 3.11, 3.16, 4.5, 4.7, 5.1). Importantly, the Outer Hellefisk moraines demonstrate that ice on the shallow banks of Southern Greenland also extended to the shelf edge. A review of the relevant literature provides support for these arguments but a shelf edge Greenland Ice Sheet during the LGM remains contested (e.g. Funder et al., 2011).
- Bedrock channels and gullies indicate that, during full-glacial periods and probably during the LGM, subglacial meltwater was present beneath the Greenland Ice Sheet in Southern Greenland (Figs. 3.17, 4.3, 4.4, 4.7). The subglacial meltwater is thought to have lubricated the beds of fast-flowing ice streams that drained the Greenland Ice Sheet during the LGM.
- The GZWs identified in Kangerlussuaq and Fiskenæs troughs suggest that the entire Southern Greenland Ice Sheet did not collapse catastrophically and that the ice streams, in some troughs at least, had periods of still-stands during retreat after the LGM (Figs. 3.13, 4.5). The wedges also demonstrate that ice stream retreat across

reverse sloping troughs does not necessarily result in catastrophic collapse (Fig. 3.5B).

- No moraines were identified on most of the continental shelf of Southern Greenland (Fig. 4.5). This indicates that the majority of the Southern Greenland Ice Sheet was characterised by rapid retreat from the continental shelf edge since the LGM. The literature suggests that the Greenland Ice Sheet retreated from the shelf edge at around 17,000 years BP in the southeast and between 15,000 – 13,000 years BP in the southwest and that the ice sheet reached the present day coastline by 10,000 years BP (Jennings et al., 2002, 2006; Roberts et al., 2008; Bennike et al., 2011).
- Iceberg ploughmarks identified on the continental shelf of Southeast Greenland suggest that iceberg calving was the dominant mechanism of mass loss from this sector of the Greenland Ice Sheet after the LGM (Fig. 4.6).
- A number of lines of evidence suggest that surface ablation was the dominant mechanism of mass loss from Southwest Greenland after the LGM. No iceberg ploughmarks were identified on the continental shelf and evidence of large amounts of meltwater sedimentation was identified in Frederikshåb Trough (3.21). The wide, flat-floored valleys on the continental slopes offshore of cross-shelf troughs in Southwest Greenland are interpreted as evidence for large subglacial outburst flows caused by increased subglacial meltwater, perhaps from increased surface melting just after the LGM. These features were not observed on the continental slopes of Southeast Greenland which suggests that less meltwater was produced during deglaciation in this sector.
- The difference in the nature and mechanisms of retreat of ice streams from the continental shelf edge east and west of Greenland implies that retreat across the continental shelf was spatially variable and highly complex. The Southeast Greenland Ice Sheet responded to warming ocean temperatures impinging on the shelf and retreated rapidly from the shelf edge to the present day coastline. The Southwest Greenland Ice Sheet did not initially respond to warming air and water temperatures and remained at the continental shelf edge for a relatively longer period of time.

Surface melting then thinned the ice sheet, making it more susceptible to collapse and, after a certain period of time, it became ungrounded from the shelf edge and retreated rapidly to the present day coastline. This suggests that marine-based ice sheets exhibit threshold behaviour and can respond in lagged and non-linear fashion to external forcing. This raises concerns about the only marine-based ice sheet today, the West Antarctic Ice Sheet.

6.2. Assessment of the Olex database and its limitations

The Olex database was the main source of bathymetric data used in this study. This section provides a review of the data to inform future investigations. To date, only a few studies have utilised the Olex database for high-latitude bathymetric investigations (e.g. Bradwell et al., 2008; Shaw et al., 2009, 2012; Spagnolo and Clark, 2009). A number of geomorphological features on the continental margins of Southern Greenland have been identified from the Olex data which have not been identified in previous investigations of this area. The profile tool and the ability to change the azimuth of the light source in the Olex database enables large features such as cross-shelf troughs and GZWs to be identified easily. When the track line density is high, (>10 per km²; Section 2.7.1), smaller features such as iceberg ploughmarks with widths and depths of less than 50 m and moraines with heights of less than 25 m could also be identified. The wide geographical coverage of the Olex database (Fig. 2.1) means that features can be identified from a range of different geomorphological settings at a resolution that is often much better than the latest IBCAO Version 3.0 (Jakobsson et al., 2012).

The resolution of the Olex database is, however, highly variable. On the continental margins of Southern Greenland, there is almost no coverage of the continental slope of Southwest Greenland or the inner shelf of Southeast Greenland. This is because these areas are not regularly visited by fishing vessels. In these areas, no features could be identified. Furthermore, in areas where the Olex data coverage appears to be good, the resolution of the data may actually be poor. This is because the Olex database interpolates a large number of cells around one measured depth value which gives the appearance of good data coverage. To avoid this, the density of ship track lines must be viewed in order to make confident descriptions about the submarine geomorphology. The main limitations of the database are that the contributors of the data are almost exclusively equipped with single-beam echosounders.

In the future, there is potential for commercial shipping vessels to be equipped with multi-beam echo-sounders (C. Wilson, Olex, pers. comm., 2013). This will improve the resolution of the Olex database. Forthcoming releases of the Olex database will also improve the resolution and reduce the number of poorly calculated depth values as more voluntarily contributed data are provided. This will allow new and smaller landforms to be identified. Overall, the Olex database is an invaluable source of bathymetric data and was used effectively in this study to investigate the geomorphology of the Southern Greenland continental margin.

7. References

- Alley, R.B., Andrews, J.T., Brigham-Grette, J., Clarke, G.K.C., Cuffey, K.M., Fitzpatrick, J.J., Funder, S., Marshall, S.J., Miller, G.H., Mitrovica, J.X., Muhs, D.R., Otto-Bliesner, B.L., Polyak, L., White, J.W.C., 2010. History of the Greenland Ice Sheet: paleoclimatic insights. *Quaternary Science Reviews* 29, 1728-1756.
- Anderson, J.B., Oakes-Fretwell, U.O., 2008. Geomorphology of the onset area of a paleo-ice stream, Marguerite Bay, Antarctic Peninsula. *Earth Surface Processes and Landforms* 33, 503-512.
- Andrews, J.T., Smith, L.M., Preston, R., Cooper, T., Jennings, A.E., 1997. Spatial and temporal patterns of iceberg rafting (IRD) along the East Greenland margin, ca 68 degrees N, over the last 14 cal ka. *Journal of Quaternary Science* 12, 1-13.
- Baeten, N.J., Laberg, J.S., Forwick, M., Vorren, T.O., Vanneste, M., Forsberg, C.F., Kvalstad, T.J., Ivanov, M., 2013. Morphology and origin of smaller-scale mass movements on the continental slope off northern Norway. *Geomorphology* 187, 122-134.
- Bartholomew, I., Nienow, P., Mair, D., Hubbard, A., King, M.A., Sole, A., 2010. Seasonal evolution of subglacial drainage and acceleration in a Greenland outlet glacier. *Nature Geoscience* 3, 408-411.
- Batchelor, C., Dowdeswell, J.A., In Press. The physiography of High Arctic cross-shelf troughs. *Quaternary Science Reviews*.
- Bell, R.E., Studinger, M., Shuman, C.A., Fahnestock, M.A., Joughin, I., 2007. Large subglacial lakes in East Antarctica at the onset of fast-flowing ice streams. *Nature* 445, 904-907.
- Benn, D.I., Evans, D.J.A., 2010. *Glaciers and Glaciation*. London, Arnold, 2nd Edition.
- Bennett, M.R., 2003. Ice streams as the arteries of an ice sheet: their mechanics, stability and significance. *Earth-Science Reviews* 61, 309-339.
- Bennett, M.R., Glasser, N.F. 2009. *Glacial geology: Ice sheets and landforms*. Chichester, Wiley-Blackwell, 2nd Edition.
- Bennike, O., Björck, S., 2002. Chronology of the last recession of the Greenland Ice Sheet.

Journal of Quaternary Science 17, 211-219.

Bennike, O., Björck, S., Lambeck, K., 2002. Estimates of South Greenland late-glacial ice limits from a new relative sea level curve. *Earth and Planetary Science Letters* 197, 171-186.

Bennike, O., Wagner, B., Richter, A., 2011. Relative sea level changes during the Holocene in the Sisimiut area, south-western Greenland. *Journal of Quaternary Science* 26, 353-361.

Björck, S., Walker, M.J.C., Cwynar, L.C., Johnsen, S., Knudsen, K.L., Lowe, J.J., Wohlfarth, B., Members, I., 1998. An event stratigraphy for the Last Termination in the north Atlantic region based on the Greenland ice-core record: a proposal by the INTIMATE group. *Journal of Quaternary Science* 13, 283-292.

Boulton, G.S., Lunn, R., Vidstrand, P., Zatsepin, S., 2007a. Subglacial drainage by groundwater-channel coupling, and the origin of esker systems: Part 1-glaciological observations. *Quaternary Science Reviews* 26, 1067-1090.

Boulton, G.S., Lunn, R., Vidstrand, P., Zatsepin, S., 2007b. Subglacial drainage by groundwater-channel coupling, and the origin of esker systems: part II-theory and simulation of a modern system. *Quaternary Science Reviews* 26, 1091-1105.

Bradwell, T., Stoker, M.S., Golledge, N.R., Wilson, C.K., Merritt, J.W., Long, D., Everest, J.D., Hestvik, O.B., Stevenson, A.G., Hubbard, A.L., Finlayson, A.G., Mathers, H.E., 2008. The northern sector of the last British Ice Sheet: Maximum extent and demise. *Earth-Science Reviews* 88, 207-226.

Brett, C.P., Zarudzki, E.F.K., 1979. Project Westmar, a shallow marine geophysical survey on the West Greenland shelf. *Grønlands Geologiske Undersøgelse Rapport* 87.

Bulgakov, N.P, Lomakin, P.D., (1994). Large-scale vertical hydroacoustic structure of the North Atlantic and its seasonal variability. *Physical Oceanography* 5, 259-267.

Canals, M., Urgeles, R., Calafat, A.M., 2000. Deep sea-floor evidence of past ice streams off the Antarctic Peninsula. *Geology* 28, 31-34.

Caress, D.W., Spitzak, S.E., Chayes, D.N., 1996. Software for multibeam sonars. *Sea Technology* 37, 54-57.

Carlson, A., Stoner, J.S., Donnelly, J.P., Hillaire-Marcel, C., 2008. Response of the southern

Greenland Ice Sheet during the last two deglaciations. *Geology* 36, 359-362.

Carlson, A.E., Winsor, K., 2012. Northern Hemisphere ice-sheet responses to past climate warming. *Nature Geoscience* 5, 607-613.

Christoffersen, P., Mugford, R.I., Heywood, K.J., Joughin, I., Dowdeswell, J.A., Syvitski, J.P.M., Luckman, A., Benham, T.J., 2011. Warming of waters in an East Greenland fjord prior to glacier retreat: mechanisms and connection to large-scale atmospheric conditions. *Cryosphere* 5, 701-714.

Clark, C.D., 1993. Mega-scale glacial lineations and cross-cutting ice-flow landforms. *Earth Surface Processes and Landforms* 18, 1-29.

Clark, P.U., Walder, J.S., 1994. Subglacial drainage, eskers, and deforming beds beneath the Laurentide and Eurasian ice sheets. *Geological Society of America Bulletin* 106, 304-314.

Clarke, K.C., (1995). *Analytical and Computer Cartography*. New Jersey, Prentice Hall. 1st Edition.

Dahl Jensen, D., Mosegaard, K., Gundestrup, N., Clow, G.D., Johnsen, S.J., Hansen, A.W., Balling, N., 1998. Past temperatures directly from the Greenland Ice Sheet. *Science* 282, 268-271.

Dansgaard, W., Johnsen, S.J., Clausen, H.B., Dahl Jensen, D., Gundestrup, N., Hammer, C.U., Oeschger, H. 1984: North Atlantic climatic oscillations revealed by deep Greenland ice cores. In: Hansen, J.E. & Takahashi, T. (eds): *Climate processes and climate sensitivity*. Geophysical Monograph 29, 288–298.

Dansgaard, W., 2004. *Frozen annals, Greenland ice sheet research*. Copenhagen, The Niels Bohr Institute for Astronomy, Physics and Geophysics.

Das, S.B., Joughin, I., Behn, M.D., Howat, I.M., King, M.A., Lizarralde, D., Bhatia, M.P., 2008. Fracture propagation to the base of the Greenland Ice Sheet during supraglacial lake drainage. *Science* 320, 778-781.

Domack, E., Amblas, D., Gilbert, R., Brachfeld, S., Camerlenghi, A., Rebesco, M., Canals, M., Urgeles, R., 2006. Subglacial morphology and glacial evolution of the Palmer deep outlet system, Antarctic Peninsula. *Geomorphology* 75, 125-142.

- Dowdeswell, J.A., Villinger, H., Whittington, R.J., Marienfeld, P., 1993. Iceberg scouring in Scoresby Sund and on the East Greenland continental-shelf. *Marine Geology* 111, 37-53.
- Dowdeswell, J.A., Uenzelmannneben, G., Whittington, R.J., Marienfeld, P., 1994. The Late Quaternary sedimentary record in Scoresby Sund, East Greenland. *Boreas* 23, 294-310.
- Dowdeswell, J.A., Kenyon, N.H., Elverhoi, A., Laberg, J.S., Hollender, F.J., Mienert, J., Siegert, M.J., 1996. Large-scale sedimentation on the glacier-influenced Polar North Atlantic margins: Long-range side-scan sonar evidence. *Geophysical Research Letters* 23, 3535-3538.
- Dowdeswell, J.A., Kenyon, N.H., Laberg, J.S., 1997. The glacier-influenced Scoresby Sund Fan, east Greenland continental margin: evidence from GLORIA and 3.5 kHz records. *Marine Geology* 143, 207-221.
- Dowdeswell, J.A., Elverhoi, A., Spielhagen, R., 1998. Glacimarine sedimentary processes and facies on the Polar North Atlantic margins. *Quaternary Science Reviews* 17, 243-272.
- Dowdeswell, J.A., Siegert, M.J., 1999. Ice-sheet numerical modeling and marine geophysical measurement of glacier-derived sedimentation on the Eurasian Arctic continental margins. *Geological Society of America Bulletin* 111, 1080-1097.
- Dowdeswell, J.A., Elverhoi, A., 2002. The timing of initiation of fast-flowing ice streams during a glacial cycle inferred from glacimarine sedimentation. *Marine Geology* 188, 3-14.
- Dowdeswell, J.A., Ó Cofaigh, C., Taylor, J., Kenyon, N.H., Mienert, J., Wilken, M., 2002. On the architecture of high-latitude continental margins: the influence of ice-sheet and sea-ice processes in the Polar North Atlantic. *Glacier-Influenced Sedimentation on High-Latitude Continental Margins* 203, 33-54.
- Dowdeswell, J.A., Ó Cofaigh, C., Pudsey, C.J., 2004. Continental slope morphology and sedimentary processes at the mouth of an Antarctic palaeo-ice stream. *Marine Geology* 204, 303-214.
- Dowdeswell, J.A., Evans, J., Ó Cofaigh, C., Anderson, J.B., 2006. Morphology and sedimentary processes on the continental slope off Pine Island Bay, Amundsen Sea, West Antarctica. *Geological Society of America Bulletin* 118, 606-619.
- Dowdeswell, J.A., Bamber, J.L., 2007. Keel depths of modern Antarctic icebergs and implications for sea-floor scouring in the geological record. *Marine Geology* 243, 120-131.

Dowdeswell, J.A., Ottesen, D., Evans, J., Ó Cofaigh, C., Anderson, J.B., 2008. Submarine glacial landforms and rates of ice-stream collapse. *Geology* 36, 819-822.

Dowdeswell, J.A., Evans, J., Ó Cofaigh, C., 2010. Submarine landforms and shallow acoustic stratigraphy of a 400 km-long fjord-shelf-slope transect, Kangerlussuaq margin, East Greenland. *Quaternary Science Reviews* 29, 3359-3369.

Dowdeswell, J.A., Fugelli, E.M.G., 2012. The seismic architecture and geometry of grounding-zone wedges formed at the marine margins of past ice sheets. *Geological Society of America Bulletin* 124, 1750-1761.

Dowdeswell, J.A., Hogan, K.A., Ó Cofaigh, C., Fugelli, E.M., Evans, J., Noormets, R., In Press. Late Quaternary ice flow in a West Greenland fjord and cross-shelf trough system: submarine landforms from Rink Isbrae to Uummannaq shelf and slope. *Quaternary Science Reviews*.

Elliot, M., Labeyrie, L., Bond, G., Cortijo, E., Turon, J.L., Tisnerat, N., Duplessy, J.C., 1998. Millennial-scale iceberg discharges in the Irminger Basin during the last glacial period: Relationship with the Heinrich events and environmental settings. *Paleoceanography* 13, 433-446.

Elverhoi, A., Norem, H., Andersen, E.S., Dowdeswell, J.A., Fossen, I., Haflidason, H., Kenyon, N.H., Laberg, J.S., King, E.L., Sejrup, H.P., Solheim, A., Vorren, T., 1997. On the origin and flow behavior of submarine slides on deep-sea fans along the Norwegian Barents Sea continental margin. *Geo-Marine Letters* 17, 119-125.

Evans, J., Pudsey, C.J., Ó Cofaigh, C., Morris, P., Domack, E., 2005. Late Quaternary glacial history, flow dynamics and sedimentation along the eastern margin of the Antarctic Peninsula Ice Sheet. *Quaternary Science Reviews* 24, 741-774.

Evans, J., Ó Cofaigh, C., Dowdeswell, J.A., Wadhams, P., 2009. Marine geophysical evidence for former expansion and flow of the Greenland Ice Sheet across the north-east Greenland continental shelf. *Journal of Quaternary Science* 24, 279-293.

Funder, S., 1989. Quaternary geology of the ice-free areas and adjacent shelves of Greenland. In: *Quaternary Geology of Canada and Greenland*, Fulton, R.J., (eds.). Geological Survey of Canada and Greenland, Ottawa, 743–792.

Funder, S., Hansen, L., 1996. The Greenland ice sheet - a model for its culmination and decay during and after the last glacial maximum. *Bulletin of the Geological Society of Denmark* 42, 137-152.

Funder, S., Kjeldsen, K.K., Kjaer, K.H., Ó Cofaigh, C., 2011. The Greenland Ice Sheet during the past 300,000 years: A review. In: Ehlers, J., Gibbard, P., Hughes, P.D., (eds.), *Quaternary Glaciations - Extent and Chronology. Part IV: A Closer Look. Developments in Quaternary Science* 15, Elsevier, Amsterdam, 699-713.

Gales, J.A., Larter, R.D., Mitchell, N.C., Hillenbrand, C.D., Osterhus, S., Shoosmith, D.R., 2012. Southern Weddell Sea shelf edge geomorphology: Implications for gully formation by the overflow of high-salinity water. *Journal of Geophysical Research-Earth Surface* 117, doi:10.1029/2012JF002357.

Gales, J.A., Larter, R.D., Mitchell, N.C., Dowdeswell, J.A., 2013. Geomorphic signature of Antarctic submarine gullies: Implications for continental slope processes. *Marine Geology* 337, 112-124.

García, M., Dowdeswell, J.A., Ercilla, G., Jakobsson, M., 2012. Recent glacially influenced sedimentary processes on the East Greenland continental slope and deep Greenland Basin. *Quaternary Science Reviews* 49, 64-81.

Graham, A.G.C., Larter, R.D., Gohl, K., Hillenbrand, C.-D., Smith, J.A., Kuhn, G., 2009. Bedform signature of a West Antarctic palaeo-ice stream reveals a multi-temporal record of flow and substrate control. *Quaternary Science Reviews* 28, 2774-2793.

Hanebuth, T., Statteger, K., Grootes, P.M., 2000. Rapid flooding of the Sunda Shelf: A late-glacial sea-level record. *Science* 288, 1033-1035.

Harbor, J.M., 1992. Numerical modeling of the development of U-shaped valleys by glacial erosion. *Geological Society of America Bulletin* 104, 1364-1375.

Heroy, D.C., Anderson, J.B., 2005. Ice-sheet extent of the Antarctic Peninsula region during the Last Glacial Maximum (LGM) - Insights from glacial geomorphology. *Geological Society of America Bulletin* 117, 1497-1512.

Hogan, K.A., Dix, J.K., Lloyd, J.M., Long, A.J., Cotterill, C.J., 2011. Seismic stratigraphy records the deglacial history of Jakobshavn Isbrae, West Greenland. *Journal of Quaternary*

Science 26, 757-766.

Hogan, K.A., Dowdeswell, J.A., Ó Cofaigh, C., 2012. Glacimarine sedimentary processes and depositional environments in an embayment fed by West Greenland ice streams. *Marine Geology* 311, 1-16.

Holland, D.M., Thomas, R.H., De Young, B., Ribergaard, M.H., Lyberth, B., 2008. Acceleration of Jakobshavn Isbrae triggered by warm subsurface ocean waters. *Nature Geoscience* 1, 659-664.

Holtedahl, O., 1970. On the morphology of the West Greenland shelf with general remarks on the "marginal channel" problem. *Marine Geology* 8, 155-172.

Howat, I.M., Eddy, A., 2011. Multi-decadal retreat of Greenland's marine-terminating glaciers. *Journal of Glaciology* 57, 389-396.

Ingólfsson, O., Frich, P., Funder, S., Humlum, O., 1990. Paleoclimatic implications of an early Holocene glacier advance on Disko Island, West Greenland. *Boreas* 19, 297-311.

IPCC, 2007. *Climate Change 2007: Synthesis Report. Contribution of Working Groups I, II and III to the Fourth Assessment Report of the Intergovernmental Panel on Climate Change* [Core Writing Team, Pachauri, R.K., Reisinger, A. (eds.)]. IPCC, Geneva, Switzerland.

Jaeger, J.M., Nittrouer, C.A., 1999. Sediment deposition in an Alaskan Fjord: Controls on the formation and preservation of sedimentary structures in Icy Bay. *Journal of Sedimentary Research*. 69, 1011-1026.

Jakobsson, M., Mayer, L., Coakley, B., Dowdeswell, J.A., Forbes, S., Fridman, B., Hodnesdal, H., Noormets, R., Pedersen, R., Rebesco, M., Schenke, H.W., Zarayskaya, Y., Accettella, D., Armstrong, A., Anderson, R.M., Bienhoff, P., Camerlenghi, A., Church, I., Edwards, M., Gardner, J.V., Hall, J.K., Hell, B., Hestvik, O., Kristoffersen, Y., Marcussen, C., Mohammad, R., Mosher, D., Nghiem, S.V., Teresa Pedrosa, M., Travaglini, P.G., Weatherall, P., 2012. The International Bathymetric Chart of the Arctic Ocean (IBCAO) Version 3.0. *Geophysical Research Letters* 39, doi:10.1029/2012GL052219.

Jennings, A.E., Gronvold, K., Hilberman, R., Smith, M., Hald, M., 2002. High-resolution study of Icelandic tephra in the Kangerlussuaq Trough, southeast Greenland, during the last deglaciation. *Journal of Quaternary Science* 17, 747-757.

- Jennings, A.E., Hald, M., Smith, M., Andrews, J.T., 2006. Freshwater forcing from the Greenland Ice Sheet during the Younger Dryas: evidence from southeastern Greenland shelf cores. *Quaternary Science Reviews* 25, 282-298.
- Johnson, G.L., Sommerhoff, G., Egloff, J., 1975. Structure and morphology of the west Reykjanes basin and the southeast Greenland continental margin. *Marine Geology* 18, 175-196.
- Joughin, I., Abdalati, W., Fahnestock, M., 2004. Large fluctuations in speed on Greenland's Jakobshavn Isbrae glacier. *Nature* 432, 608-610.
- Joughin, I., Das, S.B., King, M.A., Smith, B.E., Howat, I.M., Moon, T., 2008. Seasonal speedup along the western flank of the Greenland Ice Sheet. *Science* 320, 781-783.
- Joughin, I., Alley, R.B., 2011. Stability of the West Antarctic ice sheet in a warming world. *Nature Geoscience* 4, doi: 10.1038/NCEO1194.
- Kargel, J.S., Ahlstrom, A.P., Alley, R.B., Bamber, J.L., Benham, T.J., Box, J.E., Chen, C., Christoffersen, P., Citterio, M., Cogley, J.G., Jiskoot, H., Leonard, G.J., Morin, P., Scambos, T., Sheldon, T., Willis, I., 2012. Greenland's shrinking ice cover: "fast times" but not that fast. *Cryosphere* 6, 533-537.
- Katz, R.F., Worster, M.G., 2010. Stability of ice-sheet grounding lines. *Proceedings of the Royal Society a-Mathematical Physical and Engineering Sciences* 466, 1597-1620.
- Kelly, M. (1985). A review of the Quaternary geology of western Greenland. In: Andrews, J. T. (eds.) *Quaternary Environments of Eastern Canadian Arctic, Baffin Bay and Western Greenland*. Boston, Allen and Unwin, 461-501.
- King, E.L., Sejrup, H.P., Haflidason, H., Elverhoi, A., Aarseth, I., 1996. Quaternary seismic stratigraphy of the North Sea Fan: Glacially-fed gravity flow aprons, hemipelagic sediments, and large submarine slides. *Marine Geology* 130, 293-315.
- Kleman, J., Marchant, D., Borgstrom, I., 2001. Geomorphic evidence for late glacial ice dynamics on southern Baffin Island and in outer Hudson Strait, Nunavut, Canada. *Arctic Antarctic and Alpine Research* 33, 249-257.
- Knutz, P.C., Sicre, M.-A., Ebbesen, H., Christiansen, S., Kuijpers, A., 2011. Multiple-stage deglacial retreat of the southern Greenland Ice Sheet linked with Irminger Current warm

water transport. *Paleoceanography* 26, doi:10.1029/2010PA002053.

Kuijpers, A., Dalhoff, F., Brandt, M.P., Huembs, P., Schott, T., Zotova, A., 2007. Giant iceberg plow marks at more than 1 km water depth offshore West Greenland. *Marine Geology* 246, 60-64.

Kuijpers, A., Troelstra, S.R., Prins, M.A., Linthout, K., Akhmetzhanov, A., Bouryak, S., Bachmann, M.F., Lassen, S., Rasmussen, S., Jensen, J.B., 2003. Late Quaternary sedimentary processes and ocean circulation changes at the Southeast Greenland margin. *Marine Geology* 195, 109-129.

Kuijpers, A., Werner, F., 2007. Extremely deep-draft iceberg scouring in the glacial North Atlantic Ocean. *Geo-Marine Letters* 27, 383-389.

Laberg, J.S., Vorren, T.O., 1995. Late Weichselian submarine debris flow deposits on the Bear Island Trough Mouth Fan. *Marine Geology* 127, 45-72.

Laberg, J.S., Vorren, T.O., 1996. The Middle and Late Pleistocene evolution of the Bear Island Trough Mouth Fan. *Global and Planetary Change* 12, 309-330.

Laberg, J.S., Vorren, T.O., 2000. The Traenadjupet Slide, offshore Norway - morphology, evacuation and triggering mechanisms. *Marine Geology* 171, 95-114.

Larsen, H.C., Saunders, A.D., Clift, P.D., Beget, J., Wei, W., Spezzaferri, S., Ali, J., Cambray, H., Demant, A., Fitton, G., Fram, M.S., Fukuma, K., Gieskes, J., Holmes, M.A., Hunt, J., Lacasse, C., Larsen, L.M., Lykkeanderson, H., Meltser, A., Morrison, M.L., Nemoto, N., Okay, N., Saito, S., Sinton, C., Stax, R., Vallier, T.L., Vandamme, D., Werner, R., Clift, P.D., 1994. 7-million years of glaciation in Greenland. *Science* 264, 952-955.

Lenton, T.M., Held, H., Kriegler, E., Hall, J.W., Lucht, W., Rahmstorf, S., Schellnhuber, H.J., 2008. Tipping elements in the Earth's climate system. *Proceedings of the National Academy of Sciences of the United States of America* 105, 1786-1793.

Livingstone, S.J., Ó Cofaigh, C., Stokes, C.R., Hillenbrand, C.-D., Vieli, A., Jamieson, S.S.R., 2012a. Antarctic palaeo-ice streams. *Earth-Science Reviews* 111, 90-128.

Livingstone, S.J., Clark, C.D., Piotrowski, J.A., Tranter, M., Bentley, M.J., Hodson, A., Swift, D.A., Woodward, J., 2012b. Theoretical framework and diagnostic criteria for the identification of palaeo-subglacial lakes. *Quaternary Science Reviews* 53, 88-110.

- Long, A.J., Roberts, D.H., 2003. Late Weichselian deglacial history of Disko Bugt, West Greenland, and the dynamics of the Jakobshavns Isbrae ice stream. *Boreas* 32, 208-226.
- Lowe, A.L., Anderson, J.B., 2003. Evidence for abundant subglacial meltwater beneath the paleo-ice sheet in Pine Island Bay, Antarctica. *Journal of Glaciology* 49, 125-138.
- Lurton, X., 2002. An introduction of underwater acoustics: Principles and applications. Chichester, Praxis.
- Mackenzie, K.V., 1981. Nine-term equation for sound speeds in the oceans. *Journal of the Acoustic Society of America* 70, 807-812.
- Micallef, A., Mountjoy, J.J., 2011. A topographic signature of a hydrodynamic origin for submarine gullies. *Geology* 39, 115-118.
- Mienert, J., Andrews, J.T., Milliman, J.D., 1992. The East Greenland continental margin (65°N) since the last deglaciation: Changes in seafloor properties and ocean circulation. *Marine Geology* 106, 217-238.
- Mosola, A.B., Anderson, J.B., 2006. Expansion and rapid retreat of the West Antarctic Ice Sheet in eastern Ross Sea: possible consequence of over-extended ice streams? *Quaternary Science Reviews* 25, 2177-2196.
- Mulder, T., Syvitski, J.P.M., Migeon, S., Faugères, J.-C., Savoye, B., 2003. Marine hyperpycnal flows: initiation, behaviour and related deposits: a review. *Marine and Petroleum Geology* 20, 861-882.
- Nam, S.I., Stein, R., Grobe, H., Hubberten, H., 1995. Late Quaternary glacial-interglacial changes in sediment composition at the East Greenland continental margin and their paleoceanographic implications. *Marine Geology* 122, 243-262.
- Nick, F.M., Vieli, A., Howat, I.M., Joughin, I., 2009. Large-scale changes in Greenland outlet glacier dynamics triggered at the terminus. *Nature Geoscience* 2, doi: 10.1038/NGEO394.
- Nielsen, T., De Santis, L., Dahgren, K.I.T., Kuijpers, A., Laberg, J.S., Nygard, A., Praeg, D., Stoker, M.S., 2005. A comparison of the NW European glaciated margin with other glaciated margins. *Marine and Petroleum Geology* 22, 1149-1183.
- Nielsen, T., Kuijpers, A., 2013. Only 5 southern Greenland shelf edge glaciations since the

early Pliocene. *Scientific reports* 3, doi: 10.1038/srep01875.

Nitsche, F.O., Gohl, K., Larter, R.D., Hillenbrand, C.D., Kuhn, G., Smith, J.A., Jacobs, S., Anderson, J.B., Jakobsson, M., 2013. Paleo ice flow and subglacial meltwater dynamics in Pine Island Bay, West Antarctica. *Cryosphere* 7, 249-262.

Noormets, R., Dowdeswell, J.A., Larter, R.D., Ó Cofaigh, C., Evans, J., 2009. Morphology of the upper continental slope in the Bellingshausen and Amundsen Seas - Implications for sedimentary processes at the shelf edge of West Antarctica. *Marine Geology* 258, 100-114.

Ó Cofaigh, C., Pudsey, C.J., Dowdeswell, J.A., Morris, P., 2002. Evolution of subglacial bedforms along a paleo-ice stream, Antarctic Peninsula continental shelf. *Geophysical Research Letters* 29.

Ó Cofaigh, C., Taylor, J., Dowdeswell, J.A., Pudsey, C.J., 2003. Palaeo-ice streams, trough mouth fans and high-latitude continental slope sedimentation. *Boreas* 32, 37-55.

Ó Cofaigh, C., Dowdeswell, J.A., Evans, J., Kenyon, N.H., Taylor, J., Mienert, A., Wilken, M., 2004. Timing and significance of glacially influenced mass-wasting in the submarine channels of the Greenland Basin. *Marine Geology* 207, 39-54.

Ó Cofaigh, C., Dowdeswell, J.A., Evans, J., Larter, R.D., 2008. Geological constraints on Antarctic palaeo-ice-stream retreat. *Earth Surface Processes and Landforms* 33, 513-525.

Ó Cofaigh, C., Andrews, J.T., Jennings, A.E., Dowdeswell, J.A., Hogan, K.A., Kilfeather, A.A., Sheldon, C., 2013a. Glacimarine lithofacies, provenance and depositional processes on a West Greenland trough-mouth fan. *Journal of Quaternary Science* 28, 13-26.

Ó Cofaigh, C., Dowdeswell, J.A., Jennings, A.E., Hogan, K.A., Kilfeather, A., Hiemstra, J.F., Noormets, R., Evans, J., McCarthy, D.J., Andrews, J.T., Lloyd, J.M., Moros, M., 2013b. An extensive and dynamic ice sheet on the West Greenland shelf during the last glacial cycle. *Geology* 41, 219-222.

Ottesen, D., Dowdeswell, J.A., Rise, L., 2005. Submarine landforms and the reconstruction of fast-flowing ice streams within a large Quaternary ice sheet: The 2500-km-long Norwegian-Svalbard margin (57° - 80°N). *Geological Society of America Bulletin* 117, doi: 10.1130/B25577.1.

Ottesen, D., Dowdeswell, J.A., Landvik, J.Y., Mienert, J., 2007. Dynamics of the Late

Weichselian ice sheet on Svalbard inferred from high-resolution sea-floor morphology. *Boreas* 36, 286-306.

Ottesen, D., Stokes, C.R., Rise, L., Olsen, L., 2008. Ice-sheet dynamics and ice streaming along the coastal parts of northern Norway. *Quaternary Science Reviews* 27.

Ottesen, D., Dowdeswell, J.A., 2009. An inter-ice-stream glaciated margin: Submarine landforms and a geomorphic model based on marine-geophysical data from Svalbard. *Geological Society of America Bulletin* 121, 1647-1665.

Parsons, J.D., Bush, J., Syvitski, J.P.M., 2001. Hyperpycnal flow formation with small sediment concentrations. *Sedimentology* 48, 465–478.

Piper, D.J.W., Shaw, J., Skene, K.I., 2007. Stratigraphic and sedimentological evidence for late Wisconsinan sub-glacial outburst floods to Laurentian Fan. *Palaeogeography Palaeoclimatology Palaeoecology* 246, 101-119.

Piper, D.J.W., Normark, W.R., 2009. Processes that initiate turbidity currents and their influence on turbidites: A marine geology perspective. *Journal of Sedimentary Research* 79, 347-362.

Piper, D.J.W., Deptuck, M.E., Mosher, D.C., Hughes-Clark, J.E., Migeon, S., 2012. Erosional and depositional features of glacial meltwater discharges on the Eastern Canadian continental margin. *Application of the Principles of Seismic Geomorphology to Continental- Slope and Base-of-Slope Systems: Case Studies from Seafloor and Near-Seafloor Analogues SEPM Special Publication* 99.

Powell, R.D., 1984. Glaciomarine processes and inductive lithofacies modeling of ice shelf and tidewater glacier sediments based on Quaternary examples. *Marine Geology* 57, 1-52.

Powell, R.D., Domack, E., 2002. Modern glaciomarine environments. In: Menzies, J. (eds.): *Modern and Past Glacial Environments*, 445–486. Butterworth-Heinemann, Oxford.

Pritchard, H.D., Arthern, R.J., Vaughan, D.G., Edwards, L.A., 2009. Extensive dynamic thinning on the margins of the Greenland and Antarctic ice sheets. *Nature* 461, doi:10.1038/nature08471.

Rebesco, M., Liu, Y., Camerlenghi, A., Winsborrow, M., Laberg, J.S., Caburlotto, A., Diviacco, P., Accettella, D., Sauli, C., Wardell, N., Tomini, I., 2011. Deglaciation of the

western margin of the Barents Sea Ice Sheet - A swath bathymetric and sub-bottom seismic study from the Kveithola Trough. *Marine Geology* 279, 141-147.

Reeh, N., Mayer, C., Miller, H., Thomsen, H.H., Weidick, A., 1999. Present and past climate control on fjord glaciations in Greenland: Implications for IRD-deposition in the sea. *Geophysical Research Letters* 26, 1039-1042.

Rignot, E., Kanagaratnam, P., 2006. Changes in the velocity structure of the Greenland ice sheet. *Science* 311, 986-990.

Rinterknecht, V., Gorokhovitch, Y., Schaefer, J., Caffee, M., 2009. Preliminary ¹⁰Be chronology for the last deglaciation of the western margin of the Greenland Ice Sheet. *Journal of Quaternary Science* 24, 270-278.

Roberts, D.H., Long, A.J., 2005. Streamlined bedrock terrain and fast ice flow, Jakobshavns Isbrae, West Greenland: implications for ice stream and ice sheet dynamics. *Boreas* 34, 25-42.

Roberts, D.H., Long, A.J., Schnabel, C., Freeman, S., Simpson, M.J.R., 2008. The deglacial history of southeast sector of the Greenland Ice Sheet during the Last Glacial Maximum. *Quaternary Science Reviews* 27, 1505-1516.

Roberts, D.H., Long, A.J., Schnabel, C., Davies, B.J., Xu, S., Simpson, M.J.R., Huybrechts, P., 2009. Ice sheet extent and early deglacial history of the southwestern sector of the Greenland Ice Sheet. *Quaternary Science Reviews* 28, 2760-2773.

Roberts, D.H., Long, A.J., Davies, B.J., Simpson, M.J.R., Schnabel, C., 2010. Ice stream influence on West Greenland Ice Sheet dynamics during the Last Glacial Maximum. *Journal of Quaternary Science* 25, doi: 10.1002/jqs.1354.

Roksandić, M.M., 1979. Geology of the continental shelf off West Greenland between 61°15'N and 64°00'N: an interpretation of sparker seismic and echo sounder data. *Grønlands Geologiske Undersøgelse Rapport* 92.

Schoof, C., 2007. Ice sheet grounding line dynamics: Steady states, stability, and hysteresis. *Journal of Geophysical Research-Earth Surface* 112, doi: 10.1029/2006JF000664.

Shaw, J., Piper, D.J.W., Skulski, T., Lamplugh, M.J., Craft, A., Roy, A., 2012. New evidence for widespread mass transport on the Northeast Newfoundland Shelf revealed by Olex single-

beam echo sounding. *Geo-Marine Letters* 32, doi: 10.1007/s00367-011-0233-3.

Shaw, J., Todd, B.J., Brushett, D., Parrott, D.R., Bell, T., 2009. Late Wisconsinan glacial landsystems on Atlantic Canadian shelves: New evidence from multibeam and single-beam sonar data. *Boreas* 38, 146-159.

Shepherd, A., Hubbard, A., Nienow, P., King, M., McMillan, M., Joughin, I., 2009. Greenland ice sheet motion coupled with daily melting in late summer. *Geophysical Research Letters* 36, doi: 10.1029/2008GL035758.

Shepherd, A., Ivins, E.R., Geruo, A., Barletta, V.R., Bentley, M.J., Bettadpur, S., Briggs, K.H., Bromwich, D.H., Forsberg, R., Galin, N., Horwath, M., Jacobs, S., Joughin, I., King, M.A., Lenaerts, J.T.M., Li, J., Ligtenberg, S.R.M., Luckman, A., Luthcke, S.B., McMillan, M., Meister, R., Milne, G., Mouginot, J., Muir, A., Nicolas, J.P., Paden, J., Payne, A.J., Pritchard, H., Rignot, E., Rott, H., Sorensen, L.S., Scambos, T.A., Scheuchl, B., Schrama, E.J.O., Smith, B., Sundal, A.V., van Angelen, J.H., van de Berg, W.J., van den Broeke, M.R., Vaughan, D.G., Velicogna, I., Wahr, J., Whitehouse, P.L., Wingham, D.J., Yi, D., Young, D., Zwally, H.J., 2012. A Reconciled Estimate of Ice-Sheet Mass Balance. *Science* 338, 1183-1189.

Shepherd, A., Wingham, D., 2007. Recent sea-level contributions of the Antarctic and Greenland ice sheets. *Science* 315, doi: 10.1126/science.1136776.

Shipp, S., Anderson, J., Domack, E., 1999. Late Pleistocene-Holocene retreat of the West Antarctic Ice-Sheet system in the Ross Sea: Part 1 - Geophysical results. *Geological Society of America Bulletin* 111, 1486-1516.

Shipp, S.S., Wellner, J.S., Anderson, J.B., 2002. Retreat signature of a polar ice stream: subglacial geomorphic features and sediments from the Ross Sea, Antarctica. *Glacier-Influenced Sedimentation on High-Latitude Continental Margins* 203, 277-304.

Shreve, R.L., 1972. Movement of water in glaciers. *Journal of Glaciology* 11, 205-214.

Simpson, M.J.R., Milne, G.A., Huybrechts, P., Long, A.J., 2009. Calibrating a glaciological model of the Greenland ice sheet from the Last Glacial Maximum to present-day using field observations of relative sea level and ice extent. *Quaternary Science Reviews* 28, 1631-1657.

Smith, M.J., Clark, C.D., 2005. Methods for the visualization of digital elevation models for

landform mapping. *Earth Surface Processes and Landforms* 30, 885-900.

Sommerhoff, G., 1975. Glaziale Gestaltung und marine Überformung der Schelfbänke vor SW-Grönland. *Polarforschung* 45, 22–31.

Sommerhoff, G., 1981. Geomorphologische Prozesse in der Labrador-und Irmingersee. Ein Beitrag zur submarinen Geomorphologie einer subpolaren Meeresregion. *Polarforschung* 51, 175-191.

Spagnolo, M., Clark, C.D., 2009. A geomorphological overview of glacial landforms on the Icelandic continental shelf. *Journal of Maps*, 37-52.

Sparrenbom, C.J., Bennike, O., Björck, S., Lambeck, K., 2006. Relative sea-level changes since 15,000 cal. yr BP in the Nanortalik area, southern Greenland. *Journal of Quaternary Science* 21, 29-48.

Stanford, J.D., Rohling, E.J., Hunter, S.E., Roberts, A.P., Rasmussen, S.O., Bard, E., McManus, J., Fairbanks, R.G., 2006. Timing of meltwater pulse 1a and climate responses to meltwater injections. *Paleoceanography* 21, doi: 10.1029/2006PA001340.

Steffensen, J.P., Andersen, K.K., Bigler, M., Clausen, H.B., Dahl-Jensen, D., Fischer, H., Goto-Azuma, K., Hansson, M., Johnsen, S.J., Jouzel, J., Masson-Delmotte, V., Popp, T., Rasmussen, S.O., Roethlisberger, R., Ruth, U., Stauffer, B., Siggaard-Andersen, M.-L., Sveinbjörnsdóttir, A.E., Svensson, A., White, J.W.C., 2008. High-resolution Greenland Ice Core data show abrupt climate change happens in few years. *Science* 321, 680-684.

Stokes, C.R., Clark, C.D., 1999. Geomorphological criteria for identifying Pleistocene ice streams. *Annals of Glaciology* 28, 67-74.

Stokes, C.R., Clark, C.D., 2001. Palaeo-ice streams. *Quaternary Science Reviews* 20, 1437-1457.

Stokes, C.R., Clark, C.D., 2003. The Dubawnt Lake palaeo-ice stream: evidence for dynamic ice sheet behaviour on the Canadian Shield and insights regarding the controls on ice-stream location and vigour. *Boreas* 32, 263-279.

Syvitski, J.P.M., Stein, A.B., Andrews, J.T., Milliman, J.D., 2001. Icebergs and the sea floor of the East Greenland (Kangerlussuaq) continental margin. *Arctic Antarctic and Alpine Research* 33, 52-61.

ten Brink, U.S., Schneider, C., 1995. Glacial morphology and depositional sequences of the Antarctic continental shelf. *Geology* 23, 580-584.

Tripsanas, E.K., Piper, D.M., 2008. Glacigenic debris-flow deposits of Orphan Basin, offshore Eastern Canada: Sedimentological and rheological properties, origin, and relationship to meltwater discharge. *Journal of Sedimentary Research* 78, 724-744.

Tulaczyk, S., Kamb, B., Scherer, R.P., Engelhardt, H.F., 1998. Sedimentary processes at the base of a West Antarctic ice stream: Constraints from textural and compositional properties of subglacial debris. *Journal of Sedimentary Research* 68, 487-496.

Vachtman, D., Mitchell, N.C., Gawthorpe, R., 2013. Morphologic signatures in submarine canyons and gullies, central USA Atlantic continental margins. *Marine and Petroleum Geology* 41, 250-263.

van den Broeke, M., Bamber, J., Ettema, J., Rignot, E., Schrama, E., van de Berg, W.J., van Meijgaard, E., Velicogna, I., Wouters, B., 2009. Partitioning Recent Greenland Mass Loss. *Science* 326, 984-986.

Vanneste, L.E., Larter, R.D., 1995. Deep-tow boomer survey on the Antarctic Peninsula Pacific margin: an investigation of the morphology and acoustic characteristics of late Quaternary sedimentary deposits on the outer continental shelf and upper slope. In: Cooper, A.K., et al. (Ed.), *Geology and Seismic Stratigraphy of the Antarctic Margin*, Antarctic Research Series, 68. AGU, Washington, DC, 97-121.

Vanneste, M., Mienert, J., Bunz, S., 2006. The Hinlopen Slide: A giant, submarine slope failure on the northern Svalbard margin, Arctic Ocean. *Earth and Planetary Science Letters* 245, 373-388.

Vorren, T.O., Hald, M., Lebesbye, E., 1988. Late Cenozoic environments in the Barents Sea. *Paleoceanography* 3, 601-612.

Vorren, T.O., Lebesbye, E., Andreassen, K., Larsen, K.B., 1989. Glacigenic sediments on passive a continental margin as exemplified by the Barents Sea. *Marine Geology* 85, 251-272.

Vorren, T.O., Laberg, J.S., 1997. Trough mouth fans - Palaeoclimate and ice-sheet monitors. *Quaternary Science Reviews* 16, 865-881.

- Vorren, T.O., Laberg, J.S., Blaume, F., Dowdeswell, J.A., Kenyon, N.H., Mienert, J., Rumohr, J., Werner, F., 1998. The Norwegian Greenland Sea continental margins: Morphology and late Quaternary sedimentary processes and environment. *Quaternary Science Reviews* 17, 273-302.
- Walsh, K.M., Howat, I.M., Ahn, Y., Enderlin, E.M., 2012. Changes in the marine-terminating glaciers of central east Greenland, 2000-2010. *Cryosphere* 6, 211-220.
- Weidick, A., Oerter, H., Reeh, N., Thomsen, H.H., Thorning, L., 1990. The recession of the inland ice margin during the Holocene climatic optimum in the Jakobshavn Isfjord area of West Greenland. *Global and Planetary Change* 82, 389-399.
- Weidick, A., Kelly, M., Bennike, O., 2004. Late Quaternary development of the southern sector of the Greenland Ice Sheet, with particular reference to the Qassimiut lobe. *Boreas* 33, 284-299.
- Weidick, A., Bennike, O., 2007. Quaternary glaciation history and glaciology of Jakobshavn Isbrae and the Disko Bugt region, West Greenland: A review. *Geological Survey of Denmark and Greenland Bulletin* 14.
- Wellner, J.S., Lowe, A.L., Shipp, S.S., Anderson, J.B., 2001. Distribution of glacial geomorphic features on the Antarctic continental shelf and correlation with substrate: implications for ice behavior. *Journal of Glaciology* 47, 397-411.
- Wellner, J.S., Heroy, D.C., Anderson, J.B., 2006. The death mask of the Antarctic Ice Sheet: Comparison of glacial geomorphic features across the continental shelf. *Geomorphology* 75, 157-171.
- Wilken, M., Mienert, J., 2006. Submarine glacial debris flows, deep-sea channels and past ice-stream behaviour of the East Greenland continental margin. *Quaternary Science Reviews* 25, 784-810.
- Wingham, D.J., Siegert, M.J., Shepherd, A., Muir, A.S., 2006. Rapid discharge connects Antarctic subglacial lakes. *Nature* 440, 1033-1036.
- Zwally, H.J., Abdalati, W., Herring, T., Larson, K., Saba, J., Steffen, K., 2002. Surface melt-induced acceleration of Greenland ice-sheet flow. *Science* 297, 218-222.